A DISSERTATION
SUBMITTED TO THE FACULTY OF THE GRADUATE SCHOOL
OF THE UNIVERSITY OF MINNESOTA
BY

Savitha Krishnan

IN PARTIAL FULFILLMENT OF THE REQUIREMENTS
FOR THE DEGREE OF
DOCTOR OF [PHILOSOPHY/EDUCATION]

Prof. Gary Reineccius

December 2008

Acknowledgements

I express my deep gratitude to my advisor Dr. Gary Reineccius for his encouragement, support and guidance throughout this course work. My experience working with him has had a profound impact on me and I will carry the many words of wisdom he has kindly shared with me throughout my life. Next, I would like to extend my thanks to Dr. David Smith, Dr. Baraem Ismail, Dr. Steve Severtson, Dr. Roger Moon, Dr. Christian Milo and Dr. Raj Suryanarayanan for agreeing to serve on my committee. I would like to express my sincerest gratitude to Dr. Roger Moon for helping me with the statistical design and analysis. I thank Nestle Research Center for providing funding support for this project. I would also acknowledge both personal and professional help extended by all the flavor lab members (esp. Jean Paul, Josephine and Jian) and my friends for making my stay in Minneapolis a memorable one. I wish them success in their endeavors. I would also like to acknowledge the unconditional support extended by my boyfriend Madhukar. I simply cannot put to words the amount of respect I have for my parents for their unwavering support and encouragement they provided and to them, I dedicate this thesis.

Abstract

The primary objective of this research was to comprehensively evaluate the applicability and utility of alkyl modified silica matrices for flavor encapsulation. These silicate matrices were generated through a sol-gel process by co-hydrolyzing and co-polymerizing a simple alkoxysilane and a long chain alkylalkoxysilane. In the first study, a response surface model was designed to determine the statistically significant variables of the sol-gel process on the encapsulation efficiency of a hydrophobic flavor molecule (limonene).

In Study 2 and 3, two formulations that exhibited the highest encapsulation efficiency from Study 1 were employed to encapsulate a complex flavor mixture consisting of compounds (diacetyl, methyl propanal, methyl pyrrole and damascenone) having a wide range of physicochemical properties. As the losses of flavor compounds in silicate matrices were high during drying, the matrices were blended with an emulsifying starch before freeze drying. Flavor mixture consisting of compounds was incorporated into medium chain triglycerides (MCT's), limonene and neat before being added into the carrier matrix. We examined the efficacy of these proposed matrices by conducting a comprehensive evaluation of the stability of encapsulated flavor compounds in silica: starch blends during storage and examining the release profiles of these compounds in a food application. While hydrophilic silica blends outperformed the hybrid silica blends in the absence of the solvent, the latter performed better in the presence of solvents. Further, the differences in release properties between matrices were primarily attributed to the differences in % retention during drying; the effect of which may have surpassed the effect of flavor solvents or manufacturing formulation/process.

Table of Contents

Chapter 1 : Literature Review 1
Introduction 1
Properties of encapsulated matrices 3
Commonly used coating materials for encapsulation 4
Gum Acacia 4
Modified or Emulsifying Starch (Starch Octenyl Succinate) 4
Starch hydrolysis products 5
Silica sol-gel matrices for encapsulation 5
Properties of silica gels and precipitates generated through sol-gel reaction 7
Generation of flavor-loaded silicate matrices 8
Surface modification of silicate matrices 15
Generation of alkyl modified (hybrid) silicate sol-gel matrices 16
Studies on alkyl modified silicate sol-gel matrices 16
Influence of alkyl substitutions on the reaction rates (hydrolysis and polymerization rate) of sol-gel reaction 18
Characterization of silicate sol-gel particles generated 19
Light Scattering 20
Transmission Electron Microscopy (TEM) 20
TEM-EDAX (Transmission electron microscopy-Energy Dispersive X-ray spectrum) 21
Confocal Microscopy 21
Nitrogen Adsorption Isotherms 22
Factors affecting volatile retention during storage of dry encapsulated materials 23
Flavor release from encapsulated matrices 25
Mechanisms of Release 26
Diffusion 26
Erosion 30
Swelling or solvent-activated release 32
Rates of release 33
Factors affecting the release of flavors from food matrices 34
Proton Transfer Reaction – Mass Spectrometry 36

Chapter 2 : Preliminary Experiments/Encapsulation of orange oil in silica sol-gel matrices with gelation (Part I) 39
Introduction 39
Materials and Methods 40
Materials 40
Preparation of silica sol-gels 40
Characterization of the silica powder 42
Particle sizing 42
Moisture Content of the powders 42
Flavor load and release determination by gas chromatography 42

Results and Discussion 43
Summary 44

Chapter 3 : Preliminary Experiments/Encapsulation of orange oil in silica sol-gel matrices without gelation (Part 2) 47
Introduction 47
Materials and Methods 48
Materials 48
Synthesis of nanocapsules 48
Synthesis of precipitates 49
Characterization of the nanocapsules and precipitates 50
TEM of the nanocapsules and precipitates 50
Particle size analysis of the precipitates 50
Statistical analysis 51
TEM-EDAX (Transmission electron microscopy-Energy Dispersive X-ray spectrum) 51
Instrumental techniques for the monitoring the sol-gel reaction 51
Results and Discussion 52
Summary 54

Chapter 4 : The evaluation of silica based self-assembling matrices for orange oil encapsulation (Study 1) 60
Abstract 60
Introduction 61
Materials and Methods 62
Materials 62
Protocol for the synthesis of alkyl modified silica matrices 62
Characterization of the precipitates generated 63
Particle size analysis of the system 63
% Extractable limonene from the generated matrices 63
Confocal microscopy of the silica matrices 64
Determination of the significant reaction variables of the sol-gel reaction 64
Influence of concentration of hydrophilic silica on the formation of silica sol-gels 64
Influence of concentration of hydrophobic silica on the formation of silica sol-gels 65
Results and Discussion 65
Conclusion 67

Chapter 5 : Flavor retention in silicate matrices (Study 2) 77
Abstract 77
Introduction 78
Materials and Methods 79
Materials 79
Synthesis of precipitates 80
Characterization of the freeze-dried powder 81

Particle size analysis of the freeze-dried powder 81
Karl Fischer method for moisture determination of the freeze-dried powder 81
Extraction of aroma compounds from encapsulated matrices 81
Statistical analysis 82
Results and Discussion 83
Retention during plating/ drying 83
Rate of degradation of compounds in encapsulated matrices 84
Retention after nine weeks storage at room temperature 85
Summary 88

Chapter 6 : Flavor release from sol-gel silicate matrices (Study 3) 102
Abstract 102
Introduction 102
Materials and Methods 105
Characterization of the freeze-dried powder 105
Real-time measurement of release 105
Data Analysis 106
Results and Discussion 107
Summary 112

Chapter 7 : Conclusions 122

References:……..... 126

Chapter 8 : Appendices 135
Appendix 1 (Chapter 3) 135
Analysis of Variance Table: Particle size of the system 135
Appendix 2 (Chapter 3) 136
Pearson's Square for the addition of BVO 136
Appendix 3 (Chapter 3) 137
Silicomolybdic acid spectrophotometric method 137
Appendix 4 (Chapter 4) 138
Appendix 5 (Chapter 4) 139
Regression Analysis for the central composite design 139
Release during polymerization of the sol-gel reaction 143
Appendix 6 (Chapter 4) 144
Controlled release of limonene from the synthesized precipitates 144
Appendix 7 (Chapter 4) 146
Calculation of the amount of orange oil present in centrifuged silica precipitates by ash test and GC 146
Appendix 8 (Chapter 5) 149
Rate plots for encapsulated matrices 149
Appendix 9 (Chapter 6) 159
Individual plots for release properties of the curve 159

Release patterns of encapsulated powders in water 165

List of Figures

Figure 1-1: Gels generated through the sol-gel process..... 8
Figure 1-2: Precipitates generated through the sol-gel process 8
Figure 1-3: Type of physisorption isotherms (Point B is the stage in which monolayer coverage is complete and multilayer adsorption begins) (Singh et al., 1985) 23
Figure 1-4: Diffusion controlled matrix systems (Baker, 1987)..... 27
Figure 1-5: Reservoir System (Baker, 1987) 28
Figure 1-6: Matrix System (Baker, 1987)..... 30
Figure 1-7: Erosion Controlled Matrix Systems (Baker, 1987)..... 31
Figure 1-8: Zero-order, first-order, and $t^{-1/2}$ release patterns from devices containing the active agent content (Baker, 1987) 34
Figure 1-9: Proton Transfer Reaction-Mass Spectrometer (Lindinger et al., 1998)..... 38
Figure 2-1: Steps involved in the sol-gel polymerization reactions 45
Figure 2-2: “Release” of limonene from various sol-gels 45
Figure 3-1: Steps involved in sol-gel polymerization reaction..... 56
Figure 3-2: Particle size of the sol with increase in polymerization time..... 56
Figure 3-3: TEM images of the nanocapsules (samples 1 and 2 are replicates), with dark areas representing the cores (orange oil) stained with OsO_4 surrounded by a lighter, unstained silicate shell. 57
Figure 3-4**:** TEM images of precipitates obtained using sol-gel polymerization with dark areas representing the cores (orange oil) stained with OsO_4 surrounded by a lighter, unstained silicate shell. 58
Figure 3-5: EDAX of the core-shell nanocapsule contains similar composition (peaks have similar heights) for all the elements 59
Figure 3-6: EDAX of the core nanocapsule (it contains more Br and OsM than Si) 59
Figure 4-1: Steps involved in sol-gel polymerization reaction..... 69
Figure 4-2: Main effects of predictor variables observed on the particle size of the system 70
Figure 4-3: Main effects of predictor variables observed on % extractable limonene from the system..... 71
Figure 5-1: Flow chart for the silica sol-gel encapsulation process (step 1) 89
Figure 5-2: Flow chart for the silica sol-gel encapsulation process (step 2) 89
Figure 5-3: The influence of flavor solvent and manufacturing formulation/process on flavor retention during drying..... 90
Figure 5-4: The influence of flavor solvent and manufacturing formulation/process on flavor retention during storage for nine weeks 91
Figure 5-5: The influence of different capsule formation processes on the loss of methyl propanal (in MCT) during storage 92
Figure 5-6: The influence of different capsule formation processes on the loss of methyl propanal (in limonene) during storage..... 92
Figure 5-7: The influence of different capsule formation processes on the loss of methyl propanal (neat) during storage 93

Figure 5-8: The influence of different capsule formation processes on the loss of diacetyl (in MCT) during storage 93
Figure 5-9: The influence of different capsule formation processes on the loss of diacetyl (in limonene) during storage 94
Figure 5-10: The influence of different capsule formation processes on the loss of diacetyl (neat) during storage 94
Figure 5-11: The influence of different capsule formation processes on the loss of methyl pyrrole (in MCT) during storage 95
Figure 5-12: The influence of different capsule formation processes on the loss of methyl pyrrole (in limonene) during storage 95
Figure 5-13: The influence of different capsule formation processes on the loss of methyl pyrrole (neat) during storage 96
Figure 5-14: The influence of different capsule formation processes on the loss of damascenone (in MCT) during storage 96
Figure 5-15: The influence of different capsule formation processes on the loss of methyl pyrrole (in limonene) during storage 97
Figure 5-16: The influence of different capsule formation processes on the loss of methyl pyrrole (in neat) during storage 97
Figure 6-1: Flavor release sampling system (Nestle Research Center) 113
Figure 6-2: Three dimensional scatter plot for methyl propanal, a1- AUC (ppb); a2-I_{max} (ppb); a3 – surface release, (ppb) 114
Figure 6-3: The influence of volatile retention during drying on volatile release 114
Figure 6-4: Three dimensional scatter plot for methyl pyrrole, a1- AUC (ppb); a2-I_{max} (ppb); a3 – surface release, (ppb) 115
Figure 6-5: The influence of volatile retention during drying on volatile release 115
Figure 6-6: Three dimensional scatter plot diacetyl, a1- AUC (ppb); a2-I_{max} (ppb); a3 – surface release, (ppb) 116
Figure 6-7: The influence of volatile retention during drying on volatile release 116
Figure 6-8: Three dimensional scatter plot for damascenone, a1- AUC (ppb); a2-I_{max} (ppb); a3 – surface release, (ppb) 117
Figure 6-9: The influence of volatile retention during drying on volatile release 117
Figure 8-1: Interaction plot between predictor variables and response variable (particle size of the system) 141
Figure 8-2: Interaction plot between predictor variables and response variable (% extractable limonene) 142
Figure 8-3: % Extractable limonene through the time of polymerization 143
Figure 8-4: % Release of limonene from precipitates from in acetone-water mixture 144
Figure 8-5: % Release of limonene from precipitates in acetone-water mixture 145
Figure 8-6: First-order rate plot for compounds encapsulated in Capsul/MCT matrix 149
Figure 8-7: First-order rate plot for compounds encapsulated in hybrid silica sol-gel: starch blend/MCT matrix 149
Figure 8-8: First-order rate plot for compounds encapsulated in hydrophilic silica sol-gel: starch blend/MCT matrix 150

Figure 8-9: Zero-order rate plot for compounds encapsulated in hydrophilic silica sol-gel: starch blend/MCT matrix 150
Figure 8-10: First-order rate plot for compounds encapsulated in plating silica/MCT matrix 151
Figure 8-11: First-order rate plots for compounds encapsulated in Capsul/MCT matrix151
Figure 8-12: First-order rate plot for compounds encapsulated in hybrid silica sol-gel: starch blend/limonene matrix 152
Figure 8-13: First-order rate plot for compounds encapsulated in hydrophilic silica sol-gel: starch blend/limonene matrix 152
Figure 8-14: First-order rate plot for compounds encapsulated in hydrophilic silica sol-gel: starch blend/limonene matrix 153
Figure 8-15: First-order rate plot for compounds encapsulated in Capsul/no solvent matrix 153
Figure 8-16: Zero-order rate plot for compounds encapsulated in Capsul/no solvent matrix 154
Figure 8-17: First-order rate plot for compounds encapsulated in hybrid silica sol-gel: starch blend /no solvent matrix 154
Figure 8-18: Zero-order rate plot for compounds encapsulated in hybrid silica sol-gel: starch blend/no solvent matrix 155
Figure 8-19: Zero-order rate plot for compounds encapsulated in hydrophilic silica sol-gel: starch blend/no solvent matrix 155
Figure 8-20: First-order rate plot for compounds plated on to commercial silica/no solvent matrix 156
Figure 8-21: Cumulative area under the release curve for methyl propanal in different matrices 159
Figure 8-22: I_{max} of methyl propanal in different matrices 159
Figure 8-23: Area under the release curve for methyl propanal in different matrices before the addition of water (surface release) 160
Figure 8-24: Cumulative area under the release curve for methyl pyrrole in different matrices 160
Figure 8-25: I_{max} of methyl pyrrole in different matrices 161
Figure 8-26: Area under the release curve for methyl pyrrole in different matrices before the addition of water (surface release) 161
Figure 8-27: Cumulative area under the release curve for diacetyl in different matrices162
Figure 8-28: I_{max} of diacetyl in different matrices 162
Figure 8-29: Area under the release curve for diacetyl in different matrices before 163
Figure 8-30: Cumulative area under the release curve for damascenone in different matrices 163
Figure 8-31: I_{max} of damascenone in different matrices 164
Figure 8-32: Area under the release curve for damascenone in different matrices before the addition of water (surface release) 164
Figure 8-33: Release patterns of methyl propanal from encapsulated matrices using MCT as a solvent 165

Figure 8-34: Release patterns of methyl propanal from encapsulated matrices using limonene as a solvent 165
Figure 8-35: Release patterns of methyl pyrrole from encapsulated matrices using MCT as solvent 166
Figure 8-36: Release pattern of methyl pyrrole from encapsulated matrices using limonene as a solvent 166
Figure 8-37: Release patterns of diacetyl from encapsulated matrices using MCT as a solvent 167
Figure 8-38: Release patterns of diacetyl from encapsulated matrices using limonene as a solvent 167
Figure 8-39: Release patterns of damascenone from encapsulated matrices using MCT as a solvent 168
Figure 8-40: Release patterns of damascenone from encapsulated matrices using limonene as a solvent 168

List of Tables

Table 4-1: Fischer LSD for % extractable limonene from silicate matrices..... 76
Table 5-1: Physicochemical properties of compounds present in the flavor mixture..... 98
Table 5-2: Moisture content and particle size of the freeze-dried powders..... 98
Table 5-3: Fischer LSD tests on % retention of flavor compounds during drying for different matrices 99
Table5-4: Fischer LSD test on slopes estimated for different flavor compounds for matrices during first week..... 100
Table 5-5: Fischer LSD test on % retention of different flavor compounds for matrices after nine weeks 101
Table 6-1: Fischer LSD on the properties of the release curves for methyl propanal 118
Table 6-2: Fischer LSD on the properties of the release curves for methyl pyrrole..... 119
Table 6-3: Fischer LSD on the properties of the release curves for diacetyl..... 120
Table 6-4: Fischer LSD on the properties of release curve for damascenone 121
Table 8-1: Experimental conditions of the sol-gel reaction (Central Composite Design) 138
Table 8-2: Multiple regression on the particle size of system 139
Table 8-3: Multiple regression on the % extractable release of limonene..... 140
Table 8-4: Results for the ash test for the blank and flavor loaded samples 146
Table 8-5: Percentage limonene present in the silica samples based on GC analysis ... 147
Table 8-6 : Reaction kinetics of degradation of compounds encapsulated in different matrices..... 157

Chapter 1 : Literature Review

Introduction

Flavor is very important for consumer approval of a food product. However, during manufacturing and storage of some food products, majority of flavor compounds are either lost or degraded affecting the acceptance of the product. In order to overcome this issue, flavors are encapsulated in various materials before being introduced into food products (Balassa and Fanger, 1971; Dziezak, 1988; Versic, 1988; Reineccius, 1991; Shahidi and Han, 1993; Reineccius, 1995; Risch, 1995a). Encapsulation is a process by which a single or a mixture of molecules is entrapped within different types of coating materials. This method was developed in the 1950's for pressure sensitive coatings made for carbonless copying paper. The process has since been practiced successfully in a wide range of applications such as pharmaceutical, health, food and cosmetic industries for several years (Balassa and Fanger, 1971). Reineccius (1991) has cited several vital reasons for flavor encapsulation:

1. Protection of volatiles from evaporation during storage of a food product
2. Protection of flavors from undesirable interactions with food
3. Minimization of flavor/flavor interactions
4. Protection of volatiles from photosensitive reactions or oxidation
5. Ease of incorporation into food products

These attributes facilitate the preservation of the organoleptic profile of the product until it is being used. Numerous techniques have been used to generate flavor delivery systems and they can be classified as follows: (Balassa and Fanger, 1971; Chandrasekaran and King, 1971; Dziezak, 1988; Jackson and Lee, 1991; King, 1995; Dezarn, 1995; Risch, 1995b; Bhandari and D'Arcy, 1996)

- Drying processes: the evaporation of water is used to generate a structure that entraps the dispersion of micron sized flavor droplets. Carbohydrates, proteins and gums are the coating materials frequently used for these processes. Spray drying, fluidized bed drying, freeze drying and tray drying are the commonly employed drying techniques.

- Hot melt processes: The transition from glassy to rubbery state due to temperature modifications in some flavor carrier materials have been exploited to build structures around flavor droplets.

- Polymer complexation or Complex coacervation: Polymers have different charges under different pH conditions depending on their isoelectric point. In this process, flavor droplet is encapsulated in a complex insoluble barrier generated from two oppositely charged polymers.

- Molecular Inclusion: α-, β-, and γ- cyclodextrins contain a lipophilic cavity that can hold flavor molecules due to hydrophobic interactions.

- Adsorption/Plating: The porous nature of silica has been used to adsorb/absorb flavor compounds. Zeller et al. (1995) has highlighted the potential of other microporous flavor carrier materials such as porous carbohydrates as effective adsorbent aroma carriers.

- Biological Systems: microbial cells such as yeast can effectively incorporate flavors functioning as a controlled release system.

- Chemical methods: Flavor compounds are preserved as precursors and are generated during the cooking process or Maillard reactions.

Spray drying has been primarily employed in the food industry for encapsulating flavor compounds (Dzieak, 1988; Reineccius, 1988; Goubet et al., 1998). Amorphous systems in their glassy state are formed during the spray drying process are extremely effective in reducing the diffusion of flavor molecules; however, these barriers are still permeable to oxygen resulting in the degradation of sensitive flavor molecules. Therefore, the type of encapsulation process chosen is dependent on nature of the flavor compound (Voilley and Simatos, 1980; Rosenberg et al., 1990).

Properties of encapsulated matrices

The shapes (films, spheres, particles irregular), structures (porous or compact) and physical states (crystalline or amorphous) of the encapsulated matrices generated are contingent upon the materials and methods used to prepare them. The simplest of encapsulated matrices consist of a core surrounded by a coating which may range from several μm to mm in size (Madene et al., 2006). The core may be composed of just one or several different types of ingredients and similarly, the wall may be single or multi layered. The choice of coating materials can be natural (gum acacia, gelatin, dextrin etc), synthetic (co-polymers such as aluminum monostearate) or semi synthetic (methyl cellulose) and is dependent on the nature of the core material and their applications. The following properties are important when choosing a particular carrier material (Reineccius, 1991):

1) Cost and legal status
2) Emulsion stabilization and film forming
3) Solution viscosity and hygroscopicity
4) Bland taste and odor
5) Flavor retention during drying and storage
6) Mechanisms of flavor release
7) Nature of the flavor compound

8) Final product application

The polarity of the core material is frequently the deciding factor for the choice of carrier materials, as some of them are stable in hydrophilic wall materials and some others are stable in hydrophobic (Madene et al., 2006). In addition, the final application of the product is also critical because the mechanism of release will primarily govern the delivery of flavor in a food product (Chang et al., 1988; Whorton, 1995; Whorton & Reineccius, 1995; Goubet et al., 1998). Carbohydrates such as hydrolyzed starches, emulsifying starches and gums serve as the most common wall materials used in the food industry for the generation of microcapsules (Shahidi and Han, 1993; King, 1995).

Commonly used coating materials for encapsulation

Gum Acacia

The most conventional material used for the encapsulation of flavors is gum Acacia. It is an arbinolgalactan protein that is comprised of several sugars (D-galactose, L-arabinose, L-rhamnose and D-partially methylated glucuronic acids) and a protein moiety (Thevenet, 1988). Gum Acacia possesses exceptional properties required for encapsulation such as bland flavor, relatively low viscosity at high solids, excellent emulsification and film forming properties (Thevenet, 1988; Leahy et al., 1988). Several studies have exhibited the excellent retention of volatiles during drying and storage in gum Acacia due to its properties. However, its relatively expensive cost and limited availability has encouraged researchers to search for cheaper alternative carrier materials (Risch and Reineccius, 1990).

Modified or Emulsifying Starch (Starch Octenyl Succinate)

The development of modified starches for food applications was a result of the increasing costs of gum Acacia. Emulsifying starch is generated through the reaction of starch with

a chemical reagent called 1-octenyl succinic anhydride. The concentration of this agent is restricted to 3 % by total weight of starch (21 CFR 172.892 (d)). This reaction incorporates hydrophobicity into the matrix and therefore, the resulting product (octenyl succinate) has amphiphilic properties. The presence of hydrophilic and hydrophobic groups confers the starch, emulsifying properties that are required for stabilizing emulsions. Some of the other advantages include its good oxidative stability, protection against volatile losses, low cost and consistent supply. The disadvantages in using modified starches are their synthetic nature and shorter shelf-life. Several studies have indicated that these starches are capable of performing similar or even better to gum Acacia due to their physicochemical properties. For instance, studies conducted on spray drying of lemon oil using conventional carriers (gum Acacia and modified starch) have showed that starch octenyl succinates had lower surface oil content and therefore excellent encapsulation efficiencies when compared to gum Acacia (Bangs and Reineccius, 1981). Presently, there are several good modified starches available on the market for encapsulating volatile components: Capsul^{TM}, N-Lok®, Hi-Cap^{TM} (National Starch and Chemical Company, Bridgewater, NJ) (Reineccius, 1991).

Starch hydrolysis products

Maltodextrins and corn syrup solids are the hydrolysis products of starch produced by acid, enzyme or acid/enzyme treatments of native starches. These products have low cost, low viscosity, bland flavor, high solubility in water and retain hydrophilic compounds. However, due to lack of emulsification properties they do not provide good retention of hydrophobic volatiles (Reineccius, 1991; Risch and Reineccius, 1988).

Silica sol-gel matrices for encapsulation

In recent years, silica host matrices, formed by the sol-gel process have emerged as a promising platform for the encapsulation of biomolecules such as enzymes, drugs, proteins, nutraceuticals, flavors, fragrances etc (Reetz et al., 1996; Kortesuo et al.,

2000; Pierre, 2004; Dave et al., 1997; Gill and Ballesteros,1998; Carturan et al., 1997; Veith et al., 2004). While sols are dispersions of colloidal particles (1-100 nm) in liquid, gels are interconnected, rigid networks with pore sizes ranging in the submicron scale. The sol-gel process is a chemical technique that involves a series of hydrolysis and polycondensation reactions of inorganic compounds resulting in the transformation of a colloidal suspension (sol) into a three dimensional network (gel or precipitate). These reactions are initiated at numerous sites making the kinetics of these reactions complex.

Alkoxysilanes ($Si\text{-}(OR)_4$, where R is an alkyl group) are commonly used for the synthesis of silica sol-gels, the first such work dating back to 1846 by Ebelmen (Pierre, 2004). The synthesis of monodisperse silica particles from the hydrolysis of silicon alkoxides in aqueous alcohol solution was first reported by Stober in 1968. Complete hydrolysis of alkoxysilanes result in the formation of $Si\text{-}(OH)_4$ or silicic acid. However, studies indicate that the reaction usually never goes to completion. Condensation reactions occur between two silanols or a silanol and an ethoxy group to form siloxane (Si-O-Si) producing a byproduct (water or ethanol). These reactions can be initiated either by increasing the temperature or modifying the pH of the sol. In the case of the former, water evaporates and the particles are bridged through surface hydroxyl groups or by Si-O-Si bonds. On the other hand, catalyst addition resulting in neutral pH conditions causes the particle charge and zeta potential to decrease and condensation reaction to occur. This condensation reaction forms primary crystals, which eventually grow into particles and finally associate with each other to result in chains. These networks of chains are formed throughout the liquid medium thickening the liquid and resulting in the formation of a three dimensional network (Iler, 1979; Hench and West, 1990). The sol-gel process can be explained in a two step process,

1) Hydrolysis: Induced by low pH

$$Si\text{-}(OR)_4 + H_2O \rightarrow OH - Si(OR)_3 + ROH$$

$$Si\text{-}(OR)_4 + 4\,H_2O \rightarrow Si\text{-}(OH)_4 + 4\,ROH$$

2) Condensation: A result of neutralization

$$OH - Si\text{-}(OR)_3 + OH\text{-}Si\text{-}(OR)_3 \rightarrow (OR)_3\text{-}Si - O\text{-}Si\text{-}(OR)_3 + H_2O$$

$$(OR)_3\text{-}Si\text{-}OR + OH - Si\text{-}(OR)_3 \rightarrow (OR)_3\text{-}Si\text{-}O\text{-}Si\text{-}(OR)_3 + ROH$$

Commercial grades of silica are subdivided into three classes: 1) gels: hydrogels, xerogels and aerogels; 2) fumed pyrogenic silicas; and 3) precipitates (Rodriguez and Colon, 2001).

Properties of silica gels and precipitates generated through sol-gel reaction

The four steps involved in the formation of gels or precipitates are as follows: 1) hydrolysis of alkoxide precursor; 2) formation of nuclei (oligomers) resulting from the condensation of atleast two hydrolyzed monomers; 3) agglomeration of oligomers to form primary particles; and 4) agglomeration of primary particles. Precipitated silicas have heterogeneous distribution of silica within the sol. This implies that the silica concentration is greater in the three dimensional structure than the surrounding medium. Gels, on the other hand, have higher concentration and homogeneous distribution of silica throughout the sol; which do not settle out even when centrifuged. However, both gelling and precipitation involve the bonding of two colloidal particles.

To acquire a final free flowing powder, the silica gel is dried and ground; alternatively, the precipitate is converted into a free flowing powder by filtration followed by drying. In the final dried powder form, the structure of the precipitated silica is less compressed than the dried silica gel; however both have highly open intra structures and very high pore volumes. Gels are similar to chain formation having exactly two points of contact between colloidal particles; alternatively, more than two points of contact result in the formation of aggregates or precipitates (Barby et al., 1976; Iler, 1979; Iler, 1955). Figures 1-1 and 1-2 are pictures of gels and precipitates, respectively.

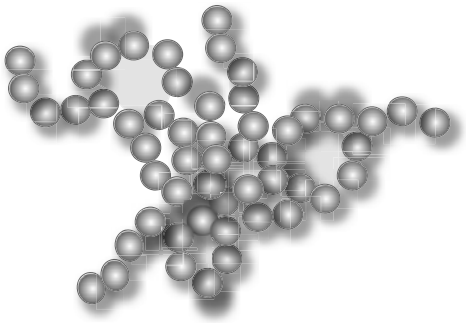

Figure 1-1: Gels generated through the sol-gel process

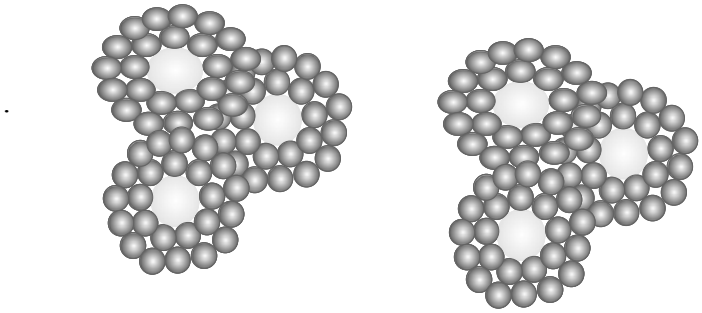

Figure 1-2: Precipitates generated through the sol-gel process

Generation of flavor-loaded silicate matrices

Alkoxysilanes such as tetraethoxysilane (TEOS) or tetramethoxysilane (TMOS) are commonly employed for the generation of silicate matrices used in encapsulation. Since alkoxysilanes are immiscible in water, a mutual solvent such as alcohol is normally used as a solubilizing agent. As described in the previous section, the hydrolysis and condensation reactions take place at localized regions; where silica

polymerizes in stages to nuclei of silica finally leading to the formation of sol particles. This is when the flavor molecules are incorporated into the sol. The successive polycondensation reactions increase the degree of crosslinking entrapping the flavor molecules in the developing network structure. It is important to mention that the hydrogen bonding groups if present on the surface of the flavor molecule can interact with the hydroxyl groups formed during the initial phase of the sol-gel reaction facilitating the condensation polymerization to occur. This resulting viscous material solidifies and leads to the formation of a porous gel or precipitate. These gels are commonly termed as simple silica matrices (Iler, 1979; Veith et al., 2004).

Comparison of plating/adsorption process and sol-gel encapsulation process

A comparison between silica plating and sol-gel encapsulation reveals that flavor retention on silica surfaces during plating is entirely by physical and/or chemical adsorption, while sol-gel encapsulation involves both adsorption and physical entrapment of flavor molecules. Iler (1979) has cited over a 1000 studies on the adsorption of compounds onto silica and has summarized that these studies recurrently demonstrate the adsorption of molecules occurring either by the formation of hydrogen bonds between the electronegative atoms of adsorbed molecules and silanol groups and/or by chemical reactions between silanol groups and the functional groups of the molecules. The amount of hydroxyl and carbonyl groups in a flavor molecule determines the level of interaction with amorphous silica and consequently, the retention of each compound. It is reported that stronger hydrogen bonds are formed with weak nitrogen bases, like pyridine and with oxygen atoms of the ether and keto groups (Iler, 1979). The residual valence electrons on siloxane (Si-O-Si) have the ability to react with water resulting in a surface covered with silanol groups (Si-OH). Adsorption of hydrophilic molecules on silica surfaces is primarily due to the presence of these hydroxyl groups. Studies carried out by Bolton and Reineccius (1992) on plating of flavors reported that improved retention and oxidative protection of flavor molecules was achieved when using fumed silicas in comparison with the other flavor carriers.

In self-assembling sol-gel encapsulation process, the reaction parameters can be modified to synthesize matrices possessing physical properties (specific surface area, pore size distribution, pore volume etc) conducive for the type of material to be encapsulated (Iler, 1979; Veith, 2004). Studies conducted by Sirisuth (2000) showed that the sol-gel reaction parameters were modified to deliver three different release profiles for a drug called metaprolol tatrate.

Use of amorphous silica in the flavor industry

There are numerous patents on the plating of flavor compounds to amorphous silica; however, there is very little literature available on the use of silica sol-gel process for flavor encapsulation. Briefly, Pillsbury Co. was granted a patent in 1968 for the use of amorphous silica as a flavor carrier (Cunningham and Hans, 1968). In 1975, International Flavor and Fragrances Inc. obtained a patent for the use of colloidal amorphous silicas to carry citrus and mint oils (Marmo and Rocco, 1975). Following that, there were several patents on the application of amorphous silica for the prolonged release of flavor in chewing gums (Bell, 1993). In 1989, there was a German patent describing the retention and stabilization of roasted coffee aroma when adsorbed to silica which was formerly lost during the grinding process. A Japanese company had a patent on the process involving the absorption of hydrolyzed meat flavors onto amorphous silica (Oshima et al., 1992). All these patents involved plating/adsorption of flavor compounds to amorphous silica.

Advantages of using silica and sol-gel process

Amorphous silica in contrast to crystalline silica is not toxic and is regularly used as a food additive and component of vitamin supplements (Noureddini and Gao, 2007). In the United States, amorphous silicas have GRAS status and are approved for use as flavor carriers; however the use of amorphous silicas cannot exceed 2 % by

weight in the final food (21CFR 172.230 and 21CFR 172.480). Some of the advantages include its chemical inertness, high specific surface areas, biocompatibility, resistance to microbial attack; silica has been used in a number of different applications. Low temperature and mild conditions are required for the sol-gel process and therefore, it is suitable for encapsulating molecules with poor thermal stability. This process does not require any complex equipment (Iler, 1979; Hench and West, 1998). Further, different functionalities can be incorporated into the silicate matrices through reaction of silanol groups present on the surface of silica. These types of structural modifications are believed to enhance the retention of encapsulated species through various types of electrostatic, covalent and hydrophobic interactions (Cellesi and Tirelli, 2000). In spite of all the potential advantages associated with the sol-gel method, characteristics of the particles obtained by this process are very sensitive to the experimental conditions such as the type of solvent, water/alkoxysilane ratio, type and concentration of alkoxysilane, time of hydrolysis and polymerization, amount of catalyst, temperature, etc (Yoldas, 1996; Livage et al., 2001; Veith et al., 2005; Dunn et al., 1998; Bhatia et al., 1998).

Processing parameters influencing the formation of silicate matrices

The processing parameters that influence the sol-gel process are as follows: (Kortesuo et al., 2002; Yoldas, 1986)

1. Type of alkoxysilane (e.g. methoxysilane, ethoxysilane etc)
2. Water/Alkoxysilane ratio
3. Type of hydrolysis medium
4. Type of catalyst (pH conditions)
5. Type of functionality introduced
6. Reaction time and temperature

Type of alkoxysilane

Studies have illustrated that the rate of hydrolysis and condensation decreased with the increase in the size of the alkoxide group. The order of relative rates of hydrolysis for alkoxysilanes was as follows: methoxysilane > ethoxysilane > propoxysilane > butoxysilane. As alcohols are generated as a byproduct during the sol-gel process, most processes use either methoxysilane or ethoxysilane with the latter being preferred due to the lower toxicity of ethanol compared to methanol (Hench and West, 1990; Kortesuo et al., 2002).

Water/alkoxysilane ratio

The influence of water content is one of the significant parameters in the determination of the morphology and size distribution of polyorganosiloxane polymers. Reports have showed that alcohol condensation is predominant when the water/alkoxide molar ratio is less than 4 leading to microporous materials. Alternatively, the microstructure of gels is not dependent on the water content when the water/alkoxide molar ratio > 10. It is important to mention that sols with lower water content have unreacted alkoxy ligands resulting in linear chain structures, whereas; higher water content sols result in the formation of more branched polymers (Hench and West, 1990; Kortesuo et al., 2002; Yoldas, 1996).

Catalyst or pH conditions

As described in the previous sections, the relative rate of hydrolysis and condensation primarily determine the morphology of the final sol-gels, which in turn is significantly influenced by the pH of the sol. Iler (1979) has categorized the polymerization process into 3 pH domains: pH < 2; pH 2-7; and pH > 7. The reaction rate is proportional to hydrogen ions below pH conditions 2 following a third order reaction, whereas, above pH 2, the reaction rate is second order reaction and primarily depends on the concentration of hydroxyl ions The neutral pH has been described as a boundary due to the significant increase in the silica solubility and hydrolysis rates above or below this particular pH.

The physical properties of the silica particles differ depending on the type of catalyst employed for the sol-gel process. While acidic catalysis results in particles having sizes between 2 and 4 nm, basic catalysis forms particles exhibiting particle sizes more than 100 nm. Nonporous polymers with small specific surface areas are formed during acidic catalysis; on the contrary, basic catalysis favors the formation of highly porous structures possessing excellent adsorption capacity. As the acidic pH conditions are close to the isoelectric point of silica (~ 2), electrophoretic mobility of particles is zero resulting in the slowest condensation rates. Linear branched polymers are formed under these conditions. On the other hand, weakly acidic to basic sols have significant amounts of deprotonated silanol groups (SiO^-); which are capable of increasing the condensation rate forming highly branched species. (Cellesi and Tirelli, 2000).

At extreme pH conditions all particles possess similar charge resulting in no aggregation due to electrostatic repulsion. Alternatively, at intermediate pH conditions the repulsive forces between particles are low resulting in frequent particle collisions. In addition under these intermediate pH conditions, there is an optimum balance of hydroxyl ions to catalyze the formation of siloxane bonds resulting in three dimensional networks.

In commercial processes, silica gels are manufactured at more alkaline pH conditions (7-10.5) in order to achieve larger particles and highly porous structures. In spite of these studies emphasizing the influence of catalysis on porosities; reports indicate that silicate matrices incorporated with longer alkyl chains are generally mesoporous irrespective of the pH used for synthesis (Hench and West, 1990; Kortesuo et al., 2002; Yoldas, 1996).

Time and temperature

Longer reaction times and higher temperatures shift the molecular size distribution of the polymer to higher values. One study reported that the sol-gel reaction conducted for 7 days at 20°C produced similar effects as 60°C exposure for 24 h. The

effects of time and temperature are highly pronounced in formulations that use higher concentrations of alkoxysilanes and higher water/alkoxysilane ratio (Yoldas, 1996).

Hydrolysis medium

Studies conducted with different types of alcohol (methanol, ethanol and propanol) as hydrolysis medium have showed that the amount of polymer (Si-O-Si) generated using methanol was higher than ethanol and propanol. In fact, propanol showed incomplete hydrolysis and low molecular weight polymers. Reports have explained that the diffusion dependent polymer growth was higher in methanol due to its low molecular weight. However, researchers have explained that this effect diminishes at higher concentrations due to smaller molecular separations (Yoldas, 1996).

In order to avoid the use of alcohols in our systems, THEOS (tetrakis (2-hydroxy-ethyl) ester) has been used in our systems. It is a chemical synthesized from TEOS and glycol and has been successfully exchanged for TEOS due to similarity in properties. The compound's solubility in water facilitates the delivery of a single homogeneous phase, unlike TEOS, where alcohol is required to avoid phase separation. The hydrolysis of THEOS results in the formation of glycol and silicic acid which eventually condenses into silica sol-gels (Meyer et al., 2002).

Functionality

Different types of functionalities (amino groups, alkyl groups) can be incorporated into silica sol-gels through the free hydroxyl groups on the surface. In this work, we focus on the modification of silica sol-gel matrices using organoalkoxysilanes (Yoldas, 1996). The influence of incorporating different chain lengths of alkylalkoxysilanes will be explained in detail in the section below.

Surface modification of silicate matrices

A number of studies have demonstrated the suitability of simple silica matrices for the encapsulation of hydrophilic molecules which can associate either chemically or physically with the hydrophilic silica surface (Veith, 2004; Bolton and Reineccius, 1992; Bhatia et al., 1998; Barbe et al., 2004). In fact, a recent study conducted in the year 2008 showed that mesoporous silica spheres could be used to achieve prolonged release of a hydrophilic perfume (Wang et al., 2008). Studies conducted by Veith et al. (2004) showed that hydrophilic silicate matrices selectively retained hydrophilic flavor compounds. The author's results further demonstrated that hydrophobic molecules such as limonene and myrcene, major compounds of citrus oils were retained poorly in simple silica matrices generated from TEOS (Veith, 2004; Bolton and Reineccius, 1992). The selective retention of compounds can lead to alteration in the flavor profile of the final product. The rationale explained for this drawback was two fold: 1) lack of interactions between the hydrophobic flavor molecules and the hydrophilic matrix (Reetz et al., 1996); and 2) diffusion losses of volatile compounds due to the porous nature of silica (Veith et al., 2004). In order to overcome these issues, alkyl modified particles have generated intense interest in a wide range of application fields in recent years (Reetz et al., 1996; Park and Komarneni, 1998).

Studies conducted unanimously concur on the observation that alkyl modifications alter the chemical reactivity of the product enhancing the hydrophobicity and decreasing the amount of surface silanol groups (Reetz et al., 1996; De Witte et al., 1996; Shimojima and Kuroda, 2002; Shimojima and Kuroda, 1998; Loy et al., 2000). One of the studies has reported that using 20 % methyltrimethoxysilane (MTMS) as a co-precursor in TMOS (tetramethoxysilane) sol-gel was adequate to make the gel completely hydrophobic (Yi et al., 2006). This enhanced hydrophobicity in alkyl modified sol-gels has been exploited to encapsulate hydrophobic molecules. Further, the addition of alkyl groups provides flexibility to the silicate network, thereby, preventing the collapse of silicate structures during drying (Park and Komarneni, 1998).

Generation of alkyl modified (hybrid) silicate sol-gel matrices

Alkylalkoxysilanes such as methyltriethoxysilane (CH_3-TEOS), octyltriethoxysilane (C_8-TEOS), or octadecyltriethoxysilane (C_{18}-TEOS), in conjunction with TEOS have been used in the synthesis of surface modified silica sol-gels for the encapsulation of hydrophobic species (Unger et al., 1993; Reetz et al., 1996; Carturan, 1997). For the formation of surface modified silica particles, a simple alkoxysilane is co-hydrolyzed and co-polymerized with an alkylalkoxysilane. A series of hydrolysis and condensation reactions finally result in a cross-condensed product with alkyl groups distributed within it. This modification of inorganic silica particles with organics leads to the production of organic–inorganic hybrid particles in which organic components are chemically bonded to silica matrix. Sol–gel processing enables the preparation of such types of organic-inorganic hybrid materials with controlled pore size and size distribution (Park and Komarneni, 1998; Loy et al., 2000; Rodriguez and Colon, 1999a, 1999b; Rodriguez and Colon, 2001; De Witte et al., 1996; Shimojima et al., 2002).

Studies on alkyl modified silicate sol-gel matrices

Several studies have highlighted the influence of alkyl substitution on the physical properties such as surface area, microporosity, pore volume, pore-size distribution, surface functionality and hydrophobicity (Reetz et al., 1996; Reetz et al., 1997; De Witte et al., 1996). Studies conducted by Yi et al. (2006) showed that organically modified silica sol-gels possessed higher specific surface areas, but smaller pore volumes than gels derived from only TMOS. A similar effect was observed by researchers Maury and Pierre (2001). Some other researchers have demonstrated that incorporating organic groups into the gel network resulted in an overall decrease of surface area, pore volume and pore-size distribution of silica sol-gels (De Witte et al., 1996). Studies have pointed out that the differences in the physical properties of sol-gels derived from similar precursors are primarily due to the dissimilarities in the reaction

kinetics. The kinetics in turn depends on the processing parameters of hydrolysis and condensation reactions (Yoldas, 1996).

Extensive research has been carried out on the use of surface modified silica particles for encapsulation purposes. Bottcher and Slowik (1998) have showed that the release of coronary therapeuticum nifedipin from porous sol-gel made matrices in water was influenced by either particle size or partial substitution of the precursor TEOS with methyl-TEOS. Carturan et al. (1997) used alkyl modified silicate matrices for studying the encapsulation of perfume essences (geranial, β-ionone and menthol) and found that the release kinetics of these molecules was affected by the matrix porosity and the chemical interactions of organic molecules with the matrix. Alternatively, studies carried out by Reetz et al. (1996) revealed that the enhanced retainment of the activity of lipases (lipophilic enzyme) in alkyl modified sol-gels was not correlated to the degree of crosslinking, specific surface area or the pore size, however was exclusively related to alkyl modification. In detail, it was reported that the lipase activity was enhanced significantly in gels formed from a mixture of $Si\text{-}(OCH_3)_3$ and $CH_3\text{-}Si\text{-}(OCH_3)_3$ as opposed to a reaction mixture consisting of $Si\text{-}(OCH_3)_3$ alone. The rationale explained for this performance was two fold: 1) higher dispersion of the hydrophobic lipase in the modified sol-gel matrix; and 2) interaction between the lipophilic domain of the silicate matrix and hydrophobic region of lipase initiating a phenomenon similar to a classical interfacial interaction. Experimental results in this study indicated that increasing the length of the alkyl chain (methyl to propyl) enhanced the activity of the enzyme. Other studies have also reported that larger alkyl groups contribute significantly to the adsorption of molecules to the silica surface (Park and Komarneni, 1998; Shimojima and Kuroda, 2002).

Studies that used hybrid matrices as a column phase showed that hydrophobic interactions increased the chromatographic retention of hydrophobic compounds resulting in the efficient separation of compounds (Constantin et al., 2000; Rodriguez and Colon, 1999a, 1999b; Rodriguez and Colon, 2001). One other study

conducted in the controlled release of drugs showed that the release rate of codeine (lipophilic drug) was significantly reduced in the presence of octyl groups from the silica gel matrix (Unger et al., 1993). On the other hand, some studies in drug research have pointed out the permanent entrapment of hydrophobic drug molecules into the intra particle volume within the silica xerogels, which would be one of the limitations of such systems (Barbe et al., 2004).

Influence of alkyl substitutions on the reaction rates (hydrolysis and polymerization rate) of sol-gel reaction

In order to synthesize homogeneous three dimensional networks in hybrid mixtures, it is essential to understand the reaction rates (hydrolysis and polymerization) of introduced monomers. Studies conducted with alkyl group substitutions such as methyl and ethyl groups demonstrate that alkylalkoxysilanes have hydrolysis rates higher than simple alkoxysilanes in simple systems (when reacted alone). The rationale for this phenomenon has been explained as the *inductive* effect of alkyl groups on silicon atom (Loy et al., 2000). Alternatively, Si-NMR studies conducted by some other researchers with higher chain alkyl groups such as hexyl and octyl groups showed that the rate of hydrolysis of TEOS is 5 times faster than octyl-TEOS suggesting that *inductive* effects do not exclusively determine the reaction rate (Rodriguez and Colon, 2001). The study pointed out one other important factor contributing to the hydrolysis and condensation behavior of alkoxysilanes and was identified as the *steric* effect. It has been proposed that steric bulky alkyl groups can impede the accessibility of the water molecules with the reactive site. Similar effects have been observed for alkyl substituents on the alkoxy groups; methoxysilanes reacted faster than the corresponding ethoxysilanes (Yoldas, 1996). Accordingly, the *inductive* effect due to the presence of octyl (alkyl) groups should lower the positive charge on the silicon atoms, driving the hydrolysis reaction, however, the slower rate of hydrolysis observed for octyl-TEOS indicated that the *steric* effect caused by the hydrophobic group dominated the *inductive* effect (Loy et al., 2000).

Conversely, in hybrid systems consisting of both TEOS and octyl-TEOS, the rates of hydrolysis for octyl-TEOS and TEOS were similar. Reports indicated that the condensation reactions between the hydrolyzed species of octyl-TEOS and TEOS drove the hydrolysis of octyl-TEOS enforcing similar rates (Rodriguez and Colon, 1999a; Rodriguez and Colon, 1999b; Rodriguez and Colon, 2001). These observations may imply that there is no necessity for the addition of octyl-TEOS prior to TEOS. However, examination of the condensation kinetics in these systems revealed an interesting trend. Studies illustrated that a reaction system consisting of TEOS alone had a higher degree of condensation compared to systems incorporated with alkyl modifications (Park and Komarneni, 1998). Researchers have explained that the cross condensation reactions occurring between the alkyl substituted silanols and silanols from TEOS contribute to the overall decrease in the rate of condensation in hybrid systems, thereby lowering the formation of bridged species. Studies have further showed that the condensation rates decreased as the chain length of the alkyl group increased (methyl to propyl) (Loy et al., 2000). The condensation rate influences the degree of crosslinking modifying the internal structure of the silicate matrix (Schmidt, 1989; Lev et al., 1995; Mah and Chung, 1995). Similar to condensation rate, the degree of cross linking also decreases with the volume of the alkyl group. In fact, gels or precipitates cannot be obtained from mixtures containing only long chain alkyl-TEOS. Reports have explained that this is primarily due to the phase separation of monomers from the sol-gel mixture followed by the *steric* effect.

Characterization of silicate sol-gel particles generated

Silicate matrices generated by the sol-gel process are generally characterized by their particle sizes, pore size distribution and specific surface areas. While particle sizes are frequently measured through light scattering methods and microscopic techniques, pore size distribution and specific surface areas are measured by nitrogen adsorption isotherms.

Light Scattering

Laser Light Scattering is a rapid technique for measuring size distribution of particles typically ranging from 1-1000 μm. It is based on the principle that particles transiting through a laser beam scatter light at an angle, which indeed has an association with their particle sizes (Tan, 1997). The scattered light measurements are made using a series of photo detectors placed at different angles and is often described as the diffraction pattern. At low particle concentrations, the instrument follows Beer-Lamberts law which postulates that turbidity (i.e. log of the inverse of the transmission, or a measure of the incident light lost due to scattering) is linear with concentration. However, this is not true for higher particle concentration as the particles are in close proximity that they are rescattered by other particles. Two assumptions are made during particle size measurement using this method: 1) Particles are assumed to be spherical. Laser diffraction is highly sensitive to the volume of the particle; as a result particle diameters are computed from the measured volume of the particle assuming a sphere of equivalent volume. 2) Suspension is assumed to be dilute so that radiation scattered by a particle is directly measured by the detector (i.e. single scattering) and does not undergo multiple scattering prior to reaching the detector. In contrary to emulsions or powders having similar particle sizes, most samples are polydisperse forming a distribution (Jillavenkatesa, 2001).

Transmission Electron Microscopy (TEM)

TEM is a microscopy technique in which a beam of electrons is transmitted through the specimen and as a result an image is formed. Electrons are generated using a tungsten filament by a process called thermionic emission and are accelerated by an electric potential to be focused by electrostatic and electromagnetic lenses onto the sample. These electrons interact with the sample as they pass through creating an image. The image created is then magnified and focused by an objective lens and finally appears on an imaging screen. Heavy metals such as osmium, lead or uranium are used as stains to enhance the contrast by scattering electrons out of the beam and selectively depositing

electron dense atoms in or on the sample (TEM tutorial guide, Imaging Center, University of Minnesota).

TEM-EDAX (Transmission electron microscopy-Energy Dispersive X-ray spectrum)

X-rays are generated when materials are irradiated with an electron beam. These high-energy electrons excite the electrons in the electron shells around the atoms in the material, causing them to jump to higher energy shells. When the electrons fall back to the lower energy shells, they emit electromagnetic radiation in the form of X-rays. The wavelengths, and hence energies of the X-rays are characteristic of the electron shell energies, and therefore the spectrum of X-rays can be used to identify different elements. As a result, X-ray spectrum produced by materials in a TEM can be used to determine the composition of many materials. High-resolution measurements can determine the differences in composition in different portions on a sample. In recent years, this technique has been frequently used to determine the elemental composition of emulsions and encapsulated materials (TEM-EDAX tutorial guide, Imaging Center, University of Minnesota).

Confocal Microscopy

This microscopic technique has been frequently employed to view food colloids such as butter, cheese, ice creams etc. In confocal microscopy, a laser beam is transmitted through a light source aperture and then focused by an objective lens into a small focal volume within a fluorescent specimen. The reflected laser light from the illuminated spot along with the emitted fluorescent light is collected by the objective lens. A beam splitter is used to alienate the light mixture providing way for the laser light to transmit and reflecting the fluorescent light into the detection apparatus. The fluorescent light passes through a pinhole and is detected by the photo detection device transforming the light signal into an electrical one and is recorded by the computer. The detector aperture allows the light only emerging from the focal point and the out-of-focus is

blocked by a pinhole, resulting in sharper images than those from conventional fluorescence microscopy techniques. This technique can be used to obtain images of various z axis planes of the sample (Confocal Microscopy tutorial guide, Imaging Center, University of Minnesota).

Nitrogen Adsorption Isotherms

Nitrogen adsorption isotherm is the most common technique employed for characterizing sol-gel materials for physical characteristics such as total pore volume, surface area and pore size distribution. According to the International Union of Pure and Applied Chemistry (IUPAC), the majority of adsorption-desorption isotherms may be categorized into six types as showed in Figure 1-3. The reversible *Type I* isotherms are characteristic of microporous solids possessing relatively small external surfaces. Non-porous or macroporous adsorbents typically show reversible *Type II* isotherms. This is a symbolic feature of adsorbents showing unrestricted monolayer-multilayer adsorption. The reversible *Type III* isotherms are not commonly observed; however, numerous systems show isotherms exhibiting gradual curvature. *Type IV* isotherms are characterized by a hysteresis loop, which is associated with capillary condensation occurring in their mesopores. *Type V* isotherms infrequently occur and are obtained with certain porous adsorbents. *Type VI* isotherms represent stepwise multilayer adsorption on a uniform non-porous surface (Singh et al., 1985).

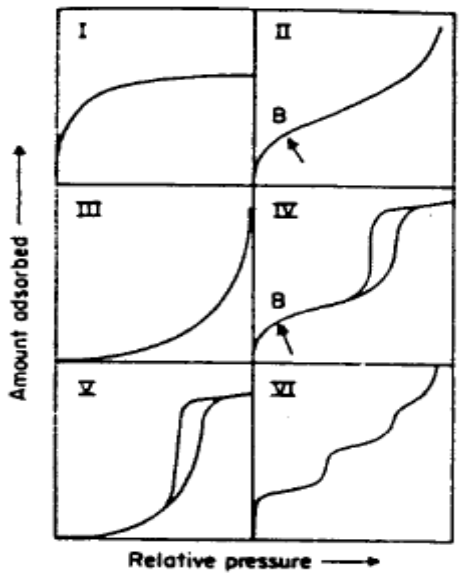

Figure 1-3: Type of physisorption isotherms (Point B is the stage in which monolayer coverage is complete and multilayer adsorption begins) (Singh et al., 1985)

Factors affecting volatile retention during storage of dry encapsulated materials

As one of the primary objectives of our research was to evaluate the loss of flavor compounds in encapsulated matrices during storage, it was important to address the factors that influence them. Differences in retention between various coating materials have been primarily attributed to the differences in the level of interaction between the carrier materials and volatiles. This implies that the physicochemical properties of the volatile flavor molecules such as functional group, molecular weight, polarity, volatility, steric hindrance etc play an important role (Goubet, 1998). In addition, it was reported that the nature of the encapsulation process and *in-feed flavor concentration* also contribute significantly for their stability (Reineccius and Coulter (1969).

Functional group

Studies on encapsulation in carbohydrates revealed that the order of retention decreased in the order of alcohols > ketones = esters > acids in carbohydrate carriers (Voilley, 1995). In detail, benzylic alcohol was the most retained volatile during freeze-drying of glucose, maltose, or DE 28.5 and DE 41.4 corn syrup solids flavored with a mixture of 16 compounds. These results were in agreement with the studies conducted by Veith et al. (2004) in silica sol-gel matrices illustrating higher retention of alcohols relative to other functional groups. The two primary reasons explained for this observation were: 1) condensation reaction occurs between the hydroxyl groups of silica and alcohol; and/or 2) hydrogen bonding occurs between the hydroxyl groups, which can lead to physisorption of molecules on the silicate surface (Iler, 1979). In addition, esters and aldehydes were also retained well in these sol-gel matrices due to the presence of carbonyl groups which can provide similar interactions as that of hydroxyl groups with the silicate surface.

Polarity

Studies have reported that polarity of flavor molecules played a more significant role in the retention performance relative to the molecular weight or boiling point. Most studies indicated that the percent retention decreased with the increase in polarity of molecules. The rationale explained for this trend was the ease of permeability of polar compounds through plasticized materials compared to non-polar compounds during drying (Rosenberg et al., 1990; Voilley, 1995). In contrast, in amorphous hydrophilic sol-gel matrices the retention of hydrophilic polar compounds was higher than non-polar compounds due to the dominant hydrogen bonding interactions occurring between the hydroxyl groups of the silicate matrices and hydrophilic compounds.

Molecular weight and size of molecules

It is well known that smaller molecules diffuse at a faster rate than bigger molecules. Hence, retention of bigger molecules is always high. Studies conducted by Rosenberg et al. (1991) reported that the retention of esters ethyl caproate (MW 144) and

ethyl butyrate (MW 116) was proportional to the molecular weight of the compounds. Similar trends were observed by Whorton et al. (2000) in spray dried maltodextrin powders containing homologous series of aldehydes ranging from C_3 to C_{11}. These trends were in agreement with studies conducted using silica sol-gel matrices (Veith et al., 2004).

Volatility

Volatility can be explained as the vapor pressure of the compound and is also an indication of the potential of a compound to transfer into the headspace. Studies conducted by Menting et al. found that the rate of evaporation of volatile components increased with the relative volatility of components. Several studies on encapsulation have pointed out the decrease in retention with the increase in volatility. Reports have explained that the volatile compounds present on the surface of the encapsulating matrix are lost due to evaporation during storage. As a result, a concentration gradient is created in the encapsulating matrix resulting in the diffusion (Fick's second law of unsteady state diffusion) of compounds from the interior to the surface (Menting et al., 1970).

Flavor release from encapsulated matrices

Flavor release in consumer applications is a critical performance criterion affecting flavor perception and thus, consumer acceptance of a food product. "Controlled release is defined as a technique by which one or more active agents or ingredients are delivered at a desired time and site" (Baker, 1987). This technology was first developed in 1964 by Folkman and Long using membranes of silicone rubber to control the release of anesthetic and cardiovascular drugs. Not surprisingly, the early commercial applications of the technology were initiated in both pharmaceutical and agricultural industries (Langer, 1990). Encapsulation has been the most common tool employed to accomplish the controlled release of active reagents.

Controlled release systems may be classified based on the physical processes or mechanisms of release. Specifically, these mechanisms may be classified into: 1) diffusion based; 2) chemical reaction based; and 3) solvent activation based (swelling and dissolution). The detailed description of the primary mechanisms of release is given in the section below. As most food grade polymer materials used for encapsulation are water soluble, the primary mechanism of release from these systems is dissolution. Therefore, the rate of dissolution of the coating material governs the release rate from these systems (Risch and Reineccius, 1995).

In contrast to carbohydrate based carriers, diffusion is the primary mechanism of release of entrapped chemical species from porous sol-gel matrices (Veith et al., 2005). Diffusion mechanism can be further subdivided into two types: 1) molecular or static diffusion; and 2) eddy or convective diffusion. While molecular diffusion is a result of random movement of molecules in a stagnant fluid; eddy diffusion is caused when elements of fluid are transported along with the dissolved solute. It has been reported that the rate/flux of eddy diffusion is typically much higher than the rate of molecular diffusion (De Roos, 2000).

Eddy diffusion has been given importance in liquid food products as studies have emphasized the importance of evaluating encapsulated matrices in the consumable form (De Roos, 2000; Roos, 2003). For instance, flavors that are incorporated into hot beverages such as tea and coffee, soup mixes, candies etc should be ideally released only during the consumption of the product or when the hot water is added to the product.

Mechanisms of Release

Diffusion

Diffusion is the most common and has been described as the most complex type of release mechanism. It is affected by a number of variables such as particle

porosity, rate of hydration *etc* (Figure 1-4). The permeability of a component through the matrix and its solubility in the wall material primarily govern the diffusion characteristics. It is well known that concentration gradient is the major driving force for diffusion to occur. For volatile compounds, the vapor pressure of the organic compound establishes a concentration gradient and initiates the diffusion process. In non-porous encapsulation systems, an active agent is transported through molecular diffusion occurring in the polymer and is explained exclusively by diffusion coefficient of the active agent or flavor in the polymer (D). Therefore, properties of the polymer such as the degree of crystallinity, crosslinking, swelling properties and molecular weight play an important role in controlling core material release. On the other hand, in porous controlled release systems having pore sizes greater than 200-500 $\mathring{A}$, the diffusion from the core is accomplished through water-filled pores. Transport through these systems is defined by an effective diffusion coefficient (D_{eff}), which is related to the diffusion coefficient of the active agent through the pores filled with a solution of active agent D_w ($D_{eff} = D_w\varepsilon/\tau$), ε is the porosity of the system and τ indicates tortuosity. Diffusion-controlled systems have been categorized into two types: a) reservoir or membrane systems; and b) matrix or monolithic systems (Baker, 1987; Langer, 1990; Washington, 1996).

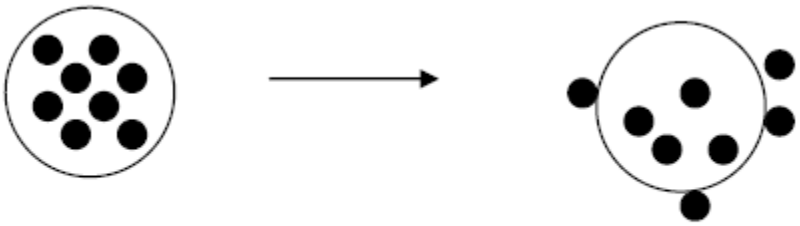

a) Diffusion Controlled

Figure 1-4: Diffusion controlled matrix systems (Baker, 1987)

Reservoir (membrane) systems

This is the simplest form of diffusion-controlled system with an active agent enclosed at relatively high concentrations within an inert membrane (Figure 1-5). Porosity of the barrier membrane can vary and release rates from these systems are primarily governed by the thickness, area and permeability of the barrier. It is interesting to note that release rates from these types of systems can be time independent and therefore, can provide a steady rate of release over a substantial period of time (zero-order kinetics). Further, the loading level of actives in these systems can be much higher than most others making it more economical (Baker, 1987; Langer, 1990; Washington, 1996).

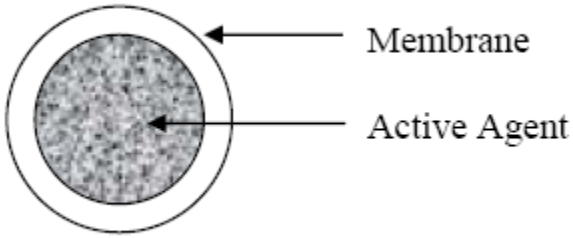

Figure 1-5: Reservoir System (Baker, 1987)

The key events associated with the release of active components in reservoir systems are: 1) first, active agent diffuses to the barrier interface of the reservoir; 2) subsequently, the active agent partitions between the reservoir carrier fluid and the barrier; 3) next, it diffuses through the barrier and partitions between the barrier and the elution medium; and 4) finally, the active agent displaces away from the barrier surface into the elution medium (Pothakamury & Barbora-Canovas, 1995). Diffusion through the barrier polymer constitutes the rate limiting step in the release of active agents from reservoir systems. Further, the specific release pattern is regulated by the concentration gradient, geometry of the device, thermodynamic characteristics of the system (solubility, through the partition coefficient, and structure of the polymer (through the diffusion coefficient)). Mathematically, the behavior of non porous diffusion controlled systems

from microcapsules is abstracted by equation:

$$dM_t/dt = 4\pi DK\Delta C r_o r_i / (r_o - r_i)$$

where D is the diffusion coefficient of the active agent through the membrane, K is the partition coefficient of active agent between the membrane and core, r_o and r_i .are the outer and inner radii of the sphere, and ΔC is the concentration difference across the membrane. It is easy to see from the above equation that maintaining constant area, thickness of the membrane, concentration gradient across the membrane will result in constant release rate from reservoir systems. On the other hand, for microporous membranes, the release rate of the active agent is given by

$$dM_t/dt = 4\pi D_w \varepsilon \Delta C r_o r_i / \tau (r_o - r_i)$$

where D_w is the diffusion coefficient of the active agent in the pore liquid phase, ε and τ are the porosity and tortuosity of the membrane, respectively (Baker, 1987; Robinson and Lee, 1987).

Matrix (monolithic) systems

Figure 1-6 shows a pictorial representation of a matrix system. In these systems, an active ingredient is either dissolved or dispersed in a rate-controlling matrix. Therefore, solubility of the active agent in the polymer becomes a controlling factor in the release from matrix. Release is achieved by diffusion when the loading of an active agent is below the solubility limit and by dissolution when it is above the solubility limit. If the active agent is dissolved in the polymer medium, it is termed as monolithic solution, alternatively; if the active agent has a limited solubility in the polymer medium, only a portion of it is dissolved and the rest is dispersed as small particles throughout the polymer and is termed as monolithic dispersion. Inspite of these systems not having a

release rate in accordance with the zero-order kinetics, it is the simplest and most convenient way to achieve prolonged release of an active agent (Baker, 1987; Pothakamury and Barbora-Canovas, 1995).

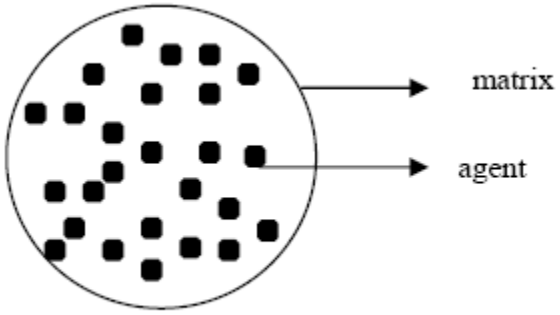

Figure 1-6: Matrix System (Baker, 1987)

Erosion

The erosion process can be categorized into 2 types: 1.) homogeneous or bulk erosion; and 2.) heterogeneous or surface erosion (Figure 1-7). In bulk erosion systems, the release of actives occurs throughout the entire matrix involving both diffusion and polymer erosion. The permeability of the active agent increases over time, however, the increase is not predictable and therefore, the release of the active molecule is also not predictable. The early period of the active agent release in these systems typically follows a first order release kinetics and is determined by simple diffusion. However, as the erosion of the polymer occurs, the release rate accelerates and is determined by a combination of diffusion and polymer erosion. One of the disadvantages of these systems is that the matrix can disintegrate before the active agent exhaustion resulting in a large burst release.

In a surface erosion process, the hydrolysis of a polymer is limited to the outer surface while the integrity of the carrier is maintained. Active agent release can be determined in these systems as it is a direct outcome of the erosion process. In addition,

these systems have the ability to deliver a constant active agent release as long as the geometry of the device remains unmodified. The type of erosion is dependent on the hydrophobicity and morphology of the polymer. While hydrophilic polymers typically undergo homogeneous erosion as they are completely permeated by water, heterogeneous erosion occurs commonly with hydrophobic polymers. Therefore, hydrophilic polymers are limited to molecules having low water solubility or macromolecules that can be physically entrapped to restrain diffusion. Heterogeneous erosion is more desirable due to the delivery of constant release rate; regardless of the chemical and physical properties of active agents (Robinson and Lee, 1987; Edlund and Albertsson, 2002; Heller, 1980). The amount of active agent released in heterogeneous erosion is given by:

$$M_t/M_\infty = 1 - [1 - k_o t/C_o r]^n$$

where M_t is the amount of active agent released at time t, M_∞ is the total amount of active agent that can be released, k_o is the erosion rate constant, C_o is the concentration of the active agent in the matrix, r is the radius of the spherical matrix and $n = 3$ for a spherical matrix (Pothakamury and Barbora-Canovas, 1995).

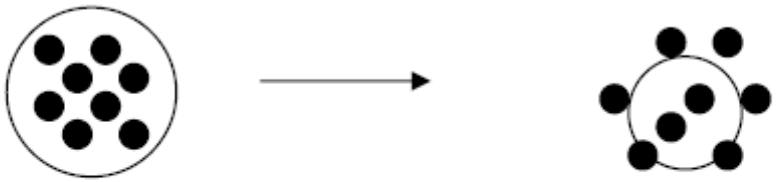

b) Erosion controlled

Figure 1-7: Erosion Controlled Matrix Systems (Baker, 1987)

Swelling or solvent-activated release

In these systems, polymer swelling occurs due to the absorption of water from external environment influencing the release kinetics of the active agent. Release mechanism from these systems is similar to diffusion controlled mechanisms, however, the membrane experiences a transition from a glassy to gel state due to the swelling of the encapsulant barrier resulting in increased release (Baker, 1987; Pothakamury and Barbora-Canovas, 1995). The swelling membrane consists of three zones: 1) a completely swollen region adjacent to the solvent surface; 2) a thin swelling zone where the polymer chains undergo hydration and relaxation; and 3) an unswollen completely dehydrated rigid polymer matrix (Baker, 1987).

The quantity of active agent M_t released at any time t is given by $M_t/M_\infty = k_a t^n$, where M_∞ is the initial active agent loading in the polymer and k_a and n are system parameters that depend on the nature of polymer-penetrant active agent interaction. Swelling leads to macromolecular relaxation of the polymers, which, in turn, influences the active agent diffusion through the polymer resulting in either case I (n = 0.5, Fickian), where the transport of molecules in the polymer matrix is dominated by the Fickian diffusion mechanism with negligible polymer relaxation, or case II (n >1.0), where the polymer relaxation primarily controls the movement of molecules with negligible diffusion of the molecules or non-Fickian (anomalous) diffusion, where both the diffusion process and polymer relaxation control the transport of molecules ($0.5 < n < 1.0$). The active agent release in these systems is primarily controlled by the velocity of the water penetration front as the agent diffusion through the glassy polymer is negligible (Washington, 1996). It is possible to achieve zero-order release in these systems by examining the swelling interface number $S_w = v\delta\ (t)/D_{ip}$, where v is the velocity of the water penetration front. For $S_w \leq 1$, zero-order release is achieved and for $S_w \geq 1$, Fickian diffusion is achieved (Pothakamury & Barbora-Canovas, 1995).

Rates of release

While the classification of encapsulated release systems in the previous section was based on the mechanisms of release, they can also be also categorized into three types based on their release kinetics: a) zero-order release; b) first-order release; and c) square-root -of-time release (Baker, 1987; Washington, 1996).

a) In zero-order release, the release rate remains constant until the active agent is exhausted. The release rate (dM_t/dt) from these systems is given as

$$dM_t/dt = k$$

where k is a constant, t is time, and M_t is the mass of the active agent released at time t.

b) In first-order release, the rate is proportional to the amount of active agent contained within the system.

$$dM_t/dt = kM_o \exp(-kt)$$

M_o is the mass of the active agent in the system at t =0. Therefore, in first order releases, the rate decreases exponentially with time.

c) The third common type of release is called square-root-of-time or $t^{-1/2}$ release. Here, the rate of compound release is linear with the reciprocal of square root of time.

$$dM_t/dt = k/\sqrt{t}$$

Figure 1-8 shows the pictorial illustration of the different release kinetics explained in the previous paragraph. Majority of controlled release applications require a constant release rate; however, in practice, release profiles are more complicated. Some of the effects that cause this deviation include: 1) burst release; and 2) time lag. The intensity of these two

effects can be estimated by the diffusion coefficient of the agent in the membrane and membrane thickness (Narasimhan et al., 1997; Huang and Brazel, 2002).

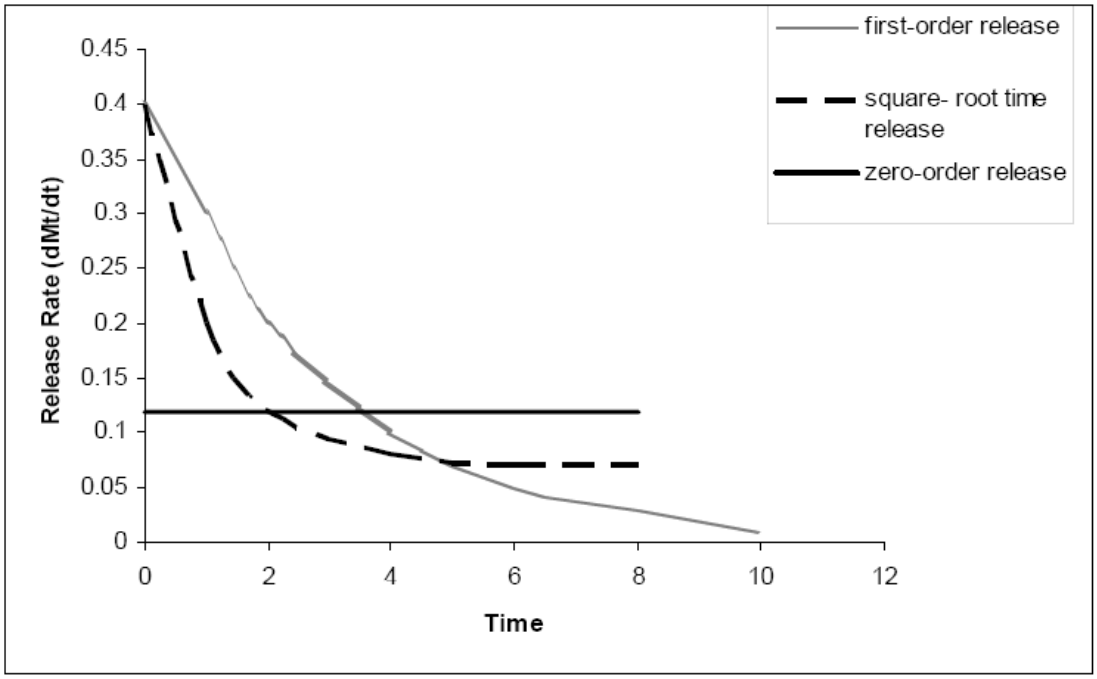

Figure 1-8: Zero-order, first-order, and $t^{-1/2}$ release patterns from devices containing the active agent content (Baker, 1987)

Factors affecting the release of flavors from food matrices

De Roos (2000) has pointed out that the two important factors that principally govern flavor release: 1.) relative volatility of a compound in a food matrix and air under equilibrium conditions (thermodynamic factor); and 2.) resistance to mass transport from product to air (kinetic factor). Therefore, in order to achieve controlled release of volatile flavor molecules in different consumer applications it is important to consider these factors. Volatility of a compound is commonly expressed as the proportion of the compound in the air and product phase under equilibrium conditions.

$$P_{ap} = C_a/C_p$$

P_{ap} is the air-product partition coefficient and C_a and C_p are the concentrations (g/L) of the volatile compound in air and product, respectively. Therefore, volatility plays an important role in flavor release only under equilibrium conditions. Alternatively, mass transport of a volatile compound from a sample base to air occurs only under non-equilibrium conditions. While the relative volatility of a flavor compound is altered as a result of its interactions with other food constituents (carbohydrates, proteins etc), mass transfer is primarily altered due to diffusion considerations. Reports indicate that the value of mass transfer coefficient can vary between 10^{-4} and 10^{-9} m/s. One approach to control the diffusion mechanism involves encapsulating the flavoring (Pothakamury and Barbosa-Canovas, 1995).

Flux from flavor containing phase to air/water interface is proportional to k_w A ΔC, where k_w is the mass transfer coefficient in the water phase, A is the interfacial area and ΔC is the concentration gradient between the matrix containing the flavor and the water/air interface. Flavor release/flux decreases with the increasing lipid level in the food matrix for hydrophobic compounds (Madene et al., 2006; Doom and Campanile, 2004). Specifically, studies conducted by Doom and Campanile (2004) indicated that the release of lipophilic flavor molecule limonene reduced with the addition of fat (2 %) into the system. The rationale explained was the physicochemical interaction occurring between the fat and lipophilic flavor molecule.

Studies conducted by De Roos (2000) on flavors loaded in vegetable oil showed reduced release of the volatile compounds compared to flavors loaded with no oil. Researchers have explained that the addition of oil increased the resistance to mass transfer and as a result enhanced the retention of flavors. However, alcohols were not retained as well as the other compounds. The rationale explained for this performance was the lower affinity of alcohols in oils. There are several instruments to measure release from encapsulated powders: 1) Proton Transfer Reaction -Mass Spectrometry

(PTR-MS); 2) Atmosphere Pressure Chemical Ionization - Mass Spectrometry (APCI-MS); 3) Purge and trap coupled with GC-MS *etc*. We have used the PTR-MS for our release measurements; therefore, there is a detailed description of the instrument below.

Proton Transfer Reaction – Mass Spectrometry

PTR-MS (Figure 1-9) is a chemical ionization technique used for the continual examination of concentration/time dynamics of volatile compounds present in complex mixtures. Some of the important advantages of the PTR-MS include:

1) It does not involve any kind of prior sample preparation or separation step
2) Quantification of volatile compounds possible for concentrations ranging from ppbv-ppmv without the use of internal standards
3) Acquisition of relatively simple spectra due to the limited fragmentation of compounds associated with the soft ionization technique

On the other hand, this unidimensional technique makes the identification of isobaric compounds (compounds that have similar masses) relatively laborious and drives us to rely on the gas chromatography-mass spectrometry for chemical identification. The main elements of the PTR-MS are the following 1) a hollow cathode discharge ionization source for the production of hydronium (H_3O^+) ions at high concentrations (up to 99 %); 2) a drift tube, where samples introduced undergo non-dissociative proton transfer with H_3O^+ ions transmitted from the ionization source into the drift tube (pressure 2.2 mbar) through a venturi-type inlet; and 3) an analyzing system consisting of a quadrupole mass spectrometer along with a signal amplifier.

The primary reaction involves the transfer of protons (H^+) from protonated water (H_3O^+) species, which in turn is produced at high intensity and purity in a hollow cathode ionization source. The reaction is capable of occurring only with volatile compounds that have proton affinities higher than that of water (165.4 kcal/mol). Most of

the volatile compounds have greater proton affinities than water which facilitates the proton transfer reaction and thereby the monitoring of ions. Further, the primary ion does not react with the natural components of air such as CO_2, N_2, O_2, due to the lower proton affinities. Volatile compounds in the gaseous phase are channeled through a heated inlet capillary line directly into the drift tube of the PTR-MS at a flow rate of approximately 18-20 ml/min. The H_3O^+ ions produced in the ionization source reacts with the volatile compounds in the reaction chamber to form the protonated form of the organic species.

The fundamental reaction is as follows

$$R + H_3O^+ \xrightarrow[k]{} RH^+ + H_2O$$

R is the reactive volatile compound and k is the reaction rate constant. The reaction rate constant of most volatile organics is equal to the respective gas kinetic collision frequencies. Followed by the generation of the product ions (RH^+), they travel through the drift tube to be monitored by the downstream quadrupole mass spectrometer. It is interesting to note that only a fraction of the primary ions react with the R species and therefore the density of the product ions is given by:

$$[RH^+] = [H_3O^+]_0 (1 - e^{-k[R]t}) \approx [H_3O^+]_0 [R]\, kt$$

k is the reaction rate constant (2×10^9 cm^3/sec) for proton transfer from H_3O^+ to R, and t is the transit time (105×10^{-6} sec) of H_3O^+ in the drift tube. The ratio of the product ion to the precursor ion is used to determine the concentration of VOC (Lindinger et al., 1998; Hansel et al., 1995)

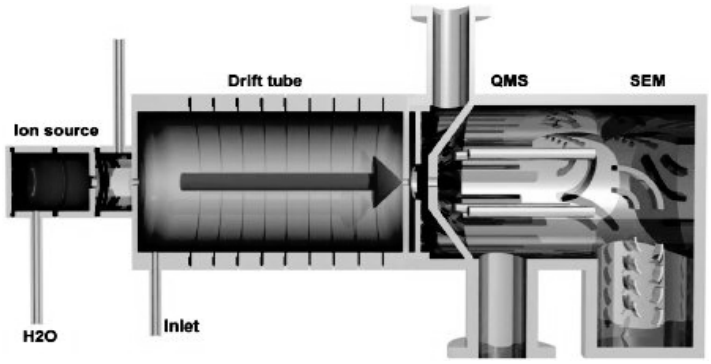

Figure 1-9: Proton Transfer Reaction-Mass Spectrometer (Lindinger et al., 1998)

Chapter 2 : Preliminary Experiments/Encapsulation of orange oil in silica sol-gel matrices with gelation (Part I)

Introduction

Alkoxysilanes ($Si-(OR)_4$, where R is an alkyl group) such as TEOS (tetraethylorthosilicate) and TMOS (tetramethylorthosilicate) are commonly used for the synthesis of silica gels and precipitates used in encapsulation (Pierre, 2004). Matrices generated from only alkoxysilanes are termed as simple silica matrices. A number of studies have demonstrated the suitability of simple silica matrices for the encapsulation of hydrophilic molecules which can associate either chemically or physically with the hydrophilic silica surface (Veith, 2004; Bolton and Reineccius, 1992; Bhatia et al., 1998; Barbe et al., 2004). In fact, a recent study conducted in the year 2008 showed that mesoporous silica spheres could be used to achieve prolonged release of a hydrophilic perfume (Wang et al., 2008). Studies conducted by Veith et al. (2004) showed that simple silicate matrices selectively retained hydrophilic flavor compounds. The author's results further demonstrated that the hydrophobic molecules such as limonene and myrcene, major compounds of essential oils were retained poorly in matrices generated from TEOS (Veith, 2004; Bolton and Reineccius, 1992). The selective retention of compounds can lead to alteration in the flavor profile of the product. In order to overcome this problem, alkyl modified silicate particles have generated intense interest in a wide range of application fields in recent years (Park and Komarneni, 1998).

Sol–gel processing enables the preparation of several types of alkyl modified materials with controlled pore size and size distribution, which are otherwise difficult to be synthesized. Although presently these types of alkyl modifications on silica have been approved only for the aromatization of packaging materials and as a food additive in pet foods, it was considered of value to study the incorporation of alkyl groups

in these matrices for the encapsulation of hydrophobic flavor compounds. The objective of this study was to evaluate the suitability of self assembling simple matrices (generated from only TEOS) and alkyl modified silica matrices (generated from both TEOS and alkyl-TEOS) for the encapsulation of hydrophobic molecule orange oil. The evaluation was performed by determining the retention of limonene (a hydrophobic compound present in orange oil) after drying and measuring the release of this compound in acetone-water system over a period of time (1- 24 h).

Materials and Methods

Materials

Octyltriethoxysilane (octyl-TEOS) and TEOS were obtained from Sigma-Aldrich Chemical Co., (St. Louis, Mo.). Orange oil was received from Robertet Flavors (Piscataway, NJ). Capsul^{TM} (a modified starch (starch octenyl succinate) was obtained from National Starch and Chemical Corp., Bridgewater, NJ).

Preparation of silica sol-gels

A sol-gel formulation that exhibited the smallest porosity by nitrogen adsorption isotherms was obtained from a paper published on sol-gels by Veith et al. (2004) for our preliminary experiments. The TEOS used in the formulation was substituted with different molar ratios of octyl-TEOS for our studies. Figure 2-1 provides a pictorial illustration of the sol-gel process and Table 2-1 shows the formulations used for the process.

Step 1: Mixing of the components

Alkoxide precursors (TEOS and octyl-TEOS), ethanol, water were mixed at room temperature in accordance with the molar ratios given in Table 2-1. As water and alkoxysilanes are immiscible, ethanol was used as a solubilizing agent (Brinker and Scherer, 1990). The acidic hydrolysis of alkoxysilanes results in the formation of silanols

[Si-$(OR)_4$]. Hydrolysis was initiated in the resulting solution by decreasing the pH to 2-3 using 0.06 M HCl (the isoelectric point of silica is approximately 2). Stirring was continued for 24 h at room temperature.

Step 2: Addition of the flavor

Following hydrolysis, the pH of the sol was increased to approximately 6 with 0.09 M NaOH. This increase in pH initiates the condensation reactions to yield a polymeric network of Si-O-Si (siloxane) (Hench and West, 1990). An emulsion of orange oil (5 g) prepared using 10 % Capsul^{TM} (starch octenyl succinate) was added to the sol and mixed well. Therefore, the flavor molecules get embedded in the polymeric network structure. The subsequent aging process facilitates an increase in the degree of cross-linking which will influence porosity (Dunn et al., 1998).

Step 3: Gelation

The resulting sol was subsequently neutralized (pH ~7) using NaOH. The increase in pH initiated the condensation of the silica species transforming the sol to a solid gel. The physical characteristics of the gel depend on the size of the particles and the extent of cross-linking.

Step 4: Aging

The gel obtained was aged for about 24 h. The reason for the aging was to increase the strength of the gel as the polycondensation continues during this process.

Step 5: Drying

Drying was carried out to remove the solvent from the interconnected pore network. Cracking of the gel was observed during drying. The gel was dried in a vacuum oven (Napco Model 5851) at 40°C and pressure of 10.8 psi (pounds/square inch) for 8 h.

Step 6: Size Reduction

The dried gel was ground in a Retch Brinkmann ZM -1 mill (250 μm screen) to obtain a free flowing powder.

Characterization of the silica powder

Particle sizing

Particle sizes and specific surface areas of the silica powders were measured using Laser diffractometry (Malvern laser diffraction apparatus, Malvern, England). The samples were dispersed in water for 5 sec by ultrasound before measurement to ensure homogeneous dispersion. A 300 mm lens was used in the measurements. The obscuration maintained was ca. 0.21. At least three measurements were recorded for each sample.

Moisture Content of the powders

The moisture content of the powders was determined using the Karl Fisher method. Sample (0.5g) was equilibrated in 2 g of dry methanol for 12 h. One µl of the methanol was injected into the Karl Fischer apparatus to determine the moisture content. This was done in duplicate.

Flavor load and release determination by gas chromatography

Sample of the powder (0.5 g) was dispersed in 4 ml of water. Then 20 ml of acetone containing 0.006 g/ml 2-octanoane (internal standard) was added slowly with agitation. The sample was allowed to soak in the acetone-water system for 24 h and the release of limonene was analyzed by GC at different time intervals by injecting 1 µl aliquot of the liquid phase into a gas chromatograph (Hewlett Packard HP 5890, Hewlett Packard) under the following conditions. A DB-5 column (30m X 0.25 mm X 1 µm) was used to determine the release of limonene (orange oil) from the sol-gels (Buffo and Reineccius, 1999). This was done in duplicate.

Column: HP-5 (Crosslinked 5 % Ph Me Silicone)
Carrier Gas: Helium
Column Head Pressure: 15 psi
Split-Ratio: 1/30

Oven Temperature Profile

Initial Temperature: 50°C

Initial Time - 0 min

Program Rate - 10 °C/min

Final Temperature - 190°C

Final time: 2 min

Detector: FID (flame ionization detector)

Results and Discussion

From Table 2-2, it can be seen that the moisture content of the powders was high (> 5 %), which shows that the drying was not carried out adequately. Figure 2-2 provides the different release profiles of limonene in an acetone-water system over a period of 24 h. The different "release" profiles for these sol-gels are likely due to the presence of octyl-TEOS, as it was the only parameter that was varied in these formulations. We have to note that we did not determine the amount of flavoring in the gels once dried. Thus, when we consider the data in Table 2-3, the difference in total release (15 – 55 %) may simply reflect the amount of flavoring remaining in the product after drying. For example, if Sol C only had 15 % of the original amount of flavoring remaining after drying, then the 15 % lost (as calculated) would really be 100 % release.

Gel C (no octyl-TEOS) had the smallest amount of flavoring after drying and it was quickly released. Gel A had a small amount of octyl-TEOS and retained nearly 3X as much flavoring as the gel without octyl-TEOS. The rate of loss was also very rapid. Gel B had the largest amount of octyl-TEOS and showed the greatest retention of flavoring and slowest release. It would appear that the addition of octyl-TEOS is desirable in improving retention in the gel and slowing release from the gel. A caveat is that the retention of flavoring also paralleled the final moisture content (Table 2-2). Different extents of drying may have been responsible for the different flavor retentions

in the gels. While the addition of octyl-TEOS appears to be desirable, we would have to repeat this experiment, determining both the amount of flavoring after drying and insuring that the drying was carried out equally across samples. We did not choose to do this because this work really did not follow our project objectives of wanting to form precipitates as opposed to forming a gel and grinding the material as we have done here.

There is a rationale for expecting the gels containing octyl-TEOS to retain flavoring better than the simple TEOS-based gels. The reason for such poor encapsulation in simple sol-gels might be due to the lack of interactions between the silanols and the non-polar compounds such as limonene. This hypothesis is supported by our observation (caveat aside) that the retention of limonene increased with the addition of alkyltriethoxysilane perhaps because of the hydrophobic interactions between the octyl chain and limonene. Studies carried out by Veith et al. (2004) showed that the amount of limonene encapsulated in simple silica sol-gels was nearly zero. In addition, studies conducted by Bolton and Reineccius (1992) also reported that the less polar compounds such as limonene were not retained well on amorphous silica carriers.

Summary

Though the association between the processing variables (stirring time, amount of TEOS, H_2O and ethanol etc) and particle characteristics (particle size, pore size, pore size distribution etc) are obvious, due to insufficient data we could not establish a correlation between them. In addition, more studies would be required to evaluate the amount of alkyl-TEOS incorporated in the sol-gels and thereby, its effect on the retention of hydrophobic flavors using the process developed by Veith et al. (2004). But as mentioned above, this process did not meet our research objectives and was abandoned.

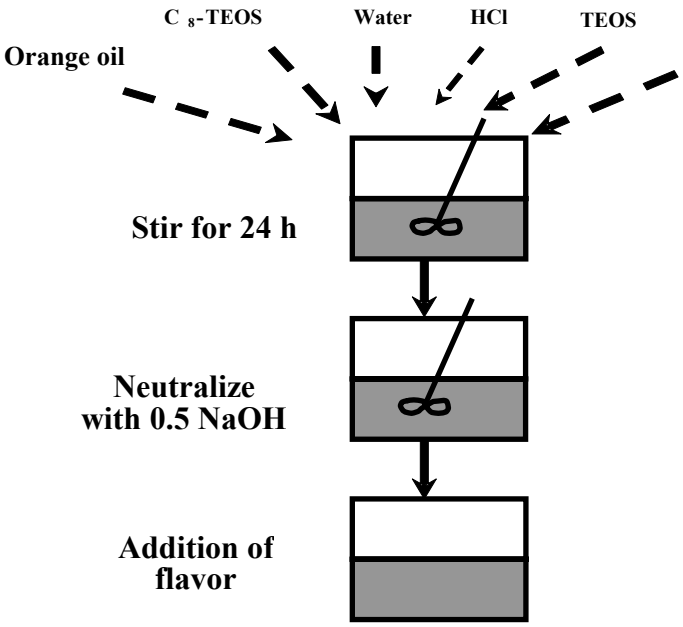

Figure 2-1: Steps involved in the sol-gel polymerization reactions

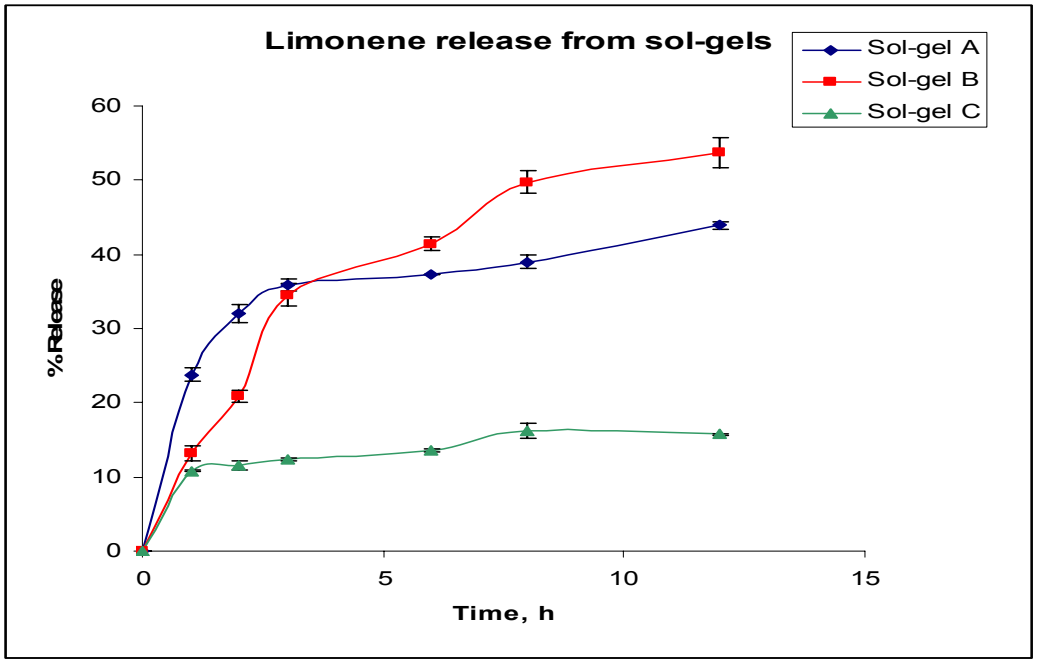

Figure 2-2: "Release" of limonene from various sol-gels

(% release was calculated assuming 100 % limonene encapsulation; each value is the average of 2 duplicate readings)

Table 2-1: Formulations of the different sol-gels generated

Formulations	**Sol A ***	**Sol B***	**Sol C***	**Sol D**
TEOS , mol %	8.3	7.25	8.7	8.7
C_8-TEOS, mol %	0.4	1.45	0	0
C_8-TEOS/ TEOS	0.05	0.2	0	0
Ethanol, mol %	47.4	47.4	47.4	47.4
H_2O, mol %	43.9	43.9	43.9	43.9
H_2O/TEOS	5.1	5.1	5.1	5.1

* Sol A, Sol B and Sol C contain 5 % flavor (orange oil emulsion) incorporated into sol-gels

* Sol D did not contain any flavor

Table 2-2: Characteristics of the different sol-gels generated

	Sol A	**Sol B**	**Sol C**	**Sol D**
Moisture Content (%)	14.6 ± 0.21	15.0 ± 0.14	11.3 ± 0.35	21.7 ± 0.28
Particle size, µm	146.2 ± 2.3	168.2 ± 1.2	166.9 ± 1.4	126.8 ± 1.8
Specific Surface Area (m^2/cc)	0.19 ± 0.0	0.20 ± 0.01	0.21 ± 0.04	0.52 ± 0.02

* Values are the average of at least duplicate determinations

Chapter 3 : Preliminary Experiments/Encapsulation of orange oil in silica sol-gel matrices without gelation (Part 2)

Introduction

Microemulsion systems (oil in water) have been used as precursors for the synthesis of silica nanocapsules in several studies. Alkoxysilanes are commonly used for the generation of silica capsules used for encapsulation. These systems have been extensively employed to study the controlled release in drugs (Chavez et al., 2005; Underhill et al., 2002; Jovanoic et al., 2005).

Oil in water (o/w) microemulsion is created by mixing oil along with two surfactants, Tween 80 (poly (oxyethylene)-sorbitane monooleate) and octyltriethoxysilane (C_8-TEOS) in aqueous solution. The acidic hydrolysis of C_8-TEOS results in the formation of a thin silicate layer on the surface of the droplets and also provides Si-OH groups for further cross-linking at the surface. Studies have reported that the hydrolysis of TEOS (tetraethylorthosilicate) occurs at a faster rate than C_8-TEOS (Underhill et al., 2002). Therefore, TEOS is added at the subsequent stage, where it undergoes hydrolysis under acidic pH conditions resulting in the formation of tetrahydroxysilane. For the formation of the shell around droplets, sol-gel polymerization reactions are initiated by increasing the pH of the sol to approximately 7. These reactions chemically connect the hydroxyl groups of C_8-TEOS and TEOS generated during hydrolysis to form a polysiloxane/silicate shell around the oil droplets. The silicate shell created stabilizes the oil droplets that are encapsulated. Transmission electron microscopy (TEM) and light scattering techniques are performed to examine the size and the shape of the synthesized capsules (Jovanoic et al., 2005).

In Chapter 2, we prepared silica gels using the sol-gel process; however the grinding of gels resulted in huge losses. Therefore, the objectives of this work were: 1) to encapsulate orange oil using silica nanocapsules generated through the sol-gel polymerization reaction; and 2) to modify of the same protocol to synthesize precipitates that do not require grinding.

Materials and Methods

Materials

Tween 80, octyltriethoxysilane (octyl-TEOS) and TEOS were purchased from Sigma-Aldrich Chemical Co., (St. Louis, Mo.). Orange oil was received from Robertet Flavors (Piscataway, NJ). Brominated vegetable oil (BVO) was also purchased from Sigma-Aldrich Chemical Co., (St. Louis, Mo.)

Synthesis of nanocapsules

The protocol for the synthesis of nanocapsules was acquired from the literature (Jovanoic et al., 2005). Microemulsions were prepared by dissolving Tween 80 (1.5 g) in 14 ml water. Orange oil (0.05 g) was added and the mixture was stirred with heating at 60 °C for 1.5 h. The mixture was cooled to room temperature and C_8-TEOS was added. The emulsion was again heated along with stirring at 60°C for 45 min to promote mixing of the two surfactants and the flavor oil. Once a homogenous emulsion was obtained, the pH was adjusted between 2.8-3.0 using 0.5 M HCl and the stirring was continued for an hour. The pH of the resulting emulsion was increased to 7 using 0.5 M NaOH. In the final step TEOS (0.05 g) was added and the mixture was stirred overnight at room temperature, after which dialysis was carried out. The product was prepared in duplicate.

Dialysis

Following the sol-gel polymerization, dialysis was performed using Spectra/Por molecular porous cellulose tubing with a molecular weight cut off of 10,000 Da to remove the unreacted ethoxy groups of the TEOS. Otherwise, TEOS continues to react under neutral conditions and eventually form a gel, which is undesirable for our system (Chavez et al., 2005; Jovanoic et al., 2005). The product obtained through the sol-gel polymerization reaction was transferred into the tubing immersed in 500 ml water. The dialysis was carried out for approximately 12 h as mentioned in the literature. The dialyzed product containing the nanocapsules was observed using TEM.

Synthesis of precipitates

The above mentioned protocol was modified to generate precipitates. Emulsion was prepared by dissolving 5 g of the mixture of orange oil (43.3 %) and BVO (56.6 %) along with 0.5 g of Tween 80 in 100 ml of water and stirring it at 60°C for 30 min (orange oil and BVO were added according to Pearson's square. To the best of my knowledge, there has not been any literature published on the criteria that determine the amount of alkyltriethoxysilane to be added to a system. However, the concentration of C_8-TEOS cannot be increased beyond a certain extent due to its insolubility in water in addition to its slow rate of hydrolysis (Chavez et al., 2005). From these initial experiments, it was expected that we would be able to determine the concentration range suitable for our system. Therefore, for our preliminary experiments, C_8-TEOS was added in small quantities on a trial and error basis. Approximately, 1.5 g of C_8-TEOS was added and stirred for 30 min at 60 °C to dissolve it. Once a homogeneous mixture was obtained, the pH was adjusted to approximately 2.8-3 using 0.5 M HCl. The acidic hydrolysis was carried out at room temperature for 48 h. The particle size of the product was measured at this stage using a Malvern Laser Diffraction Particle Sizer. Following this, TEOS (1- 6 g) was added to the emulsion and allowed to hydrolyze at room temperature for 24 h. Increasing the amount of TEOS beyond 6 % of the amount of water resulted in the formation of gels, which was undesirable for our encapsulation process. Subsequently,

the pH was increased to approximately 7 using 0.5 M NaOH and again stirred at room temperature between (1-24 h) to initiate the polymerization reaction. Particle size measurements were made at various time intervals (e.g. 1 h, 3 h. ….24 h) to observe the change in particle size during polymerization. The resultant precipitates were observed using TEM to confirm the particle sizes acquired from the light scattering methods. This experiment was conducted in duplicate.

Characterization of the nanocapsules and precipitates

TEM of the nanocapsules and precipitates

The contrast between the oil core and the silicate matrix is commonly obtained by adding a small quantity of dodecene to the oil to be encapsulated (a highly unsaturated compound that reacts with osmium tetra oxide (OsO_4) and imparts a darker electron density to the oil). The double bond present in limonene (a major compound present in orange oil) enables the oil phase of the capsules to be stained with of OsO_4 (Electron Microscopy Sciences), which can react with OsO_4 to produce similar effects as dodecene. A droplet of the emulsion was placed drop wise on a carbon–coated nickel grid and left for 4 h for the water to evaporate. The dried grid was placed in a sealed container where OsO_4 vapor diffused through the polysiloxane/silicate to stain the limonene present in the core of the nanocapsules. The grids were stained for around 30 min and the TEM images were obtained using a Philips CM12 microscope at 75 kV. In order to confirm the staining results obtained by limonene, dodecene was used as the core material in one of samples.

Particle size analysis of the precipitates

Particle size was measured by using laser diffractometry using Malvern laser diffraction apparatus (Malvern, England). The samples were dispersed in water for 5 sec by ultrasound before measurement to ensure homogeneous dispersion. A 300 mm lens was

used in the measurements. The obscuration maintained was ca. 0.21. Final sizes were obtained from the average of three reproducible results.

Statistical analysis

Analysis of variance (ANOVA) was carried out on particle sizes of precipitates obtained from different amounts of TEOS (1, 3 and 5 g) and times of polymerization (0, 1, 3, 12, 16 and 24 h) utilizing R statistical software (2008). When a factor effect or an interaction was found significant, indicated by a significant F test ($P \leq 0.05$), differences between the respective means (if more than 2 means) were determined using Least Significant Difference test

TEM-EDAX (Transmission electron microscopy-Energy Dispersive X-ray spectrum)

Elemental (qualitative) composition of the entire nanocapsule and the core of the nanocapsule were determined using TEM-EDAX. The purpose of this analysis was to confirm that orange oil is encapsulated within the silica matrix.

Instrumental techniques for the monitoring the sol-gel reaction

In spite of the literature providing us information about the kinetics of the hydrolysis and polymerization reactions of alkoxysilanes, it was required to verify if these reactions were occurring. In addition, these studies facilitate the understanding of reaction kinetics of alkoxysilanes specific for our system and therefore, provide better control over the reaction. ^{29}Si-NMR and ^{1}H-NMR spectra were acquired independently for C_8-TEOS and TEOS and for the reaction mixture using different solvents ($CHCl_3$, D_2O, H_2O) on a Varian NMR-Inova 500 spectrometer (Varian, Palo Alto, CA) according to a protocol available in the literature (Rodriguez and Colon, 2001).

Results and Discussion

Analysis of variance revealed that the interaction between the concentration of alkoxysilane and time of polymerization contributed to significant differences in the particle size of the final products. From Figure 3-1 and results tabulated in Table 3-1, it can be seen that the particle size of the system increased with the increase in the time of polymerization (1-24 h). Further, it can be observed that 1 g of TEOS was insufficient to induce a noticeable change in the particle size, however, by adding 3 or 5 g of TEOS significant increases in particle sizes were achieved at the end of polymerization reaction. This result was corroborated by the findings of one other researcher who illustrated that increasing the amount of TEOS resulted in bigger particles (Jovanoic et al., 2005). The particle size measurements for these samples varied over a wide range indicating that the product generated was not homogeneous.

Figures 3-3 and 3-4 provide the TEM pictures of the nanocapsules and precipitates, respectively. It can be seen that the use of osmium tetra oxide visually differentiated the orange oil (darker) core and the silicate (lighter) shell. Though the nanocapsules exhibited a definite shell, it can be observed that the precipitates did not have a distinct shell. Therefore, measuring the thickness of the silicate matrix was not feasible. For the synthesis of nanocapsules, the pH of the sol was increased to approximately 7 prior to the addition of TEOS. Studies have reported that the rate of hydrolysis and polymerization of TEOS is slow at neutral pH enhancing the formation of spherical silicate shells in addition to offering better control over thickness of the silicate shell (Chavez et al., 2005; Underhill et al., 2002). However, for the synthesis of precipitates, the hydrolysis of TEOS was carried out at acidic pH. The reason for the modification of protocol was due to the higher concentration of TEOS used in the generation of precipitates. Reports have indicated that the acidic pH induced a faster hydrolysis facilitating a rapid formation of silicate matrix (Jovanoic et al., 2005).

The surface crosslinking of the hydroxyl groups between TEOS and alkyl-TEOS should ideally prevent the coalescence of the oil cores. However, the results from TEM (Figure 3-4d) showed that there was coalescence in the emulsion. These may have been due to the following reasons: 1) higher concentration of flavor oil compared to TEOS; 2) inadequate stirring time resulting in phase separation of emulsion; and 3) incomplete hydrolysis and polymerization reactions. One other reason might have been due to the fact that octyltriethoxysilane, a lipophilic surfactant, requires extensive stirring to get dissolved in water and thereby hydrolyzed. Reports have indicated that the rate of hydrolysis of some alkylalkoxysilanes is slow due to the steric hindrance caused by the long chain alkyl group (Rodriguez and Colon, 1999). Therefore, we have increased the stirring time and reduced the concentration of alkyl-TEOS in our subsequent experiments for the delivery of a homogeneous mixture.

In addition, there were also differences in particle sizes of the precipitates determined by laser diffraction and TEM. TEM showed particle sizes much smaller than the light scattering measurements. This might have been due to the insensitivity of the Malvern Particle Sizer to account for smaller particles during the analysis. However, the presence of smaller particles such as Tween 80 micelles, dust particles etc cannot be ignored.

Figure 3-5 shows the elemental composition (TEM-EDAX) for the entire capsule, while Figure 3-6 shows only for the oil core. It can be observed from Figure 3-5 that the composition of all the elements (silicon, bromine and osmium) was almost similar for the entire silica matrix, whereas, the oil core showed higher bromine (presence of BVO in the oil core). This illustrated that the oil was at the center within the silicate shell.

The challenges encountered while performing NMR were the following:
1) Due to the low natural abundance of the NMR-active ^{29}Si isotope, high concentration of the silica is required to receive response. However, the concentration of silica present

in our system was low. For e.g. the concentration in our system ranged between 0.03 M – 0.30 M, while approximately 1-2 M is required to receive a valid and prompt response (Rodriguez and Colon, 2001). Further, if the concentration of silica was increased more than the above mentioned range, gelation occurred, which was undesirable for our system. Therefore, we could not monitor the progress of the reaction using ^{29}Si-NMR. Though alkoxysilanes became soluble as the reaction proceeded as a result of the low pH, the initial reaction mixture had phase separation. Due to the insolubility of alkoxysilanes in water, ethanol is commonly used as a solvent to dissolve them in aqueous systems. However, ethanol was not incorporated in our reaction mixture. Consequently, the data obtained was very complex due to the aggregation. 3) ^{1}H-NMR was also attempted, however, there were too many interferences from the other components (Tween 80, water & HCl) present in the system in addition to aggregation occurring in the tubes. In spite of using deuterium oxide to inhibit the water peak, the resolution obtained was poor

Summary

From these preliminary experiments, we explored the various factors influencing the sol-gel polymerization reactions and the techniques that facilitated the understanding of these reactions. Though NMR techniques were not successful in monitoring the sol-gel reactions, experiments have showed the applicability of a colorimetric technique for our reaction system. From the statistical analysis, an association was observed between the particle size of the system and concentration of TEOS. However, the influence of other parameters such as the concentration of alkyl-TEOS and hydrolysis times of the sol-gel reaction was not taken into consideration in these preliminary experiments. Therefore, a response surface model that accounted for all these factors was designed to gain a complete understanding these reactions. In addition, these results did not indicate if adequate encapsulation efficiency was offered by the sol-gel polymerization reaction process. Our subsequent studies measured this value by quantifying the % unencapsulated limonene from silicate matrices in a solvent. One of

the most important concerns was the solubility of alkoxysilanes in aqueous system. In order to overcome this, TEOS was replaced with tetrakis (2–hydroxyethyl) orthosilicate (THEOS) for the subsequent studies as a result of its complete solubility in water. Reports indicate that tetraalkoxysilanes can be successfully exchanged for THEOS. Further, the concentration of octyl-TEOS was decreased in our future studies to facilitate the delivery of homogeneous dispersions.

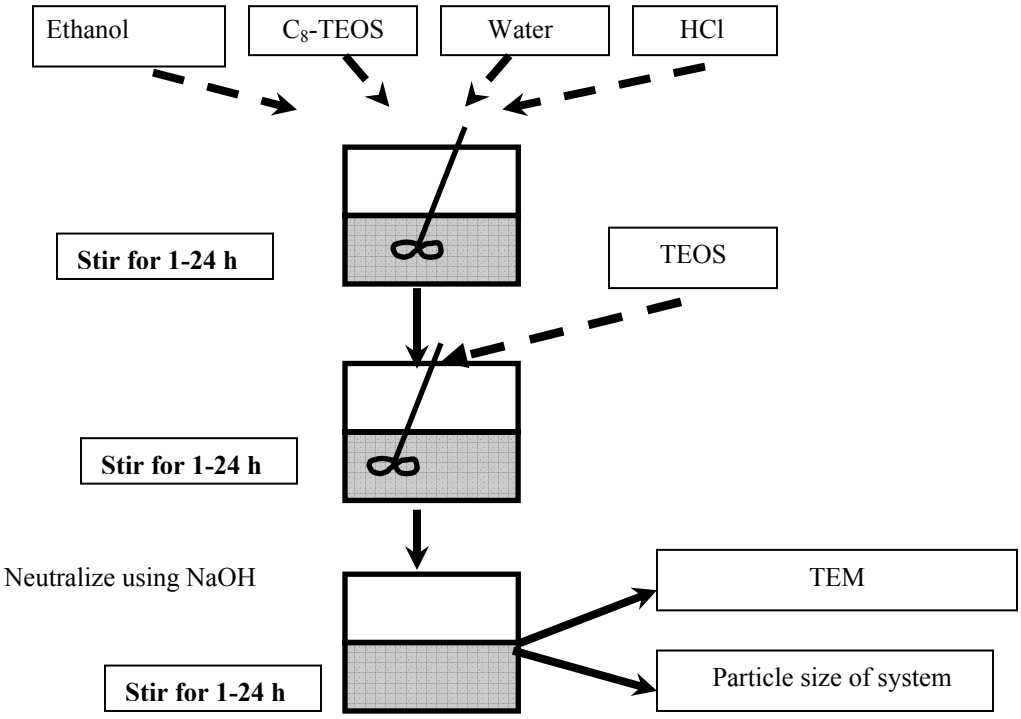

Figure 3-1: Steps involved in sol-gel polymerization reaction

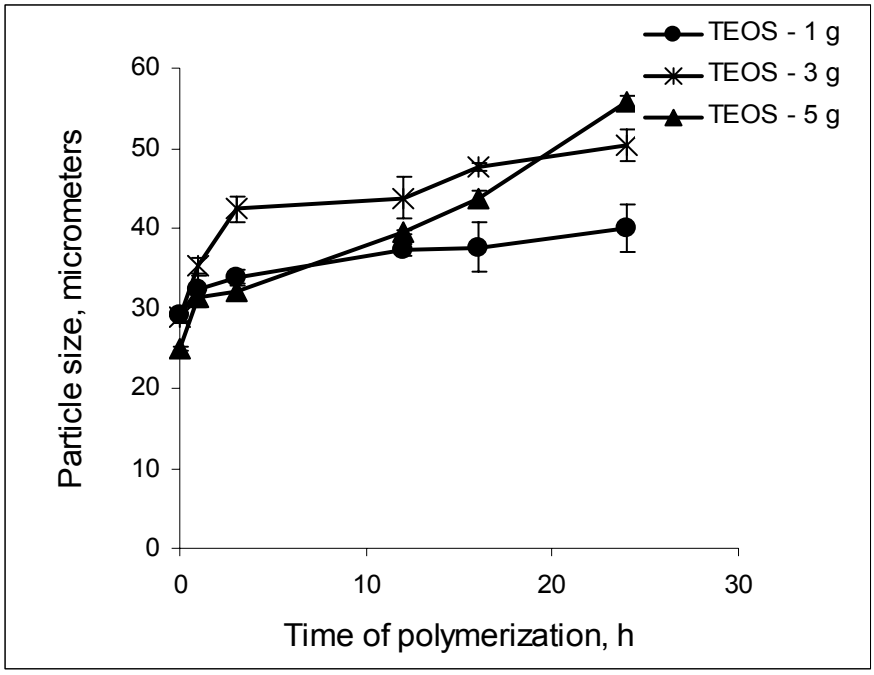

Figure 3-2: Particle size of the sol with increase in polymerization time

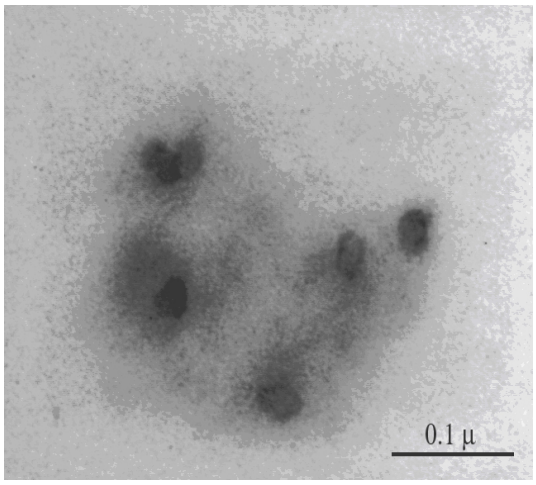

Sample 1a

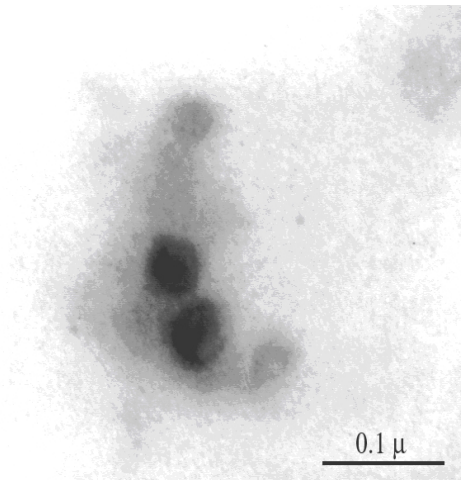

Sample 2a

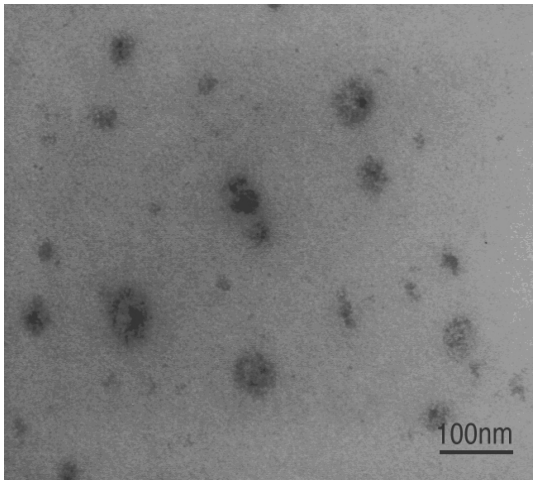

Sample 1b

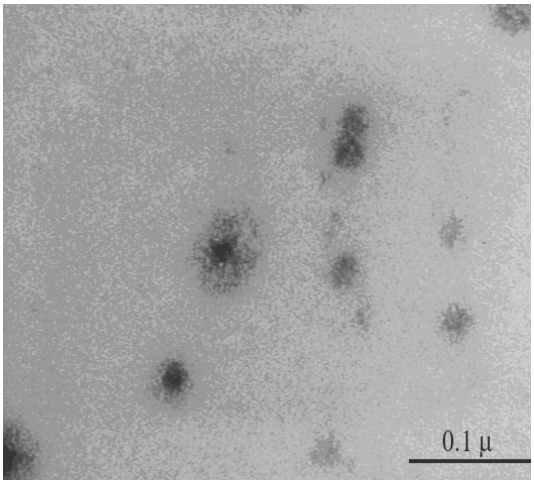

Sample 2b

Figure 3-3: TEM images of the nanocapsules (samples 1 and 2 are replicates), with dark areas representing the cores (orange oil) stained with OsO_4 surrounded by a lighter, unstained silicate shell.

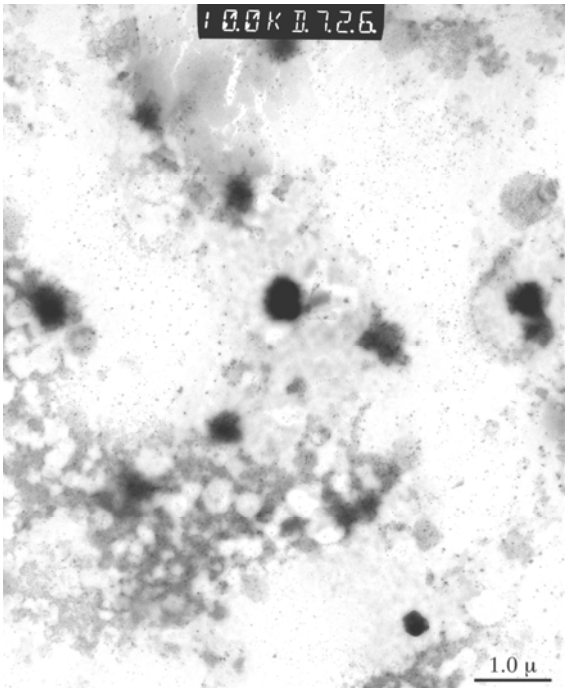

a) Orange oil and silica

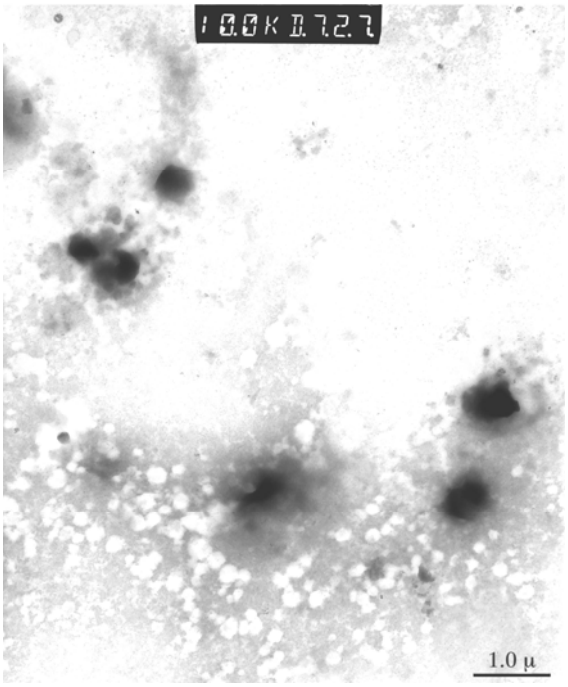

b) Orange oil and silica shell

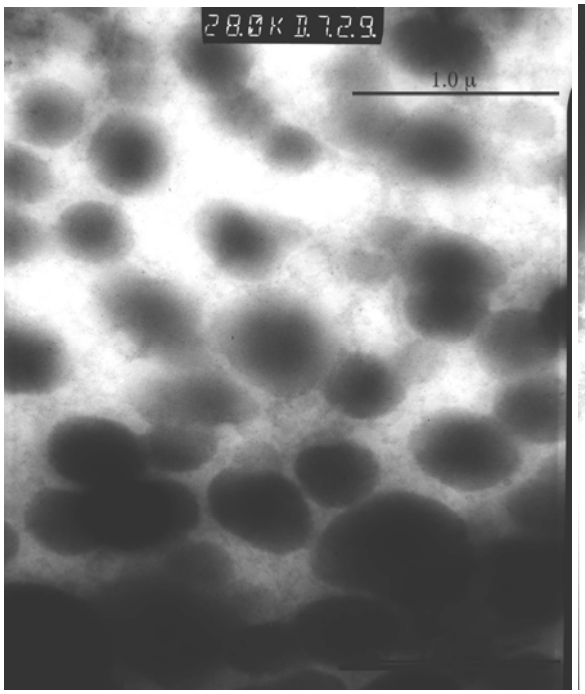

c) Dodecene and silica shell

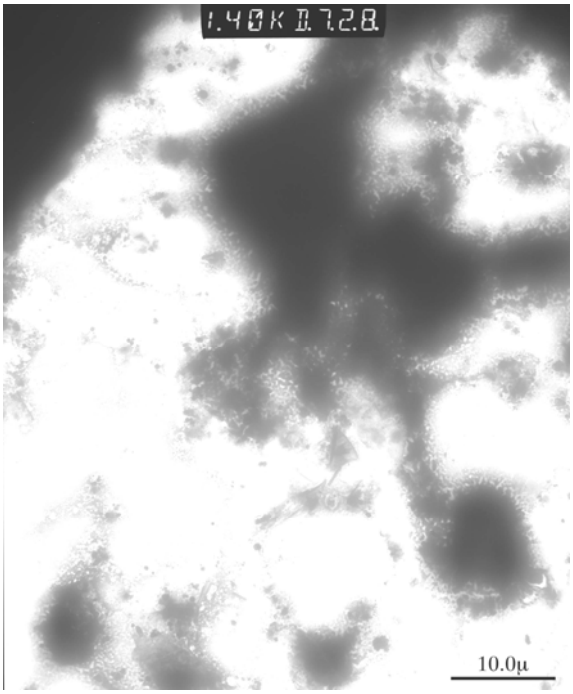

d) Orange oil Coalescence

Figure 3-4: TEM images of precipitates obtained using sol-gel polymerization with dark areas representing the cores (orange oil) stained with OsO_4 surrounded by a lighter, unstained silicate shell.

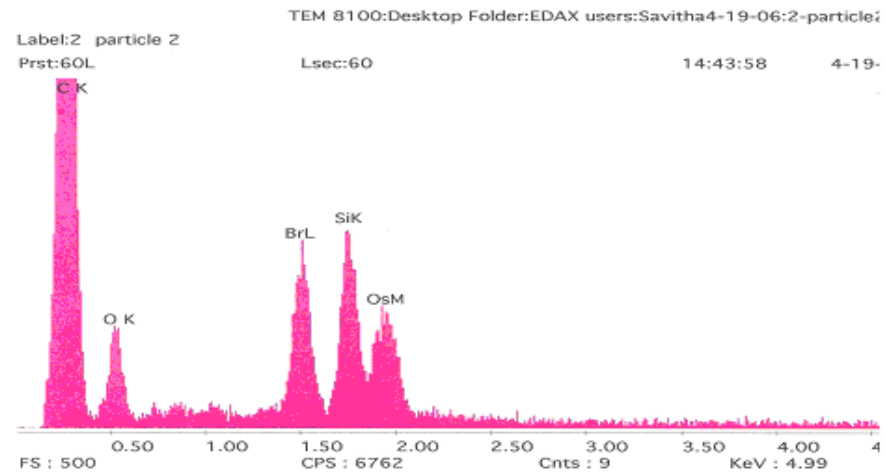

Figure 3-5: EDAX of the core-shell nanocapsule contains similar composition (peaks have similar heights) for all the elements

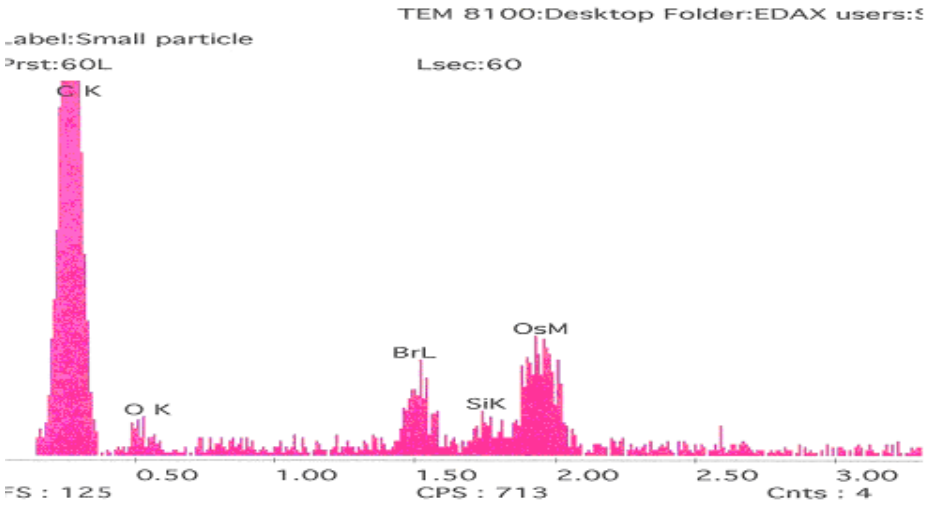

Figure 3-6: EDAX of the core nanocapsule (it contains more Br and OsM than Si)

Chapter 4 : The evaluation of silica based self-assembling matrices for orange oil encapsulation (Study 1)

Abstract

Several studies have reported that the hydrophilic environment provided by silica matrices synthesized by the sol-gel process using simple alkoxysilanes has not been favorable for the encapsulation of hydrophobic molecules resulting in their losses. To address this problem, we introduced hydrophobicity into the silica matrix in the form of long chain alkyl groups. This was accomplished by the combined hydrolysis and polymerization of an alkylalkoxysilane and a simple alkoxysilane. The matrices so generated have been used to study the encapsulation of orange oil. The objectives of this study were to formulate a protocol for the synthesis of alkyl modified silica matrices, determine the parameters of the reaction which exert an influence on the sol-gel process by observing the particle size of the system and % unencapsulated limonene. Our results revealed that all the reaction parameters identified (conc. and hydrolysis time of alkyl alkoxysilane, conc. and hydrolysis time of alkoxysilane, time of polymerization) were significant for the estimation of our observables; no correlation was observed between the particle size and % unencapsulated limonene. Results also showed that increasing the concentration of the simple alkoxysilane decreased the % unencapsulated limonene indicating the formation of compact matrices; on the other hand, increasing the concentration of the alkylalkoxysilane in the system increased the % unencapsulated limonene.

Keywords: silica matrices, sol-gels, limonene, release, entrapment, adsorption

Introduction

Silica host matrices formed by the sol-gel process have been used to encapsulate biomolecules such as enzymes, drugs, proteins, nutraceuticals, flavors and fragrances (Reetz et al., 1996; Kortesuo et al., 2000; Pierre, 2004; Dave et al., 1997; Gill and Ballesteros, 1998; Carturan et al., 1997; Veith et al., 2004). In the United States, amorphous silicas have GRAS status and are approved for use as flavor carriers; however, use cannot exceed 2 % by weight in a final food (21CFR 172.230 and 21CFR 172.480). Some of the advantages of silica include its chemical inertness, high specific surface areas, biocompatibility and resistance to microbial attack (Iler, 1979; Hench and West, 1998). Further, the process is conducted at room temperature therefore; it is conducive for encapsulating molecules with poor thermal stability. These molecules become entrapped in the growing covalent gel network during the sol-gel reaction process rather than being chemically bound to the inorganic matrix. In spite of all the potential advantages associated with the sol-gel method, characteristics of the matrices obtained by this process are very sensitive to the experimental conditions such as the type of solvent, concentration of the alkoxide, time of hydrolysis and polymerization, amount of catalyst, temperature, etc (Yoldas, 1996; Livage et al., 2001; Veith et al., 2005; Dunn et al., 1998; Bhatia et al., 1998).

In the current work, we have designed a response surface model and studied the influence of the reaction parameters on the encapsulation efficiency of the process. The predictor variables identified from Chapter 3 were: 1) concentration of alkyl-TEOS (x1); 2) time of hydrolysis of alkyl-TEOS at acidic pH (x2); 3) concentration of THEOS (x3); 4) time of hydrolysis of THEOS at acidic pH (x4); and 4) time of polymerization at neutral pH (x5). The response variables chosen for this study were: 1) particle size of the system; and 2) measurement of % extractable limonene from the system.

Materials and Methods

Materials

Octyltriethoxysilane (octyl-TEOS) and THEOS (tetrakis (2–hydroxyethyl) orthosilicate, water soluble substitute for alkoxysilane) was purchased from Sigma-Aldrich Chemical Co., (St. Louis, MO.). Orange oil was received from Robertet Flavors (Piscataway, NJ). Brominated vegetable oil (BVO) was purchased from Spectrum Chemical Mfg. Corp. (Gardena, CA).

Protocol for the synthesis of alkyl modified silica matrices

Figure 4-1 shows the flowchart for the sol-gel reaction process. To the best of our knowledge, there has been no literature published on the criteria that determine the amount of alkylalkoxysilane to be added to a system for the generation of alkyl modified silica matrices. However, the concentration of alkylalkoxysilane cannot be increased beyond a certain extent due to its poor solubility in water (Jovanoic et al., 2005). Octyl-TEOS (0.05-0.5 g) was added to 100 ml of water containing 5 g (57.5 % orange oil and 42.5 % BVO) of oil and stirred for 30 min at 60°C to dissolve it. Once a homogeneous mixture was obtained, the pH was adjusted to approximately 2.8-3 using 0.5 M HCl and allowed to stand at room temperature between 1-24 h to hydrolyze the ethoxy groups. This process enables the formation of a thin silicate layer around the orange oil droplets in addition to providing unreacted Si-OH groups for further cross-linking at the surface. Following this, THEOS (0.5 - 6 g) was added to the emulsion and allowed to co-hydrolyze with octyl-TEOS at room temperature for 1-24 h to form Si-OH groups. Subsequently, the pH was increased to approximately 7 using 0.5 M NaOH and again stirred at room temperature between 1-24 h to initiate the polymerization reaction between the hydroxyl groups formed from the hydrolysis of octyl-TEOS and THEOS. Particle size measurements of the silica matrices generated were made at the end of the

polymerization reaction. The resultant particles were observed using a confocal microscope to determine the location of the orange oil droplets and the silica matrices.

Characterization of the precipitates generated

Particle size analysis of the system

Particle size measurements were made using laser diffractometry (Malvern Laser Diffraction apparatus, Malvern, England). The samples were dispersed in water for 5 sec by ultrasound before measurement to ensure homogeneous dispersion. A 300 mm lens was used in the measurements. The obscuration maintained was ca. 0.21. At least three replicate measurements were recorded for each sample.

% Extractable limonene from the generated matrices

Sample performance was primarily based on the amount of extractable limonene from matrices in an acetone-water system; this value gave us the amount of limonene that was not encapsulated or readily available for release. A 0.35 ml aliquot of a silica product was added to a vial. To that, 10 ml of acetone containing 0.005 g/ml 2-octanoane (internal standard) was added slowly with agitation. A one μL aliquot of the liquid phase was immediately injected into a gas chromatograph for quantifying the amount of extractable limonene. An Agilent gas chromatograph (Hewlett Packard Model 5890) equipped with an HP-5 (Crosslinked 5% PhMeSilicone) column (30m x 0.25mm x 0.25μm) was used in the analysis. The operating conditions were as follows: column carrier gas: helium; column head pressure: 15 psi; split-ratio: 1/30; oven program: 50°C/0 min/10°C/min/190°C/2 min; detector: FID (flame ionization detector). The mixture was sonicated for 3 min and the injection was repeated to measure the total release of limonene. From the values of extractable and total limonene, the % unencapsulated limonene was calculated.

Confocal microscopy of the silica matrices

Silica samples generated through the sol-gel process were observed using a Biorad MRC 1024 confocal microscope. Nile red, a lipophilic fluorophore was used to differentiate between the lipophilic orange oil core and the hydrophilic silica.

Determination of the significant reaction variables of the sol-gel reaction

The influence of the identified variables on the particle size of the system (y1) and % extractable limonene (y2) was investigated using a central composite design (CCD). The quantities of alkyl-TEOS, THEOS, hydrolysis and polymerization times for each treatment were given by the central composite model designed for the study. Based on the preliminary experiments conducted, the reaction parameters were used in the following ranges, concentration of octyl-TEOS (0.05 - 0.5 % of water), THEOS (1 - 6 % of water), hydrolysis times for the silica precursors (1 - 24 h) and polymerization time (1-24 h). Increasing the concentration of THEOS beyond 6 % resulted in the formation of the gel which was undesirable for our study. A 34 experiment study was conducted with (0.5 cube + star) points of 26 and 8 replicates of the center point. The observables were the particle size measurements of the system and the % extractable limonene. Results obtained were analyzed by multiple regression using R statistical software (University of Auckland). The main effect plots of predictor variables were generated using Minitab 15 statistical software trial version (State College, Pennsylvania).

Influence of concentration of hydrophilic silica on the formation of silica sol-gels

The optimized formulation obtained from the CCD (results and discussion section of this paper) was used to specifically study the influence of concentration of hydrophilic silica by varying the concentration of the hydrophilic precursor (THEOS) at 7 different levels (0.5, 0.75, 1, 2, 3, 4 and 6 % of water) and maintaining the rest of the parameters constant. The experiment was carried out in duplicate, therefore, a total of 14 experiments

were conducted. The results obtained were then analyzed using Analysis of variance (ANOVA) in R statistical software. It was expected that with the increase in the silica precursor level in the initial solution, the silicate network generated becomes denser by condensation providing enhanced stability to the encapsulated product (Kim et al, 2003).

Influence of concentration of hydrophobic silica on the formation of silica sol-gels

The influence of hydrophobicity on the % extractable limonene release was systematically studied at 3 different total silica precursor levels (2, 4 and 6 % of water) using a full factorial model with the replicates blocked. The total silica precursor at each level was substituted with octyl-TEOS at various percentages (0, 25, 50, 75, and 100 %). A total of 30 experiments were conducted (3 × 5 =15 experiments in each block). ANOVA was used to compare the performance of different treatments. The interaction plots between the predictor variables and the response surface plots were generated using Minitab 15 statistical software trial version (State College, Pennsylvania).

Results and Discussion

Figures 4-2 and 4-3 show the main effect plots of the predictor variables on the means of the particle size of the system and % extractable limonene. From these plots, it can be observed that the lowest level of all the reaction parameters delivered the highest % extractable limonene; increasing the levels of the reaction parameters decreased the value. From the multiple regression analysis of the central composite model, a second order model was fit and a direct relation was observed between the predictor variables and the particle size of the system, whereas; an inverse relation was seen between the predictor variables and the % extractable limonene. We found the concentration of hydrophilic silica, interaction between the concentration of hydrophobic silica and hydrolysis time of hydrophilic silica, interaction between the concentration of hydrophilic silica and its hydrolysis time, interaction between the concentration of

hydrophilic silica and polymerization time, and interaction between the hydrolysis time of hydrophilic silica and polymerization time to significantly affect the particle size of the system. On the other hand, interaction between the concentration of hydrophobic silica and its hydrolysis time, interaction between the concentration of hydrophobic silica and polymerization time, interaction between hydrolysis time of hydrophobic silica and time of polymerization and interaction between the concentration of hydrophilic silica and its hydrolysis time were the significant parameters for determining the % extractable limonene. From the above mentioned significant parameters, it can be seen that almost all the predictor variables chosen were significant either in the determination of the particle size of the system or % extractable limonene. However, when the relationship between the particle size of the system and % extractable limonene was explored, it was found that there was no correlation between them as illustrated by the R^2 value of 0.033 (Figure 4-4). This means that larger mean particle sizes do not necessarily mean lower extractable orange oil.

Therefore, the conditions of the treatment (X2=24 h, X4=24 h and X5=24 h) that had delivered the lowest % extractable limonene were used for our subsequent experiments, which involved the study of concentration of hydrophilic and hydrophobic silica on % extractable limonene release.

In Figure 4-5, it can be seen that increasing the concentration of hydrophilic silica from 0.5 to 6 % decreased the % extractable limonene indicating the formation of more compact structures at higher concentrations. However, the decrease was not statistically significant beyond 3 % hydrophilic silica. Figure 4-6 (a, b, c and d) shows the confocal microscopic images of the silica matrices from systems generated using different concentrations of simple alkoxysilanes, respectively. It can be seen from the confocal images that the amount of precipitated silica generated using 0.5 % of hydrophilic silica was less; at the 2 % level some of the orange oil droplets were within individual silica matrices; while others were within a continuous silica matrix. The 4 % alkoxysilane samples showed a continuous silica matrix and the orange oil droplets were

uniformly distributed within it. At the 6 % level, a highly interconnected silicate network was formed with the droplets heterogeneously scattered in the matrix.

From Figures 4-7 and 4-8, it can be observed that the addition of octyl-TEOS did not have a positive effect on the retention of limonene: % extractable limonene increased with the introduction of hydrophobicity as opposed to decreased (at both 2 and 6 % alkoxysilane levels). At the 6 % level of alkoxysilane (100 % octyl-TEOS addition), almost 50 % of the limonene was extractable. This unexpected trend in retention might have been due to the incomplete hydrolysis of octyl-TEOS, insufficient concentration of THEOS to co-hydrolyze and co- polymerize with octyl-TEOS, and/or insufficient concentration of octyl-TEOS to have a positive effect on the release

A literature search provided information that the increase in the release of lipophilic molecules with the incorporation of alkyl groups is likely because of the less compact silicate structures formed due to the long chain alkyl groups (Loy et al., 2000). The formulation containing 25 % octyl-TEOS addition showed lower % extractable limonene than 0 % octyl-TEOS at the 4 % total silica level indicating a positive influence of hydrophobicity on the release of limonene (Table 4-1). The formulation containing 100 % octyl-TEOS at the 2, 4 and 6 % alkoxysilane level did not form a precipitate; instead there was a layer of octyl-TEOS floating at the top of the container. This observation is supported by several studies stating that solutions containing alkyl-TEOS do not gel nor form a precipitate (Shimojima et al., 2002).

Conclusion

The response surface model demonstrated that all the predictor variables affected particle size of the system and limonene retention. No correlation was observed between the particle size and % extractable limonene. It was found that the lowest level of reaction parameters resulted in the highest % extractable limonene, whereas; highest

level of reaction parameters resulted in the lowest value indicating the formation of complete silicate matrices.

It was also found that the incorporation of long chain alkyl groups into the formulation resulted in a higher value of % extractable limonene indicating the formation of less compact matrices. One of the drawbacks of this study is that the silica matrices were not characterized for their other physical properties such as the pore volume, pore size distribution and specific surface area. This information would have facilitated in explaining the rationale for the increased % extractable limonene with the addition of alkylalkoxysilane. Further, this study focused only on a single compound, future work was conducted using these systems for the encapsulation of a complex flavor mixture consisting of hydrophilic and hydrophobic flavors.

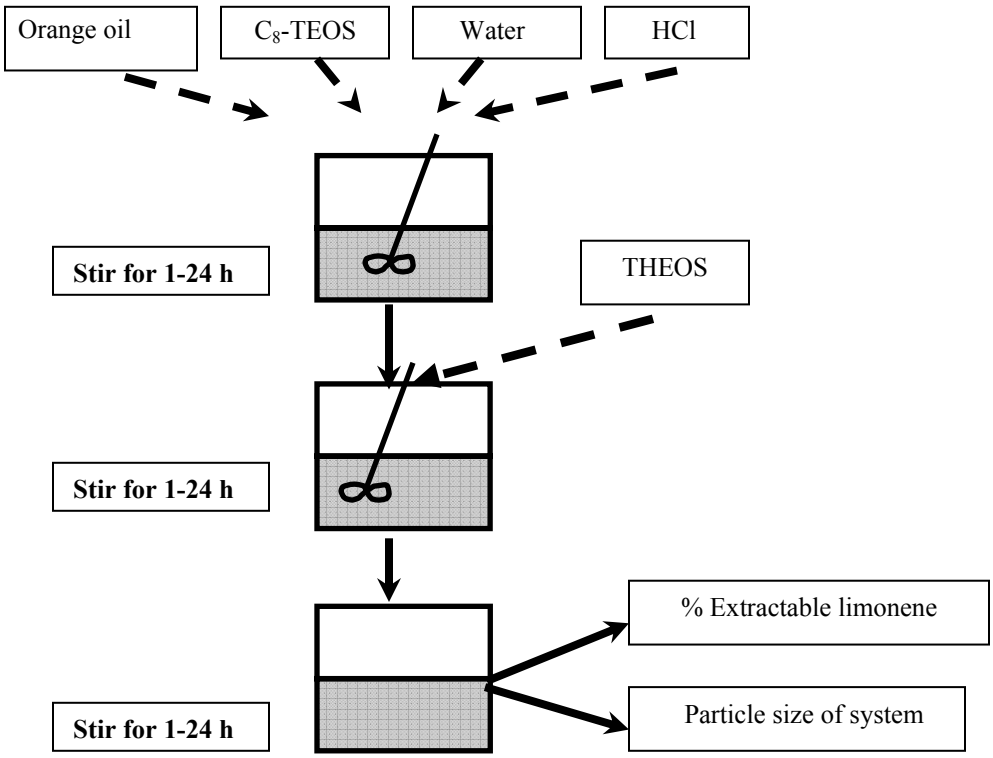

Figure 4-1: Steps involved in sol-gel polymerization reaction

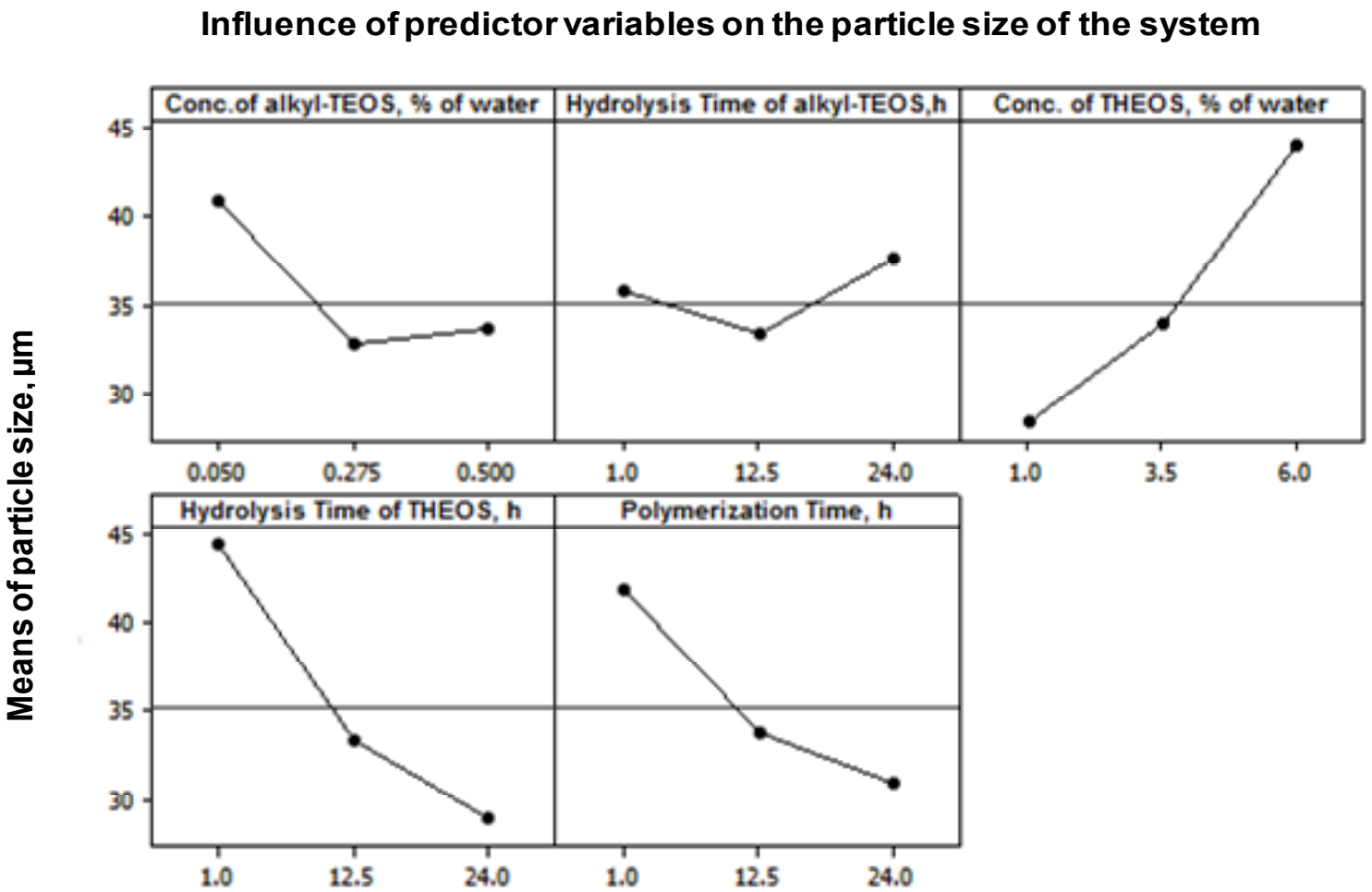

Figure 4-2: Main effects of predictor variables observed on the particle size of the system

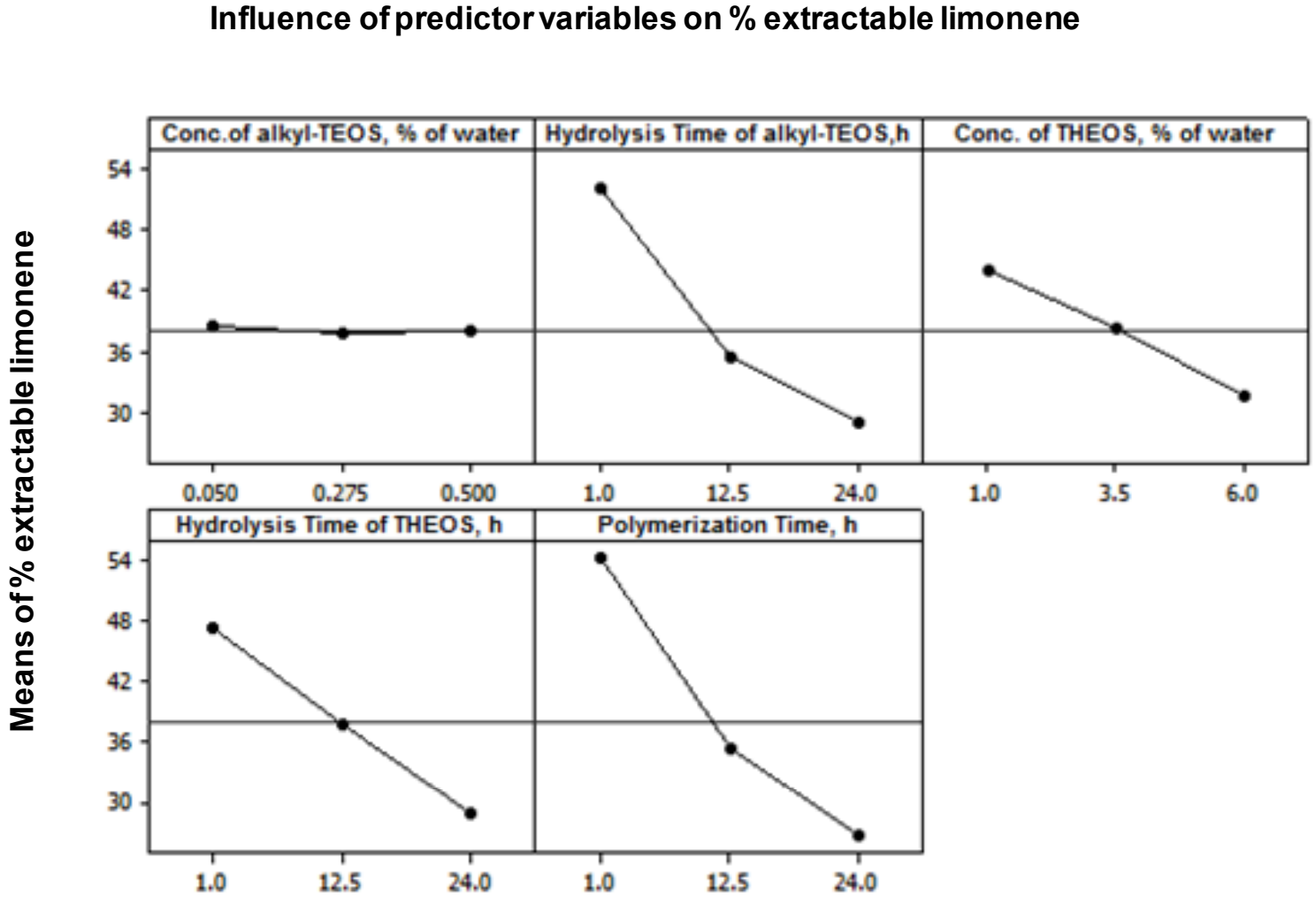

Figure 4-3: Main effects of predictor variables observed on % extractable limonene from the system

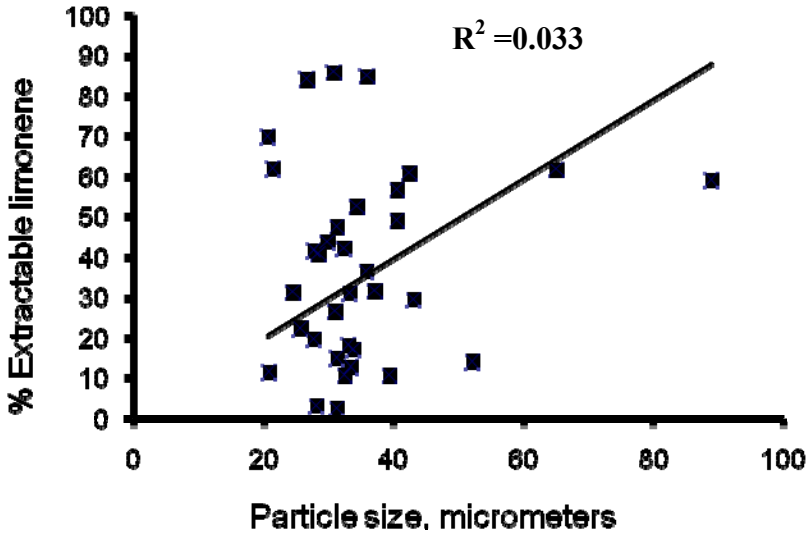

Figure 4-6: Relationship between mean particle size and % extractable release of limonene

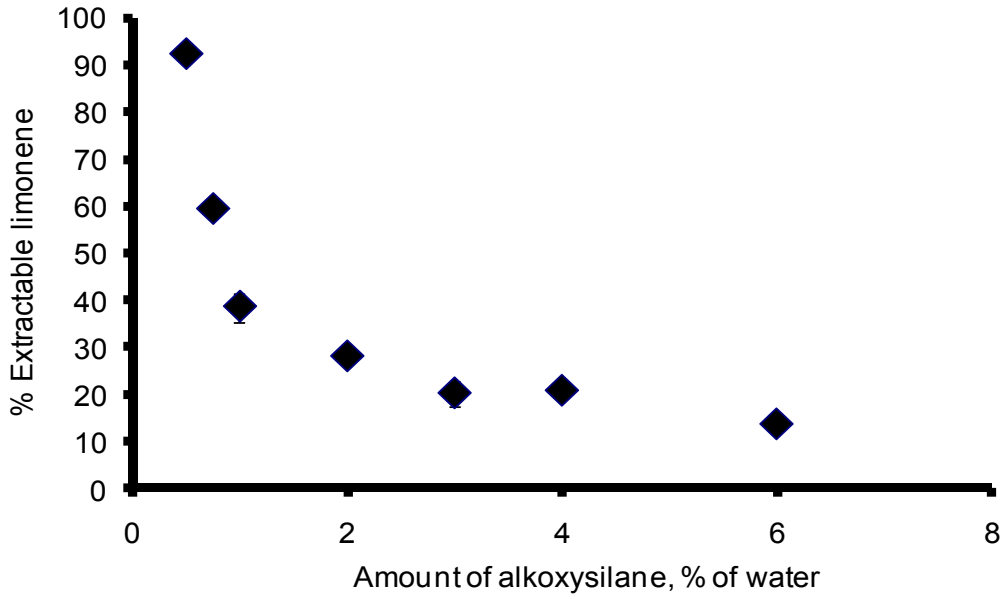

Figure 4-7: Influence of concentration of hydrophilic silica on the % extractable limonene from silica sol-gel matrices

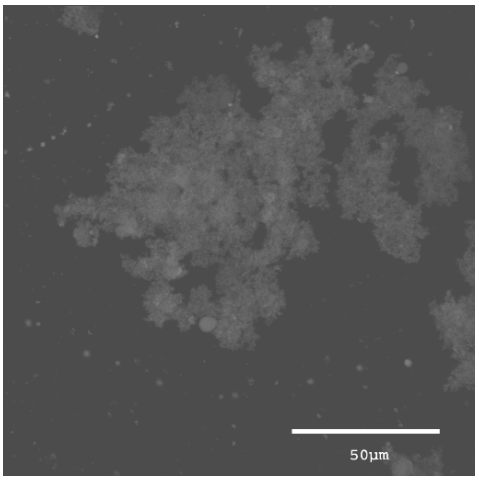

(A) 0.75 % silica

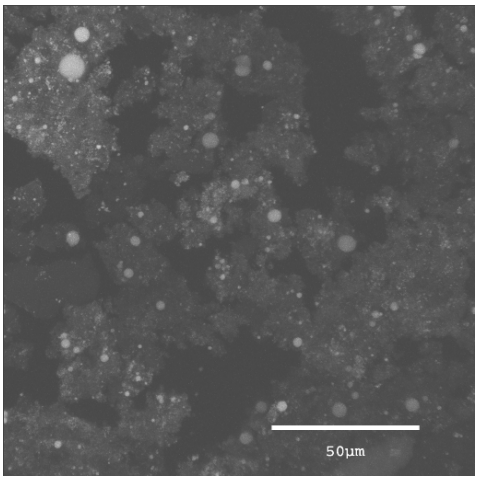

(B) 2 % silica

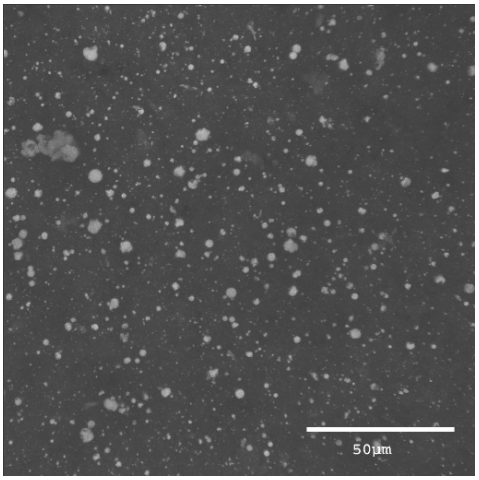

(C) 4 % silica

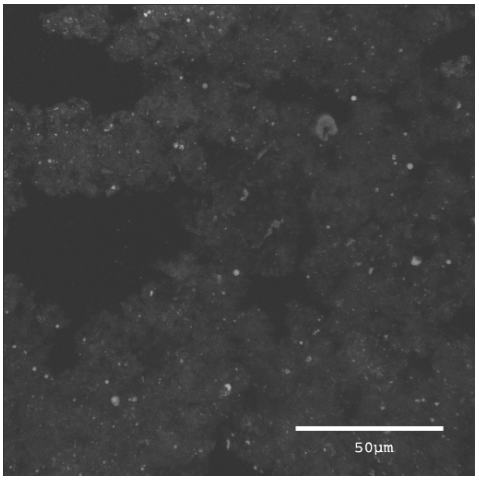

(D) 6 % silica

Figure 4-8: Confocal microscopic images of silica matrices stained with nile red containing different conc.'s of simple alkoxysilanes (bright spots represent the orange oil and the lighter matrix represent silica).

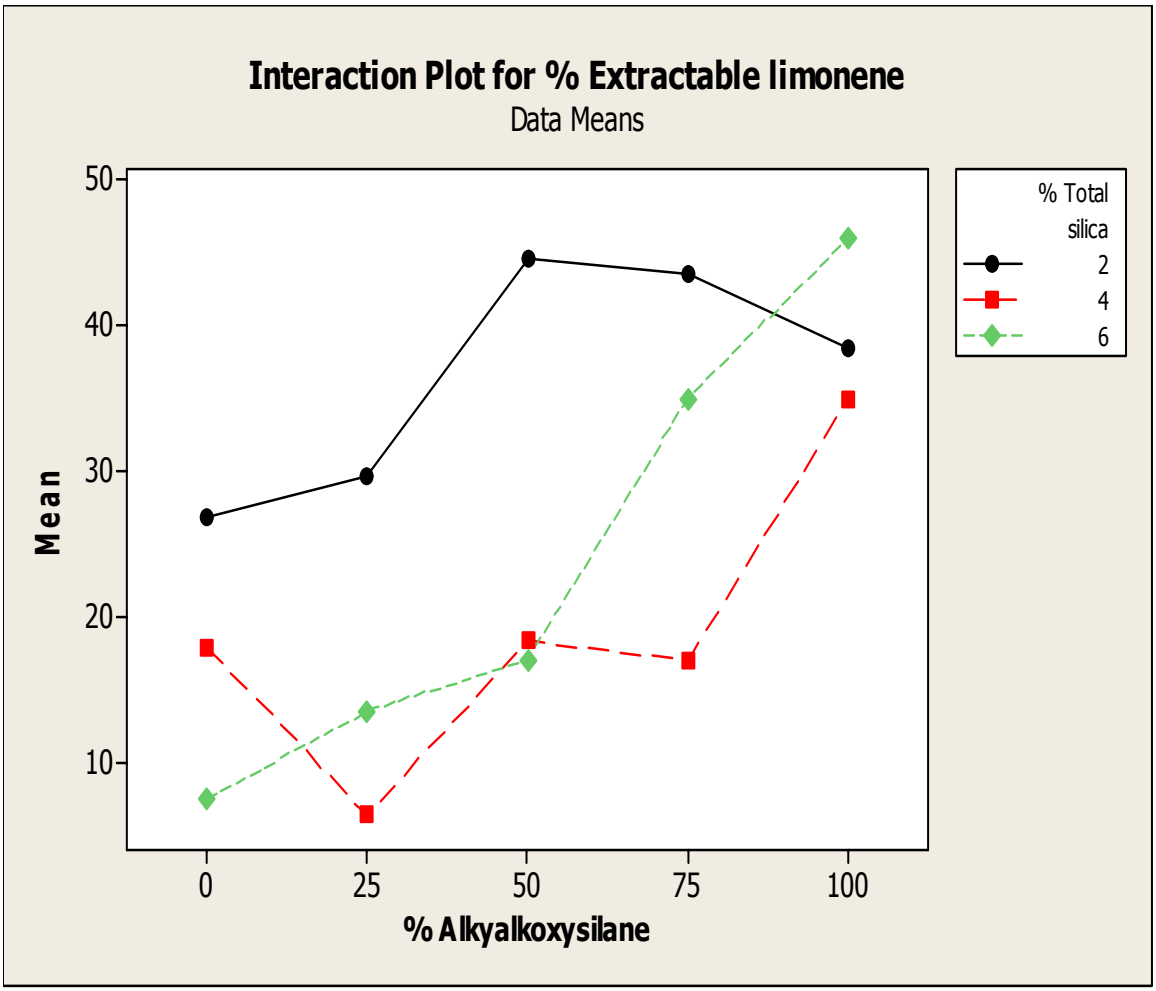

Figure 4-9: Influence of concentration of hydrophobic silica on the % extractable limonene from silica sol-gel matrices

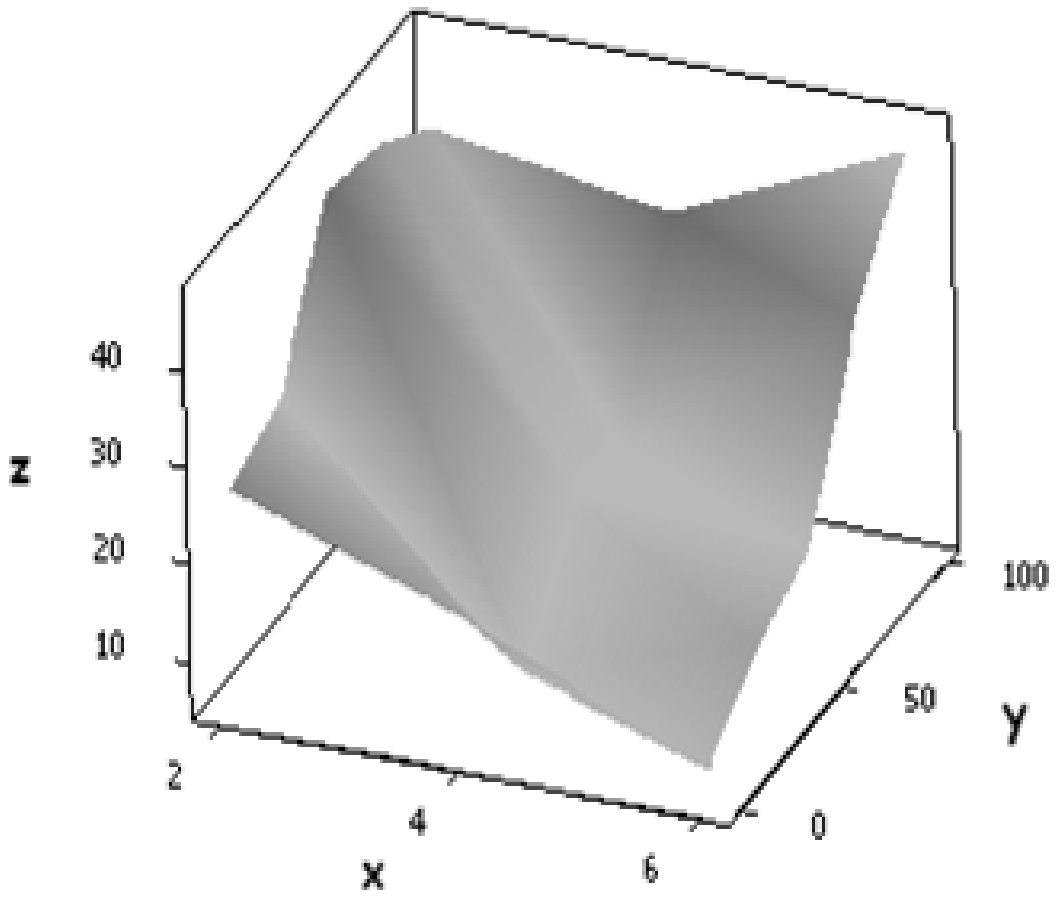

x- % Total silica; y - % Alkylalkoxysilane; and z- % Extractable limonene

Figure 4-10: Response surface plot to study the influence of concentration of hydrophobic silica

Table 4-1: Fischer LSD for % extractable limonene from silicate matrices

Total silica precursor, % of water	Alkylalkoxysilane, % of total silica precursor	% Extractable limonene
2	0	26.8 d
2	25	29.8 d
2	50	44.7 a
2	75	43.6 a
2	100	38.5 ab
4	0	17.9 e
4	25	6.3 g
4	50	18.3 e
4	75	17.0 e
4	100	35.8 bc
6	0	7.4 fg
6	25	13.5 ef
6	50	12.5 efg
6	75	33.9 bc
6	100	43.5 a

*Different letters note significant differences between matrices

Chapter 5 : Flavor retention in silicate matrices (Study 2)

Abstract

Previous studies on flavor encapsulation in silicate matrices synthesized by the sol-gel process have showed limited value because the silica remains porous to the flavorants. We have attempted to address this problem in two ways: 1) by introducing long chain alkyl groups into the silicate network; and 2) blending alkyl modified (hybrid) and unmodified sol-gel silicate (hydrophilic) matrices with a commercial emulsifying starch (Capsul^{TM}). The latter is an effort to fill the silica polymer structure with a food polymer thereby "plugging" the pores. We examined the efficacy of these approaches by conducting a comprehensive evaluation of the stability of encapsulated flavor compounds during freeze drying and storage. Performance was compared to two control samples, Capsul and commercial plating silica. A model flavor mixture consisting of diacetyl, methyl propanal, methyl pyrrole, and damascenone was incorporated into medium chain triglycerides (MCT's), limonene and neat before being added into the carrier matrix. Capsul (neat) showed the highest retention for most compounds (except methyl pyrrole). Alternatively, commercial plating silicas (neat) exhibited the lowest loss (plating) of methyl pyrrole of all delivery systems. Overall**,** results from retention during drying/storage showed that diacetyl was retained relatively better than the other compounds. While Capsul (limonene) retained volatiles the best during storage (except damascenone), commercial plating silicas performed poorly irrespective of the flavor solvents used (retaining negligible amounts at the end of nine weeks). Though the alkyl modification showed significantly lower losses during drying compared to the unmodified/hydrophilic silica blends for some compounds, it did not exhibit a positive influence during storage.

Introduction

Flavor is very important for consumer approval of a food product. During manufacturing and storage of some food products, flavor compounds are either lost or degraded affecting the acceptance of the product. In order to overcome this issue, flavors are encapsulated in various materials before being introduced into food products (Balassa and Fanger, 1971; Dziezak, 1988; Versic, 1988; Reineccius, 1991; Shahidi and Han, 1993; Reineccius, 1995; Risch, 1995). Encapsulation is a process by which a single or mixture of molecules is entrapped within different types of coating materials (Balassa and Fanger, 1971).

Silica matrices formed by the sol-gel process have emerged as a promising platform for the encapsulation of biomolecules such as enzymes, drugs, proteins, nutraceuticals, flavors and fragrances. A number of studies have showed that simple silica matrices have been excellent for the encapsulation of hydrophilic molecules, which can associate either chemically or physically with the hydrophilic silica surface (Veith, 2004; Bolton and Reineccius, 1992; Bhatia et al., 1998; Barbe et al., 2004). One of the recent studies conducted by Veith et al. (2004) demonstrated that hydrophilic silicate matrices selectively retained the hydrophilic flavor compounds. Studies have explained that the hydrogen bonding occurring between the electronegative atoms of the flavor molecules (oxygen electron donors such as ethers, alcohols and ketones) and the hydroxyl groups present on the surface of silica is primarily responsible for the retention of hydrophilic molecules (Iler, 1979). Alternatively, results have demonstrated that the hydrophobic molecules such as limonene and myrcene, major constituents of essential oil, were retained poorly in simple silica matrices generated from TEOS (Bolton and Reineccius, 1992; Veith et al., 2004). The selective retention of flavor compounds would likely lead to an alteration in the flavor profile of the product which is undesirable.

The reasons for this lack of retention are two fold: 1) a lack of interaction between the hydrophobic flavor molecule and the hydrophilic silica matrix; and 2) diffusion losses that could occur during storage due to the porous nature of silica.

Therefore, we have attempted to address this problem in two different ways: 1) to add alkyl groups to the silica gel thereby increasing the hydrophobic nature of the silica; and 2) to incorporate a food polymer into the silica gel structure which would reduce its porosity to flavor molecules. In recent years, alkyl modifications on silicate matrices have generated intense interest in a wide range of application fields (Unger et al., 1993; Reetz et al., 1996; De Witte et al., 1996; Carturan et al., 1997; Loy et al., 2000; Veith et al., 2004; Yi et al. 2006). Studies have also indicated that the introduction of alkyl groups into the silicate matrix can increase the flexibility of the three dimensional network preventing the collapse of matrices during drying (Witte et al., 1996; Loy et al., 2000). Further, some studies have reported the association of silica with proteins and polysaccharides through hydrogen bonding. One of the studies described a reaction between metal alkoxides when mixed with ethyl cellulose. These types of interactions have enhanced the retention of encapsulated molecules (Shchipunov, 2003). Examining the chemical structure of emulsifying starch (octenyl succinate), there are various possibilities for hydrogen bonding with the hydroxyl groups of the silanols.

In the current work, we have used the formulation of the sol-gel process from Chapter 4 for encapsulating a complex flavor mixture. We have studied the performance of the silicate matrices by evaluating the retention of flavor compounds during drying and storage and comparing them to conventional flavor carriers.

Materials and Methods

Materials

Gas chromatographic (GC) grade dichloromethane was purchased from Fisher Scientific (Hanover, IL). Octyl-TEOS (octyltriethoxysilane) and THEOS (tetrakis (2–hydroxyethyl) orthosilicate, a water soluble substitute for alkoxysilane) were purchased from Sigma-Aldrich Chemical Co., (St. Louis, MO). The flavor mixture consisting of compounds methyl propanal, diacetyl, methyl pyrrole and damascenone and their corresponding internal standards (methyl butanal, pentanedione, n-pyrrole and α-ionone) were also

purchased from Sigma Aldrich Chemical Co., (St. Louis, MO). Capsul^{TM} (starch octenyl succinate) was obtained from National Starch and Chemical Corp., Bridgewater, NJ and Syloid 244, commercial plating silica was purchased from W.R.Grace and Co., (Phoenix, AZ).

Synthesis of precipitates

Figures 5-1 and 5-2 illustrate the encapsulation process. Two optimized formulations of the sol-gel process (1. 4 % silica precursor with 25 % alkylalkoxysilane addition; and 2. 6 % silica precursor with addition of alkylalkoxysilane) obtained from the previous study (Chapter 4) were used to evaluate the shelf-life stability of flavor compounds. Octyl-TEOS was added to 100 ml of water and stirred for 30 min at 60°C to dissolve it. Once a homogeneous mixture was obtained, the pH was adjusted between 2.8-3 using 0.5 M HCl and hydrolyzed for 24 h under room temperature conditions for the generation of hydroxyl groups. THEOS was added subsequently and hydrolyzed under acidic conditions for 24 h. In the next step, the pH was increased to approximately 7 using 0.5 M NaOH and flavor compounds were introduced into the sol at this stage. A variable in this study was how the model flavor compounds were added, i.e. they were added with a solvent (MCT, limonene) or neat (no solvent). After the addition, the mixture was stirred at room temperature for 1 h to initiate the polymerization reaction between the hydroxyl groups formed from the hydrolysis of octyl-TEOS and THEOS. At the end of the reaction, 10 g of emulsifying starch was blended with the polymerized precipitate. The resulting slurry obtained was freeze-dried (– 40°C and 100 millitorr) and the dried powders went through a size reduction process (pestle and mortar) before being stored in polyethylene bags under room temperature conditions in a dessicator containing drierite for the study.

Control samples of Capsul (MCT, limonene and neat) were prepared by adding 20 g of the modified starch in 100 ml of water (stirring at 60°C for 1 h). Once the starch dissolved, flavor mixture (MCT, limonene and neat) was introduced into the slurry and the resulting slurry was freeze-dried under similar conditions as the silica sol-gel matrices. For the generation of flavor loaded plating silicas, the flavor mixture dissolved

in solvents (MCT, limonene and neat) was added to Syloid 244 and blended for a period of time using a hand mixer to obtain homogeneous loading.

Table 5-1 shows the physicochemical properties of the investigated aroma molecules. It can be noticed that the aroma compounds chosen had a wide range of partition coefficients. The twelve samples evaluated are listed below: 1) hybrid silica blend (MCT); 2) hybrid silica blend (limonene); 3) hybrid silica blend (neat); 4) hydrophilic silica blend (MCT); 5) hydrophilic silica blend (limonene); 6) hydrophilic silica blend (neat); 7) plating silica (MCT); 8) plating silica (limonene); 9) plating silica (neat); 10) Capsul (MCT); 11) Capsul (limonene); and 12) plating silica (neat).

Characterization of the freeze-dried powder

Particle size analysis of the freeze-dried powder

Particle size measurements were made using laser diffractometry (Malvern Laser Diffraction apparatus, Malvern, England). The samples were dispersed in ethanol for 5 sec by ultrasound before measurement to ensure homogeneous dispersion. A 300 mm lens was used in the measurements. The obscuration was maintained at ca. 0.21. At least three replicate measurements were recorded for each sample.

Karl Fischer method for moisture determination of the freeze-dried powder

The moisture content of the freeze-dried powder was determined using the Karl Fischer method. Sample (0.5 g) of the sample was equilibrated in 10 g of dry methanol for 24 h. One milliliter of the supernatant was injected into the Karl Fischer instrument to determine the moisture content. This was done in triplicate.

Extraction of aroma compounds from encapsulated matrices

Aroma load was determined by extraction using dichloromethane and subsequent GC analysis. A 0.15 g of aroma-laden silica powder was added to a vial containing 1 ml of

water and vortexed for 5 min. Next, 4 ml of dichloromethane containing internal standards was added slowly with agitation. One μL aliquot of the liquid phase was immediately injected into a gas chromatograph for quantifying the amount of each compound present in the encapsulated matrices. An Agilent gas chromatograph (Hewlett Packard Model 5890) equipped with a DB-5 column (30m x 0.25mm x 0.25μm) was used in the analysis. The operating conditions were as follows: column carrier gas: helium; column head pressure: 8 psi; splitless injection; oven program: 38°C/8 min/10°C/min/190°C/2 min; detector: FID (flame ionization detector). A standard curve was constructed with known concentrations of the corresponding pure aroma mixtures with internal standards of similar concentration. The calibration curves consisted of at least 5 points and were linear ($R^2 > 0.98$) for all the aroma compounds as showed in Table 5-1. The extraction was carried out in triplicate.

Statistical analysis

The evaluation of different combinations of carriers and solvents was conducted by: 1) measuring the losses during drying/blending and storage; and 2) determining the rate of degradation of compounds. The loss during drying was calculated by measuring the ratio of the concentration of a compound remaining in the matrix after drying over the initial concentration of the flavor loaded on to the matrix. The rate of loss for each volatile was determined for all the matrices by fitting these concentration values in the zero-order [($C-C_0$) Vs time], first-order [ln (C/C_0) Vs time] equations and plotting these points. C and C_0 are the final and initial concentrations of the flavor compound, respectively. The reaction order used in reporting was chosen based on the best fit, i.e. highest R^2. However, the slopes of these equations cannot be directly compared due to differences in reaction order between matrices.

To provide some measure of rate of loss that is comparable across all systems, we decided to express rate of loss as the slope of loss over the first week of storage. Finally, the retention during storage was expressed by the percentage of each compound (concentration of the compound remaining after 9 weeks/concentration

measured after drying) remaining at the end of the final/ninth week. Analysis of variance (ANOVA) was conducted on these values utilizing R statistical software (2008) for each of the 12 combinations of carriers and solvents. When a factor effect or an interaction was found significant, indicated by a significant F test ($P \leq 0.05$), differences between the respective means were determined using Fischer Least Significant Difference test (LSD).

Results and Discussion

Retention during plating/ drying

Methyl propanal: It can be seen from Figure 5-3 and Table 5-3 that compounds encapsulated in hybrid silica blend (limonene) and Capsul (neat) showed the highest retention of methyl propanal in the dry product (~ 55 %). The observation that using Capsul as the flavor carrier resulted in good retention is consistent with the literature (e.g. Bangs and Reineccius, 1981). The poorest retentions were obtained by simply plating the methyl propanal onto commercial silicas irrespective of the flavor solvent used (MCT, limonene and neat) retaining less than 10 % of methyl propanal. This is likely due to the low molecular weight (M.W. 72) of this compound. Studies have reported that the increase in retention with the increase in molecular weight. The rationale explained for this behavior is the influence of molecular weight on flavor diffusion occurring through the matrix during drying. Reports indicate that smaller molecules diffuse more readily than the bigger molecules (Rosenberg et al., 1990; Voilley, 1995).

Diacetyl: Most matrices exhibited exceptional retention of diacetyl showing drying losses between 0 and 10 % (Figure 5-3 and Table 5-3). Reports have indicated that compounds possessing carbonyl groups can engage in hydrogen bonding with the hydroxyl groups present on the silicate surface. In fact, the amount of hydroxyl and carbonyl groups in a flavor molecule determines the level of interaction with the silica and subsequently, the retention of each compound (Iler, 1979). Diacetyl has two carbonyl groups, which may participate in such interactions resulting in enhanced retention. However, plating this highly hydrophilic compound on to commercial silicas showed a

significantly lower retention losing close to 80 % of the compound. Based on the above results, it was apparent that these highly volatile compounds (methyl propanal and diacetyl) are likely to have been lost during the plating process. It is known that the plating process involves mere adsorption of a compound onto the silica surface; therefore, the losses of these compounds are anticipated.

Methyl pyrrole: Methyl pyrrole plated onto commercial plating silica (neat) exhibited the lowest loss of all delivery systems after the plating process retaining 61 % of the original loading (Figure 5-3 and Table 5-3). Methyl pyrrole has unpaired electrons in the nitrogen atom that can interact strongly with the silicate surface. In contrast, when MCT was used, retention dropped by ca, half (35 %). Among the matrices that were freeze-dried, Capsul (neat) retained the most (45 %). The rest of the matrices that had undergone the drying process showed poor retention with drying losses ranging between 70 – 80 %. These results indicated that the loss of this particular compound was primarily due to the freeze drying process.

Damascenone: The plating process was very efficient in retaining damascenone, a highly hydrophobic compound (Figure 5-3 and Table 5-3). Note that this compound is also relatively low in volatility and chemically inert aroma compound. The use of hydrophobic solvents (MCT and limonene) enhanced the retention of this hydrophobic compound retaining close to 100 % when they were used. The delivery systems that showed good retention were Capsul (neat) and the hybrid silica blend (flavors dissolved in MCT). While Capsul (neat) exhibited high retentions for all compounds after the drying process; the increased hydrophobicity in the hybrid silicas likely contributed to the good retention of this hydrophobic flavoring compound.

Rate of degradation of compounds in encapsulated matrices

While the first concern in flavor encapsulation is whether volatiles are retained in the encapsulation process, the second concern is for how well they are

retained on storage. As noted in the Materials and Methods section, volatile losses are expressed as the slope of the amount of each volatile remaining over the first week of storage (See Table 5-4). Statistical analysis found no significant differences between the calculated slopes for methyl propanal across all delivery systems during this initial storage period.

Diacetyl loss in the plated silica (limonene) showed the highest value indicating the most rapid loss of all systems. In fact high slopes were found for diacetyl loss from both plated systems. While the hydrophilic silica blends also had a high loss for diacetyl during this period regardless of the solvent used, hybrid silica blends and Capsul proved to have the slowest rate of degradation, when diacetyl was added neat and with MCT, respectively.

Although commercial silicas showed the highest retention of methyl pyrrole after the plating process, they had the fastest rate of loss irrespective of the solvent used. Hydrophilic silica blends and hybrid silica blends added neat protected the methyl pyrrole from degrading relatively better than the other matrices.

Damascenone adsorbed onto commercial silicas (neat) retained the best (demonstrated by the lowest slope) during the first week. Furthermore, model volatiles dissolved in hydrophobic solvents (MCT and limonene) prior to encapsulation in hybrid silica blends had slower rates of loss compared to the other combinations of solvents and carriers; this might have been due to the affinity of the hydrophobic matrix (carrier and solvent) to damascenone.

Retention after nine weeks storage at room temperature

A nine week storage study was carried out to evaluate the longer term shelf-life stability of the model volatile compounds loaded in different matrices. Table 5-

5 shows the significant differences between the percentages retained after nine weeks of storage for different matrices. Figure 5-4 is a graphical presentation of these data.

Methyl propanal: Figures 5-5, 5-6 and 5-7 show the influence of different capsule formation processes on the loss of methyl propanal during storage in solvents MCT, limonene and neat, respectively. The Capsul (limonene) exhibited the best performance retaining 30 % of the initial amount of flavoring over nine weeks of storage. The performance of the sol-gel matrices was rather poor exhibiting retentions less than 10 % during storage. Methyl propanal, being a highly volatile (B.P. 75°C) and low molecular weight compound (M.W. 72), showed very high losses relative to the other volatiles tested.

Diacetyl: Figures 5-8, 5-9 and 5-10 show the influence of different capsule formation processes on the loss of diacetyl during storage in solvents MCT, limonene and neat, respectively. Similar to methyl propanal, diacetyl was retained best in Capsul matrix (limonene) exhibiting 75 % retention after 9 weeks storage. While diacetyl encapsulated in hydrophilic silica blends exhibited higher retentions than the hybrid silica blends in the absence of solvents, the latter performed better in the presence of solvents. This implied that the interaction occurring between the hybrid carrier and the hydrophobic solvents enhanced the retention of this particular compound.

Several studies have illustrated the superior performance of hydrophilic silicas for the encapsulation of hydrophilic species (Veith, 2004; Bolton and Reineccius, 1992; Bhatia et al., 1998; Barbe et al., 2004). The plated silicas lost most of the volatiles resulting in final concentrations below the detection of the analytical method. However, the hydrophilic silica blends generated by the sol-gel process showed retentions between 30 - 38 % performing better than the plated silicas. From these results, it can also be observed that the loss of individual compounds cannot be explained only by volatility; the polarity of the compound also plays an important role. In spite of diacetyl being a highly volatile compound (B.P. 88°C); its retention in silica matrices was higher than methyl pyrrole (B.P. 112°C) and damascenone (B.P. 275°C). This is in agreement with

studies which have indicated that the amount of flavor retained on the silicate surface is also dependent on the polarity of the molecule (Iler, 1979; Bolton and Reineccius, 1992; Veith et al., 2004).

Methyl pyrrole: Figures 5-11, 5-12 and 5-13 show the influence of different capsule formation processes on the loss of methyl pyrrole during storage in solvents MCT, limonene and neat, respectively. Dissolving methyl pyrrole in limonene and its subsequent encapsulation in a Capsul matrix proved to be the best system retaining 55 % of the initial flavoring. The performance of the silica sol-gel blends for methyl pyrrole was similar to diacetyl with the hybrid silica blends performing better than hydrophilic blends in the presence of solvents. While the hydrophilic silica blend (MCT) retained 45 % of the initial flavoring; the hybrid silica blend (MCT) exhibited retention close to 53 %. The partition coefficient of methyl pyrrole is 1.43, making it a moderately hydrophobic compound. Therefore, the incorporation of hydrophobic groups in the hybrid silica blend might have resulted in the enhanced performance. Further, the addition of hydrophobic solvents to methyl pyrrole prior to the encapsulation process also appeared to improve the retention of this compound.

Damascenone: Figures 5-14, 5-15 and 5-16 show the influence of different capsule formation processes on the loss of damascenone during storage in solvents MCT, limonene and neat, respectively. Although Capsul (limonene) showed a superior performance during storage for other compounds, it was an unsuitable matrix for encapsulating damascenone (~ 12 %). The hydrophilic silica blend generated by the sol-gel process (MCT) showed an outstanding performance, ca. 75 % of the damascenone. The other solvents used resulted in retentions between 40 and 50 %. It is important to note that hybrid silica blends were used assuming they would improve the retention of hydrophobic compounds. Theoretically, incorporating damascenone, a highly hydrophobic compound (log P- 4.43), into hybrid silicas should have relatively better retention compared to hydrophilic silica matrices. However, hybrid silicates retained only ca. 35 % of the original flavoring losing more than 50 % of the initial flavoring. NMR studies revealed that the long chain alkyl groups of the alkylalkoxysilane could be pushed

to the surface during the condensation process due to the steric hindrance. Due to the presence of the alkyl groups on the surface, damascenone could also stay on the surface resulting in the faster loss of the compound.

Summary

Capsul (neat) showed the highest retention for most compounds (except methyl pyrrole) during drying. Alternatively, commercial plating silicas (neat) exhibited the lowest loss (plating) of methyl pyrrole of all delivery systems. Overall**,** results from retention during drying/storage showed that diacetyl was retained relatively better than the other compounds. While Capsul (limonene) retained volatiles the best during storage (except damascenone); commercial plating silicas performed poorly irrespective of the flavor solvents used (retaining negligible amounts at the end of nine weeks). Hybrid silica: starch blends performed better than the hydrophilic silica: starch blends during storage in the presence of solvents for most compounds except damascenone.

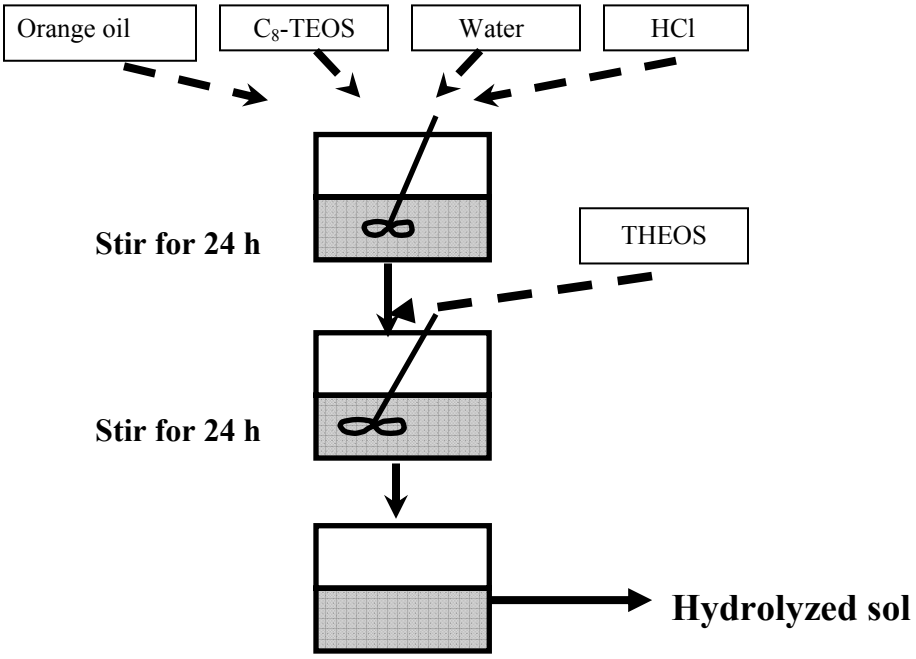

Figure 5-1: Flow chart for the silica sol-gel encapsulation process (step 1)

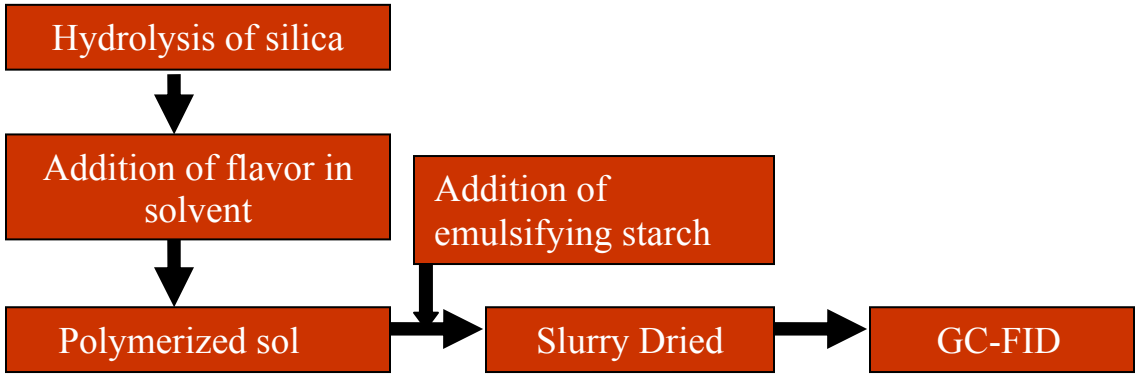

Figure 5-2: Flow chart for the silica sol-gel encapsulation process (step 2)

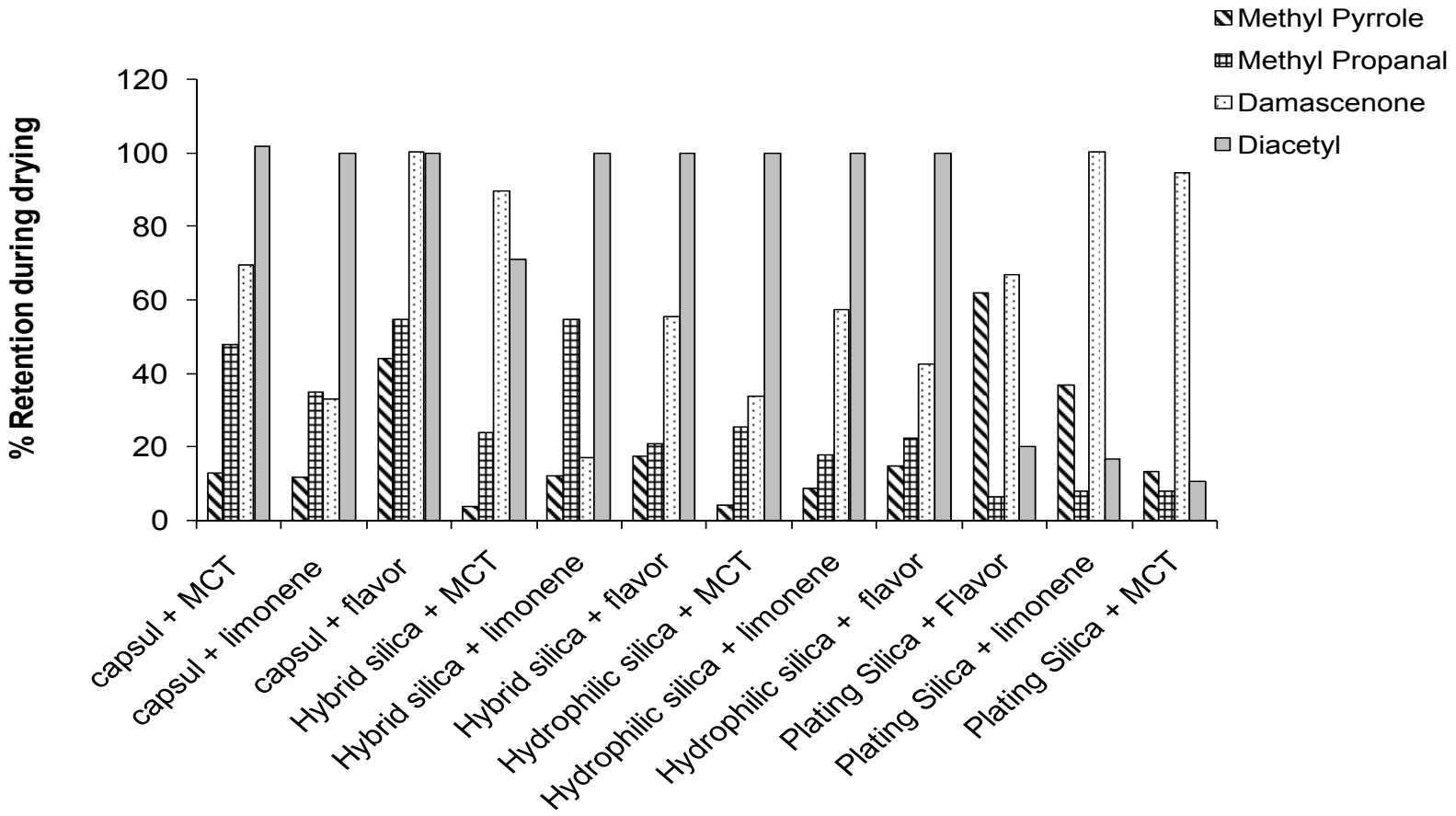

Figure 5-3: The **i**nfluence of flavor solvent and manufacturing formulation/process on flavor retention during drying

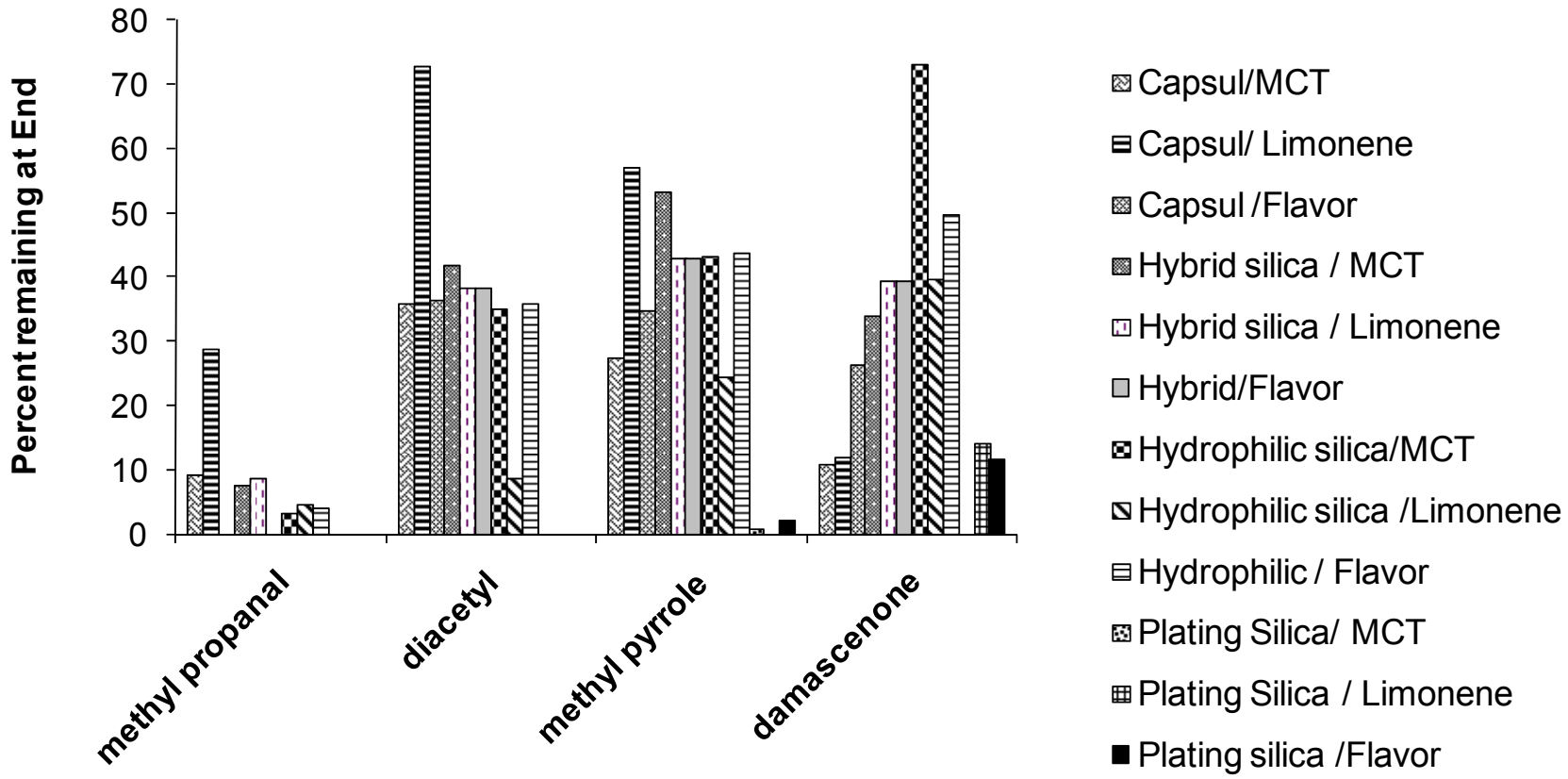

Figure 5-4: The influence of flavor solvent and manufacturing formulation/process on flavor retention during storage for nine weeks

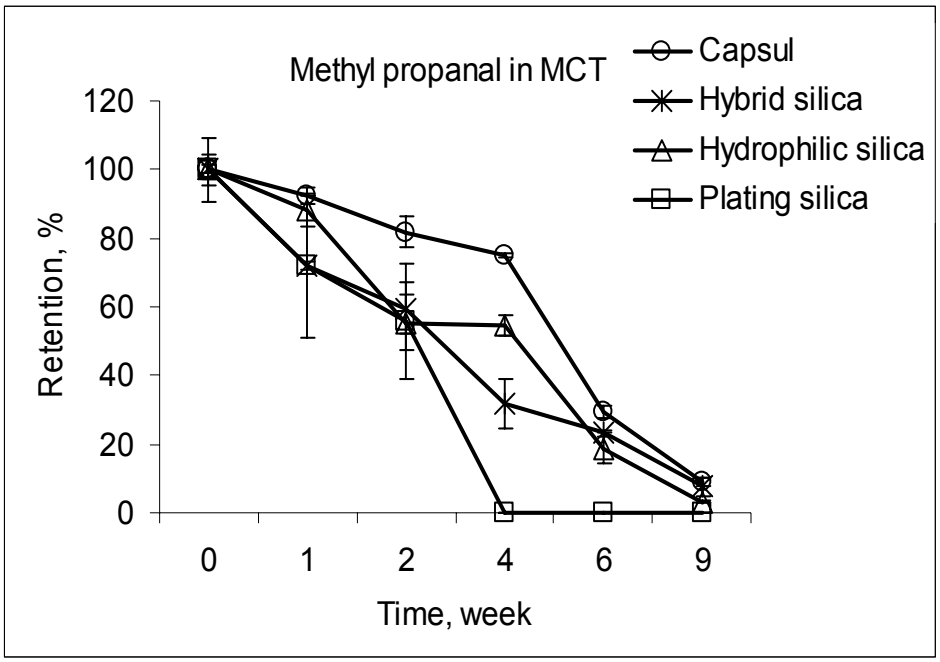

Figure 5-5: The influence of different capsule formation processes on the loss of methyl propanal (in MCT) during storage

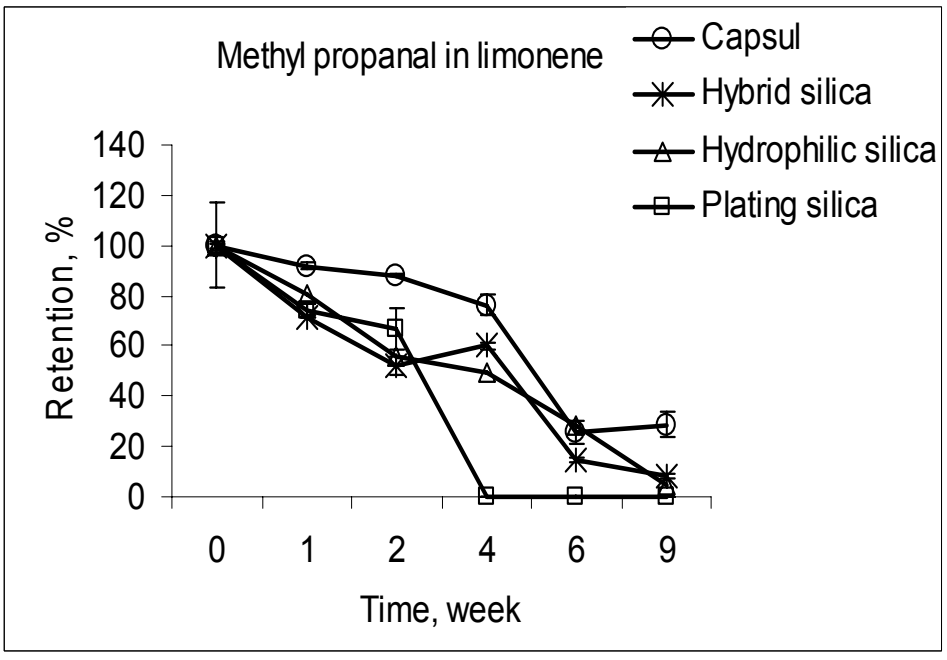

Figure 5-6: The influence of different capsule formation processes on the loss of methyl propanal (in limonene) during storage

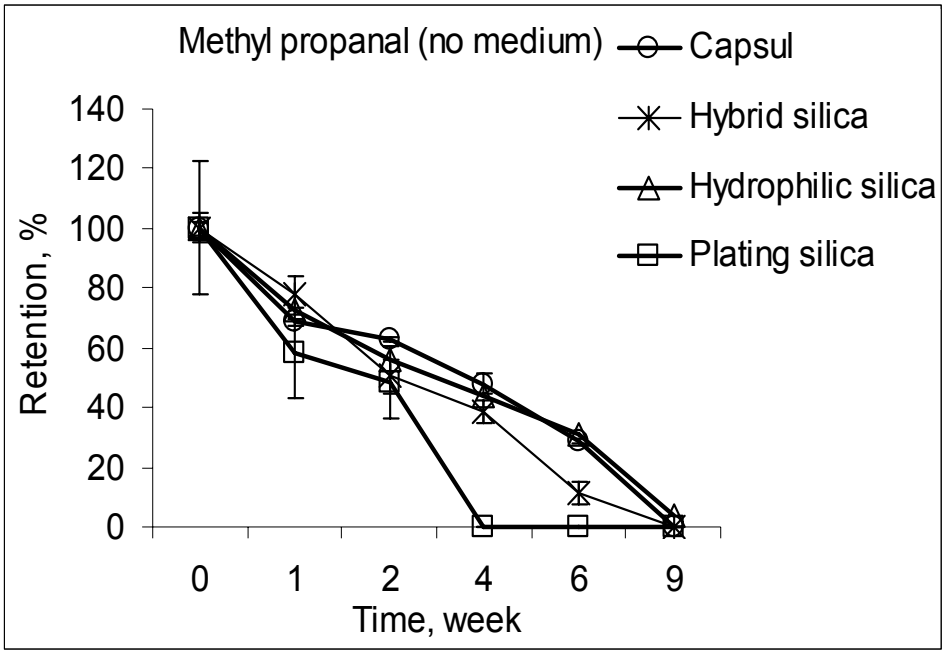

Figure 5-7: The influence of different capsule formation processes on the loss of methyl propanal (neat) during storage

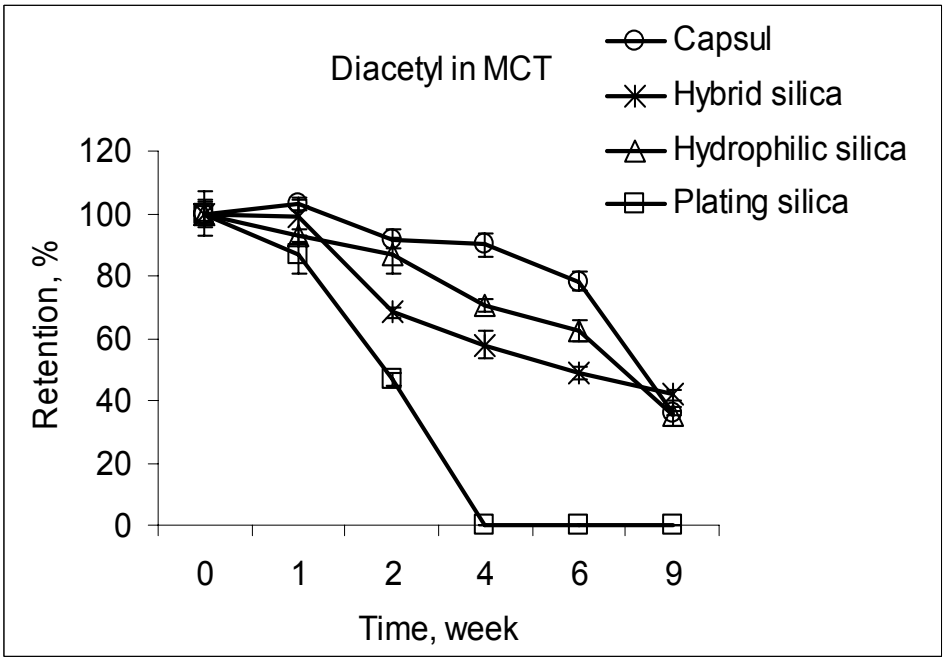

Figure 5-8: The influence of different capsule formation processes on the loss of diacetyl (in MCT) during storage

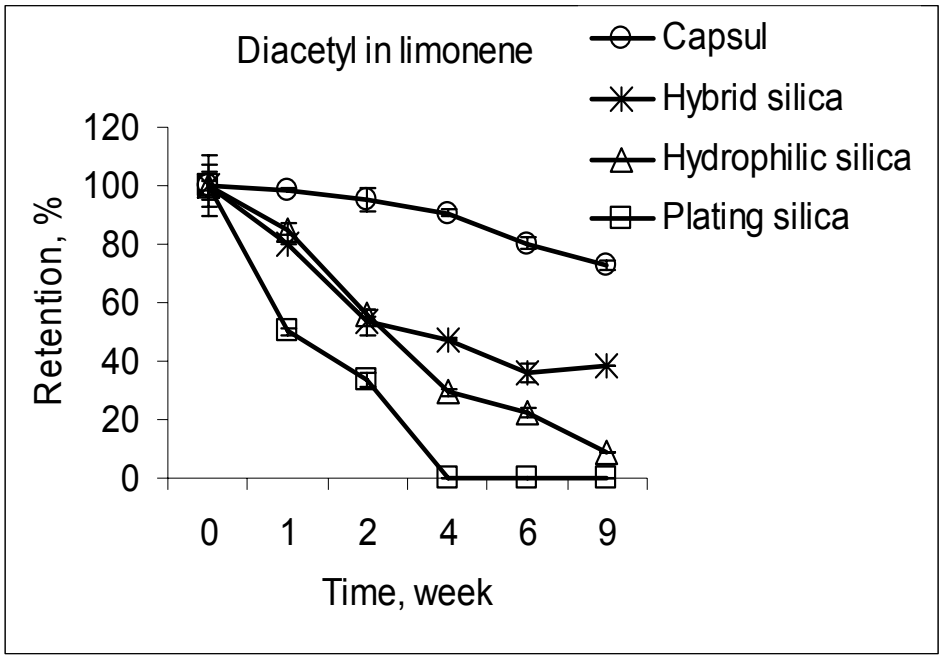

Figure 5-9: The influence of different capsule formation processes on the loss of diacetyl (in limonene) during storage

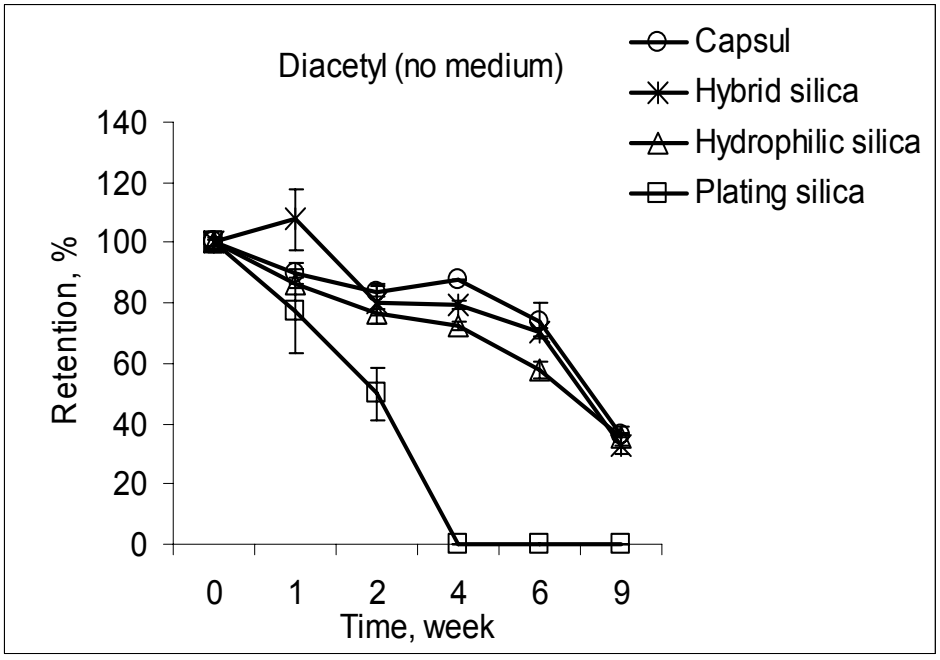

Figure 5-10: The influence of different capsule formation processes on the loss of diacetyl (neat) during storage

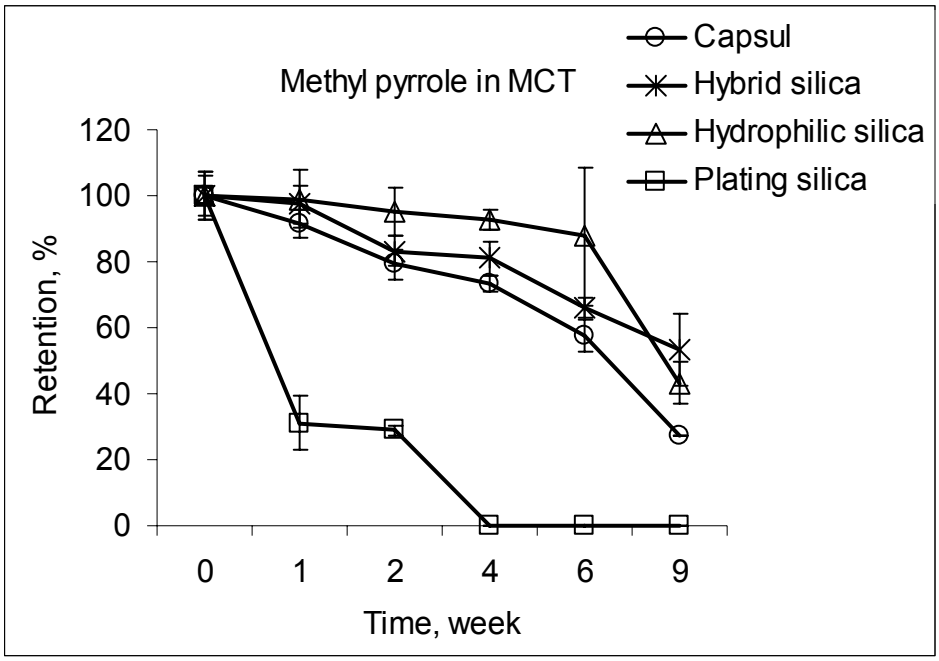

Figure 5-11: The influence of different capsule formation processes on the loss of methyl pyrrole (in MCT) during storage

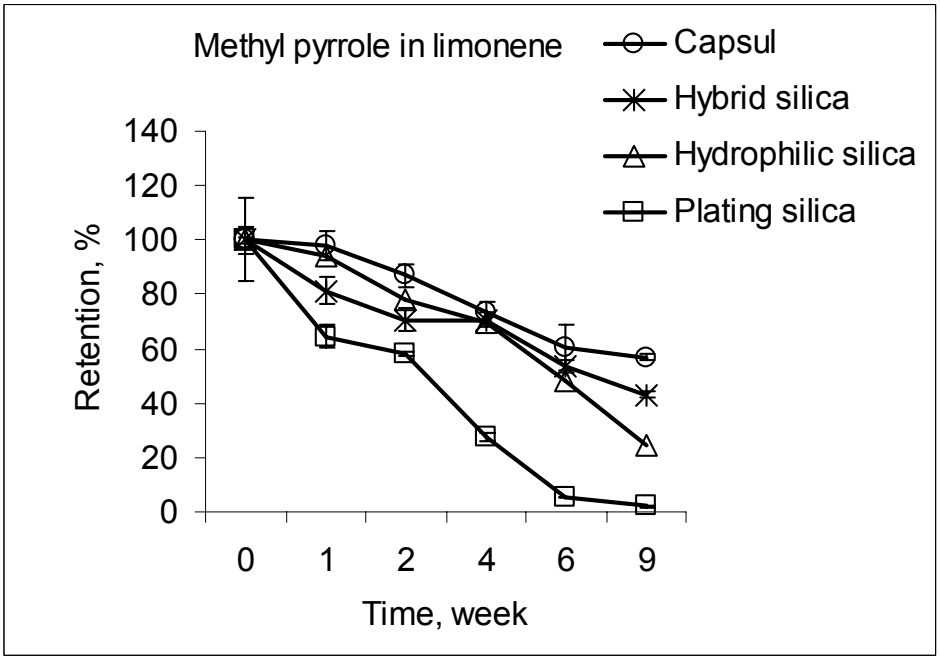

Figure 5-12: The influence of different capsule formation processes on the loss of methyl pyrrole (in limonene) during storage

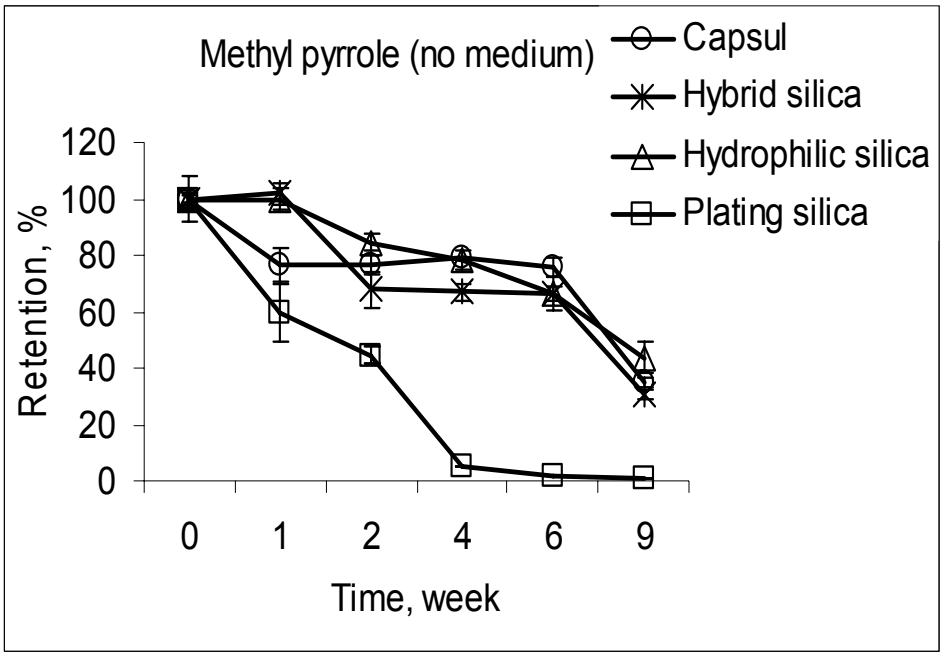

Figure 5-13: The influence of different capsule formation processes on the loss of methyl pyrrole (neat) during storage

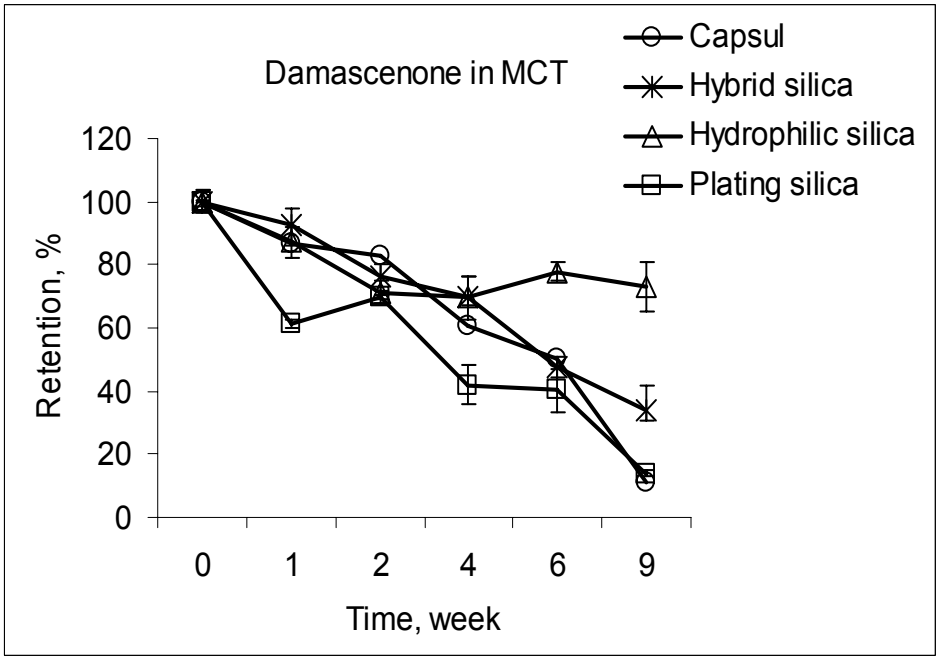

Figure 5-14: The influence of different capsule formation processes on the loss of damascenone (in MCT) during storage

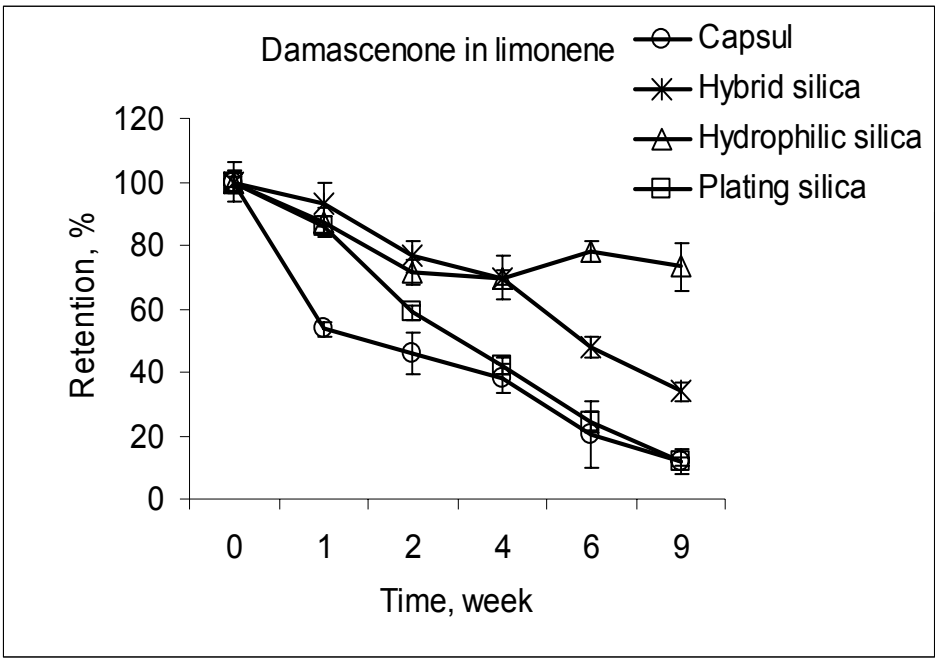

Figure 5-15: The influence of different capsule formation processes on the loss of methyl pyrrole (in limonene) during storage

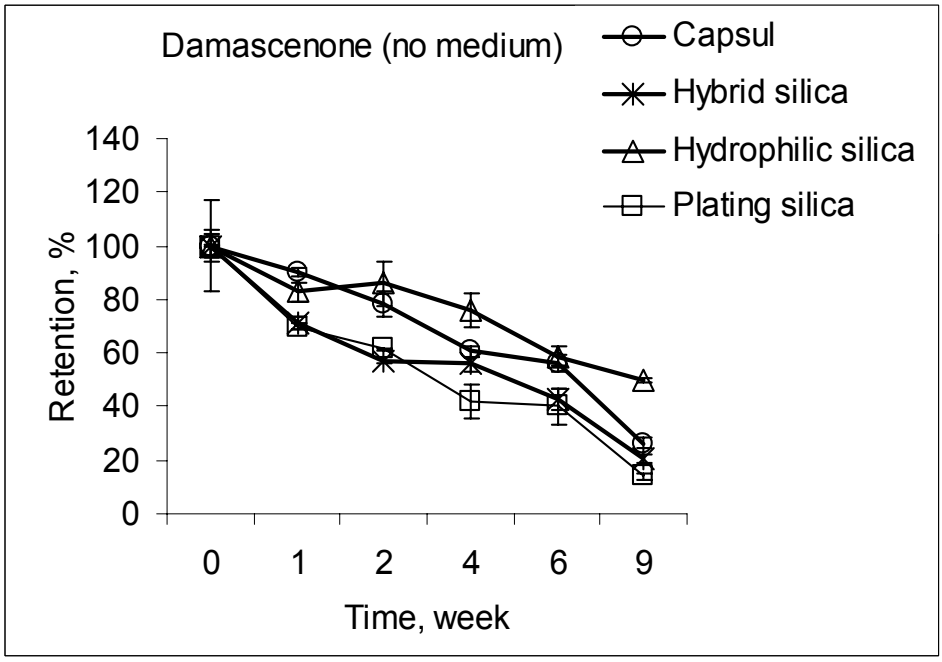

Figure 5-16: The influence of different capsule formation processes on the loss of methyl pyrrole (in neat) during storage

Table 5-1: Physicochemical properties of compounds present in the flavor mixture

Compounds	Molecular weight	Boiling point (°C)	Log P	µg /g of powder
Diacetyl	86	75	-1.7	500
Methyl propanal	72	88	0.72	500
Methyl pyrrole	81	112	1.43	2500
Damascenone	190	275	4.03	500

*Log P – Log of the partition coefficient, which is the ratio of the concentration of the compound in octanol and water (De Roos, 2000)

Table 5-2: Moisture content and particle size of the freeze-dried powders

Matrices	Moisture Content, %	Particle size , micrometers
Capsul/MCT	4.4	283.4
Capsul /Limonene	4.2	285.2
Capsul/neat	5.0	344.7
Hybrid silica blend/MCT	4.1	241.1
Hybrid silica blend/Limonene	4.0	268.7
Hybrid silica blend/ neat	3.9	267.2
Hydrophilic silica blend/ MCT	4.3	184.5
Hydrophilic silica blend/Limonene	4.4	273.0
Hydrophilic silica blend/neat	4.1	346.9
Plating silica/MCT	3.9	31.3
Plating silica/Limonene	4.3	31.3
Plating silica/neat	5.2	31.3

*Values are the average of three reproducible readings

Table 5-3: Fischer LSD tests on % retention of flavor compounds during drying for different matrices

Matrices	% Drying			
	Methyl propanal	Diacetyl	Methyl pyrrole	Damascenone
Capsul/MCT	44.7 b	95.2 b	12.7 ef	65.2 c
Capsul/limonene	32.5 c	100.0 a	11.4 fg	31.0 f
Capsul/neat	51.1 a	100.0 a	44.0 b	100.0 a
Hybrid silica silica/MCT	22.4 de	66.8 c	3.7 h	83.7 b
Hybrid silica/limonene	51.2 a	100.0 a	12.1 ef	15.8 g
Hybrid silica/neat	19.5 f	100.0 a	17.4 d	51.7 d
Hydrophilic silica/MCT	23.6 d	100.0 a	3.9 h	31.6 f
Hydrophilic silica/limonene	16.7 g	100.0 a	8.5 g	53.4 d
Hydrophilic silica/neat	20.9 ef	100.0 a	14.8 de	39.7 e
Plating silica/MCT	6.3 h	10.5 f	36.7 c	94.5 a
Plating silica/limonene	7.7 h	20.3 d	13.3 ef	100.0 a
Plating silica/neat	7.9 h	16.6 e	61.9 a	66.7 c

* Different letters note significant differences between matrices

Table5-4: Fischer LSD test on slopes estimated for different flavor compounds for matrices during first week

Matrices	Slopes			
	Methyl propanal	Diacetyl	Methyl pyrrole	Damascenone
Capsul/MCT	7.6 a	-2.7 e	8.5 def	13.2 de
Capsul/limonene	8.2 a	1.3 de	2.1 f	46.3 a
Capsul/neat	31.3 a	10.2 cd	23.2 cd	10.1 de
Hybrid silica/MCT	27.9 a	0.77 de	2.5 ef	7.1 de
Hybrid silica/limonene	28.4 a	19.7 bc	18.6 de	6.2 de
Hybrid silica/neat	22.4 a	-7.7 e	-1.7 f	28.9 bc
Hybrid silica/MCT	11.8 a	13.3 bc	0.93 f	12.8 de
Hydrophilic silica/limonene	19.5 a	14.8 bc	6.1 ef	14.7 d
Hydrophilic silica/neat	26.9 a	23.1 b	-6.6 f	17.2 cd
Plating silica/MCT	28.3 a	22.5 b	40.6 b	0.80 e
Plating silica/limonene	28.2 a	13.5 bc	69.0 a	38.5 ab
Plating silica/neat	26.3 a	49.8 a	35.3 bc	13.7 d

*Different letters note significant differences between matrices

Table 5-5: Fischer LSD test on % retention of different flavor compounds for matrices after nine weeks

Matrices	% Retention of flavor compounds after nine weeks			
	Methyl propanal	Diacetyl	Methyl pyrrole	Damascenone
Capsul/MCT	9.1 b	35.9 cd	27.2 d	10.8 f
Capsul/limonene	28.7 a	72.9 a	56.9 a	11.9 f
Capsul/no solvent	0.0 d	36.3 cd	34.7 c	26.3 d
Hybrid silica/MCT	7.5 b	41.7 b	53.3 a	33.8 c
Hybrid silica/limonene	8.5 b	38.3 c	42.9 b	39.5 c
Hybrid silica/neat	0.0 d	32.8 e	30.5 cd	20.4 de
Hydrophilic silica/MCT	3.1 c	35.0 de	43.2 b	73.1 a
Hydrophilic silica/limonene	4.5 c	8.6 f	24.2 d	39.6 c
Hydrophilic silica/neat	4.0 c	35.8 cd	43.8 b	49.8 b
Plating silica/MCT	0.0 d	0.0 g	0.7 e	0.0 g
Plating silica/limonene	0.0 d	0.0 g	0.0 e	14.0 ef
Plating silica/neat	0.0 d	0.0 g	2.1 e	11.7 f

*Different letters note significant differences between matrices

Chapter 6 : Flavor release from sol-gel silicate matrices (Study 3)

Abstract

Previous studies on flavor encapsulation in silicate matrices synthesized by the sol-gel process have showed limited value because the silica remains porous to the flavorants. We have attempted 2 ways to address this problem: 1) introduction of long chain alkyl groups into the silicate network; and 2) blending alkyl modified (hybrid) and unmodified sol-gel silicate (hydrophilic) matrices with a commercial emulsifying starch (Capsul™). The latter is an effort to fill the silica polymer structure with a food polymer thereby "plugging" the pores. In the current work, we have evaluated the efficacy of these proposed matrices by examining the release profiles of encapsulated flavor compounds using a real-time MS technique. A model flavor mixture consisting of diacetyl, methyl propanal, methyl pyrrole, and damascenone was incorporated into medium chain triglycerides (MCT's), limonene and neat before being added into the silica-based matrix. Analysis of variance (ANOVA) was conducted on the properties of the curve: cumulative area under the curve (AUC), maximum intensity reached (I_{max}), time required to reach maximum intensity (T_{max}), increasing slope in the linear portion of the curve or rate of increase, and surface release. ANOVA revealed that the interaction between the carriers and solvents showed a significant effect on most release characteristics (AUC, I_{max}, surface release, increasing slope) for all the matrices. The differences in release properties between matrices were primarily attributed to the differences in retention during drying; the effect of which may have surpassed the effect of flavor solvents or manufacturing formulation/process. However, there were some compound specific deviations to this hypothesis. Other factors that may explain exceptions to the hypothesis proposed were the location of the volatile substance in the particle and the affinity of solvents for the flavor compound.

Introduction

Flavor release in consumer applications is a critical performance criterion affecting flavor perception and thus, consumer acceptance of a food product. Flavor release is a function of the encapsulation system used in preparing a food flavoring. The two primary factors that principally govern flavor release are the inherent driving force for release, i.e. the vapor pressure of a flavor compound, and the resistance to mass transport from the product to air (kinetic factor) (De Roos, 2000). Therefore, in order to control the release of volatile flavor molecules, it is important to consider the above mentioned factors. While the relative volatility of a flavor compound is altered as a result of its interactions with other food constituents (carbohydrates, proteins etc), mass transfer is primarily altered due to diffusion considerations. One approach to control the diffusion mechanism involves encapsulating the flavoring (Pothakamury and Barbosa-Canovas, 1995).

Specifically, encapsulation is defined as a process by which a single or a mixture of molecules is entrapped within different types of coating materials (Balassa and Fanger, 1971). The release mechanisms from encapsulated systems may be broadly classified into: 1) diffusion based; 2) chemical reaction based; and 3) solvent activation or dissolution based systems (Baker, 1967). Since most food grade coating materials (gums, hydrolyzed and emulsifying starches) used for encapsulation are soluble in water, dissolution is the primary mechanism of release from these systems (Shahidi and Han, 1993; King, 1995; Risch and Reineccius, 1995).

In contrast to carbohydrate based carriers, diffusion is the primary mechanism of release of entrapped chemical species from porous sol-gel matrices (Veith et al., 2005). In diffusion controlled systems, flux from flavor containing phase to air/water interface is proportional to k_w A ΔC, where k_w is the mass transfer coefficient of the flavor in the water phase, A is the interfacial area and ΔC is the concentration gradient between the matrix containing the flavor and the water/air interface (Pothakamury and Barbosa-Canovas, 1995). Diffusion mechanism can be further sub divided into two types: 1) molecular or static diffusion; and 2) eddy or convective diffusion. While molecular diffusion is a result of random movement of molecules in a

stagnant fluid; eddy diffusion is caused when elements of fluid are transported along with the dissolved solute. It has been reported that the rate/flux of eddy diffusion is typically much higher than the rate of molecular diffusion (De Roos, 2000).

In chapter 5, we have conducted a comprehensive evaluation of drying and storage losses of flavor compounds encapsulated in the sol-gel matrices. In this chapter, we will describe the release characteristics of flavor compounds from the sol-gel matrices. Specifically, we have used a Proton Transfer Reaction-Mass Spectrometer (PTR-MS) to measure the release of flavor compounds from encapsulated matrices in the liquid applications. It is interesting to note that, eddy diffusions plays an important role in several applications (e.g. tea and coffee, soup mixes, candies etc), where food is consumed in liquid form (De Roos, 2000).

Briefly, PTR-MS is a chemical ionization technique used for the continual monitoring of concentration/time dynamics of volatile compounds present in complex mixtures (Lindinger et al., 1998; Hansel et al., 1995). The detailed description of the instrument has been previously provided in Chapter 1. The key objective of this study was to examine the release profiles of silica sol-gel matrices in a controlled experimental set up containing water. This exercise was performed by evaluating the properties of the release curves: total area under the curve (AUC) (measured by the trapezium method in Microsoft Excel 2003); maximum intensity reached (I_{max}); time required to reach maximum intensity (T_{max}); rate of increase (estimating the increasing slope in the linear portion of the curve); and finally surface release (surface release was calculated by estimating the area under the curve prior to the addition of water with only purging of air). Note that, the release measurements of the powders were made immediately after they were freeze-dried.

Materials and Methods

Materials and Methods in this work are identical to the description provided earlier in Chapter 5. The release measurements were made only for samples containing solvents (MCT and limonene).

Characterization of the freeze-dried powder

The powders were characterized for their particle size, moisture content, retention during drying and real-time measurement of release. The procedure for particle size, moisture content and retention during drying has been provided in Characterization of the freeze-dried powder in Chapter 5.

Real-time measurement of release

Figure 6-1 shows the experimental set up for the measurement of release (Courtesy: Nestle Research Center, Lausanne, Switzerland). A double-jacketed glass cell (350 ml glass vessel) was held at 75°C with a circulating water bath. The cell was connected to a double-jacketed burette filled with 100 ml of water (75°C) with the circulating water bath. The whole set-up was held at a temperature higher than 75°C in an oven heated (100°C) to avoid cold points and water condensation. The sample cell was connected to the fix-mounted top cover to be easily disconnected and filled with the sample. The headspace was purged continuously with compressed air (200 ml/min) through heated tubes penetrating through the fix-mounted top of the cell. Prior to the analysis by PTR-MS, the sample purge gas was diluted with 2 L/min of dry air in order to prevent the saturation of the mass spectrometer. When all the set-up had been thermo-stabilized, 30 mg of sample was added to the glass vessel. Subsequently, the 100 ml hot water in the burette was quickly dispensed into the sample cell and the release measurements were made. This procedure was carried out very quickly to avoid temperature changes in the sample, oven, and headspace vessel. The mixture was continuously stirred during the measurement. The flow rate of the capillary connected to the PTR-MS was 17 ml/min. The release of aroma compounds was monitored on-line with a PTR-MS in the MID (Multiple Ion Detection) mode.

PTR-MS instrumental parameters were as follows: drift tube pressure, 2 mbar; drift tube temperature, 60° C; drift voltage, 600 V. Methyl propanal, diacetyl, methyl pyrrole and damascenone were monitored as masses 73, 87, 82 and 191, respectively for a period of 10 minutes. The dwell times for these ions were every 50 ms, 50 ms, 0.1 s and 0.2 s, respectively. Masses 21 and 37 had dwell times of 0.1 s and 0.2 s, respectively. Five replicates of each sample were used to determine the release profiles.

Data Analysis

Raw PTR-MS data was converted to concentrations in parts per billion (ppbv). The data obtained from the release of the eight different encapsulated powders were analyzed by analysis of variance (ANOVA) on the properties of the curve: AUC; I_{max}; T_{max}; increasing slope in the linear portion of the curve; and surface release utilizing R statistical software (2008) for each of the 8 combinations of carriers and solvents. When a factor effect or an interaction was found to be significant, as indicated by a significant F test ($P \leq 0.05$), differences between the respective means were determined using Fischer Least Significant Difference test (LSD). The equation for the estimation of concentration in ppbv is given below:

$$R_{[ppbv]} = \frac{RH^{+}.\ 10^{9}.U\,[V].2.8\ [\mathrm{cm}^2/Vs].\ 22400.\ 1013^2\ [mbar^{\,2}].\ (273.15 + T_d)^2\ [K^2].Tr_{H3O+}}{k_i\ [\mathrm{cm}^3/\mathrm{s}].\ 9.2^2\ [cm^2].\ H_3O^{+}{}_0.\ p_d{}^2\ [\mathrm{mbar}^2].6.022.10^{23}.\ 273.15^2\ [\mathrm{K}^2].\ Tr_{(RH+)}}$$

where t is the residence time of the primary ions in the drift tube (~ 106 μs), k is the proton-transfer reaction rate constant (2×10^9 cm^3/sec) which corresponds to the ion-molecule capture collisions, U is the drift voltage, T_d is the drift tube temperature [°C], p_d is the drift tube pressure [mbar], $Tr_{(....)}$ is the mass dependent transmission for the respective ions. RH^+ and H_3O^+ are the count rates of the protonated volatile compound and the primary ion, respectively. A 3D scatterplot was designed using statistical software Minitab 15 trial version (State College, Pennsylvania) to evaluate the

relationship between the matrices based on the three main response variables (a1- AUC; a2- I_{max}; and a3 – surface release) for different compounds.

Results and Discussion

To reiterate, the volatile release measurements were made for samples containing solvents (MCT and limonene). The eight samples evaluated are listed below: 1) hybrid silica blend (MCT); 2) hybrid silica blend (limonene); 3) hydrophilic silica blend (MCT); 4) hydrophilic silica blend (limonene); 5) plating silica (MCT); 6) plating silica (limonene); 7) Capsul (MCT); and 8) Capsul (limonene). Capsul and plating silica were used as control samples.

Overall our experiments revealed four common observations: 1) From ANOVA, we found that the interaction between the carriers and solvents showed a significant effect on most release characteristics (AUC, I_{max}, surface release, slope) for all the compounds; 2) There were no significant differences in T_{max} for volatiles across matrices; 3) The release patterns for each volatile were similar between matrices exhibiting a strong burst of release instantly after the addition of water; 4) Plating silicas (limonene) exhibited higher surface release intensities for all compounds (better performing encapsulated matrices should have lower quantities of flavor on the surface and thus, less surface release). However, while we observed that all the compounds exhibited the above mentioned common behavior, compound specific differences were observed across the matrices. These specific differences across matrices for each compound are discussed below.

Methyl propanal

Table 6-1 shows the results of Fischer LSD test conducted on the release properties of the curves (AUC, $I_{max,}$ surface release, slope). From the 3D scatterplot (Figure 6-2), it can be seen that methyl propanal encapsulated in the hybrid silica blend (limonene) showed the highest total release (highest AUC), I_{max} and slope. Examining the

performance of the freeze-dried encapsulated samples, this matrix had the highest retention of methyl propanal during drying (51.2 %). The increased concentration of the compound in this matrix likely is responsible for the highest and fastest release of this compound.

The relationship between the % retention during drying and response variables (AUC, I_{max} and slope) for the eight matrices was determined using a scatterplot in Microsoft Excel. A linear relationship (acceptable R^2 values) was observed between the % retention during drying and three main response variables (AUC, I_{max} and slope) confirming that higher quantities of the compound in the final dry samples resulted in higher release (Figure 6-3). There were some inconsistencies to this general observation.

One of the inconsistencies was methyl propanal loaded onto plating silica (MCT) which showed a relatively higher release rate and intensity in spite of lower having lower retention (6.3 %) during drying. In fact, the release properties (AUC, I_{max} and rate of increase) from the plated silica were not significantly different from that of the Capsul product which had higher retention (45 %) during drying. As plating involves an adsorption process, it is possible that the flavor compounds may remain in close proximity to the surface during the blending process. This implies that the distance required to reach the air-water interface is less. This may have also contributed to the faster release in this matrix.

The properties of the release curves were not statistically different between the other sol-gel matrices (hydrophilic blends (MCT and limonene) and hybrid blends (MCT)). These matrices also showed similar % retention during freeze drying.

Methyl pyrrole

Table 6-2 shows the results of Fischer LSD test conducted on the release characteristics of methyl pyrrole (AUC, $I_{max,}$ surface release, slope). From the 3D

scatterplot (Figure 6-4) grouping, it can be seen that silica sol-gel matrices (hybrid and hydrophilic) did not exhibit differences in their release properties.

The two high I_{max} values were exhibited by the control samples plating silicas (limonene) and Capsul (MCT). Their retentions during drying were 36.7 % and 12.7 %, respectively. Plating silicas (limonene) also exhibited higher quantities of this compound on the surface indicated by the higher surface release value (ten times higher than the other matrices). This greater presence of the compound on the surface is likely to have contributed for the higher I_{max}. Alternatively, higher I_{max} values in Capsul (MCT) may have been due to the greater solubility of the starch in water than silicas. As a result of methyl pyrrole's (moderately hydrophobic compound) lower affinity with water, this result is likely to be observed.

Plating silica (MCT) showed a bimodal peak. MCT being viscous, there is a possibility for inhomogeneous distribution of flavors during the blending process resulting in bimodal peaks. As most matrices had lower or similar retentions of methyl pyrrole, the association between the % retention during drying and response variables (AUC, I_{max} and surface release) was less significant (Figure 6-5).

Diacetyl

Table 6-3 shows the results of Fischer LSD test conducted on the diacetyl release characteristics (AUC, $I_{max,}$ surface release, slope). Diacetyl incorporated into limonene prior to encapsulation showed higher I_{max} values than when incorporated into MCT with the exception of plating silica (limonene). In addition, the rate of increase was also the highest in matrices containing limonene. Examining the drying data shows that matrices containing limonene had higher retentions of diacetyl than matrices containing MCT. This increased concentration of diacetyl likely contributed to its increased release. In addition, van Ruth et al. (2000) have demonstrated a higher release of hydrophilic compounds when loaded with vegetable oil prior to its encapsulation in alginate beads and proposed that this is due to the increase in relative volatility of hydrophilic

compounds in the hydrophobic environment. Although both solvents used in our study were hydrophobic, limonene is more hydrophobic than MCT and this may have caused a similar effect and as a result increased the release of this hydrophilic molecule

The retention of diacetyl during drying for some of the generated silica sol-gels (hybrid silica (limonene), hybrid silica (MCT and limonene)) and control samples (Capsul (MCT and limonene)) were close to 90-100 %. In spite of having similar retention of the compound, the release characteristics differed between these matrices.

From the 3D scatterplot (Figure 6-6), it can be observed that diacetyl encapsulated in hybrid silica blend (limonene) showed the highest total release and I_{max}. Hydrophilic silica blends (MCT and limonene) exhibited lower release intensities despite showing similar retention to hybrid silica blend (limonene). Analyzing the results of surface release revealed that these hydrophilic silica blends exhibited the highest surface release irrespective of the solvent used. The lower intensities of AUC and I_{max} after the water addition in these sol-gels may have been due to the higher release of the compound prior to the addition of water. The amount of flavor retained on the silicate surface is dependent on the polarity of the molecule. In addition, it has been reported that the hydroxyl groups on the silicas are generally located on the surface (Iler, 1979). Methyl propanal and diacetyl being polar molecules can interact with these hydroxyl groups and remain on the surface during the flavor blending process, thereby showing higher surface release. In addition, these silica blends are likely to have more interaction with diacetyl due to their common hydrophilic nature.

In contrast to methyl pyrrole, most matrices had higher retentions of diacetyl, therefore, the association between the % retention during drying and response variables (AUC, I_{max} and surface release) was less significant (Figure 6-7).

Damascenone

Table 6-4 shows the results of Fischer LSD test conducted on the release characteristics of damascenone (AUC, $I_{max,}$ surface release, slope). In spite of the loading of damascenone (800 ppm) being similar to the other compounds (diacetyl and methyl propanal) and its superior retention during drying, the concentration (ppbv) released during the dynamic release process was relatively less during preliminary experiments. This was primarily due to two reasons: 1) slower mass transfer of this compound in the transfer line (connected from the oven containing the experimental set-up to the PTR-MS); and 2) condensation of this high molecular weight compound in the drift tube. This issue was corrected by heating the transfer line and drift tube using a silicone heating tape.

Damascenone incorporated into limonene had a relatively lower release of damascenone (in contrast to diacetyl) than when incorporated into MCT (Figure 6-8). Further, matrices containing MCT's had huge amounts of damascenone on the surface as was demonstrated by the surface release values. Examining the retention of damascenone during drying showed that higher levels of damascenone were retained when MCT was used as a solvent than when limonene was used as a solvent (with one exception - plating silica). This difference in concentration resulting from solvent choice likely explains the observed differences in release. The dissimilarities in the release properties between the hybrid and hydrophilic silica blends were also attributed to the differences in the concentrations of damascenone. These results are further corroborated by the data presented in Figure 6-9 which showed a linear relationship between the % retention and response variables (AUC, I_{max} and increasing slope). There were some deviations from this general observation.

One of the main deviations was that Capsul (MCT) (65.2 % retention) exhibited similar release intensities to plating (MCT) (90-100 %). As previously pointed out, higher release of the compound in Capsul may have been due to greater solubility of the carrier in water.

Hybrid silica blends were used assuming they would render a more controlled release (delayed T_{max} than hydrophilic silica blends) for hydrophobic compounds. Theoretically, damascenone, being a highly hydrophobic compound (log P-4.43), incorporated into hybrid silica blends should have relatively slower release compared to hydrophilic silica blends. However, these effects were not observed as the initial concentrations varied between the matrices. Similar to methyl pyrrole, bimodal peaks were obtained for plating silica (MCT).

Summary

Overall, plating silica (limonene) exhibited the highest surface release of all matrices. The reason for this for this may be: 1) larger amounts of flavor close to the surface rather than diffusing into the pores during the blending process and/or 2) the small particle size of the plating silica. The plating silicas had smaller particle sizes (31 μm) and therefore, higher specific surface area compared to other matrices, which had particle sizes between 200 and 400 μm (Table 5-2 from Chapter 5).

The differences in release properties between matrices were primarily attributed to the differences in retention during drying; the effect of which may have surpassed the effect of flavor solvents or manufacturing formulation/process. However, there were some compound specific deviations to this hypothesis. Other factors that may explain exceptions to the hypothesis proposed were the location of the volatile substance in the particle and the affinity of solvents for the flavor compound.

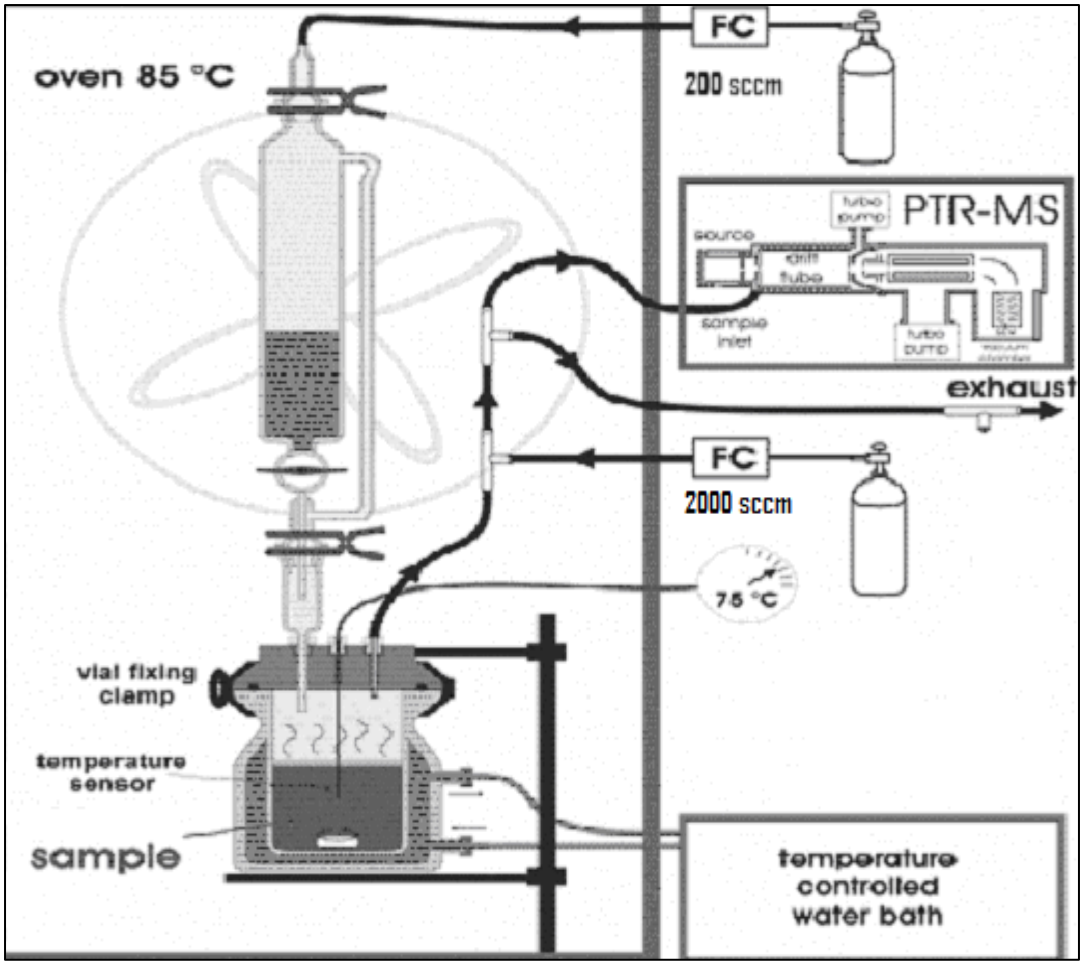

Figure 6-1: Flavor release sampling system (Nestle Research Center)

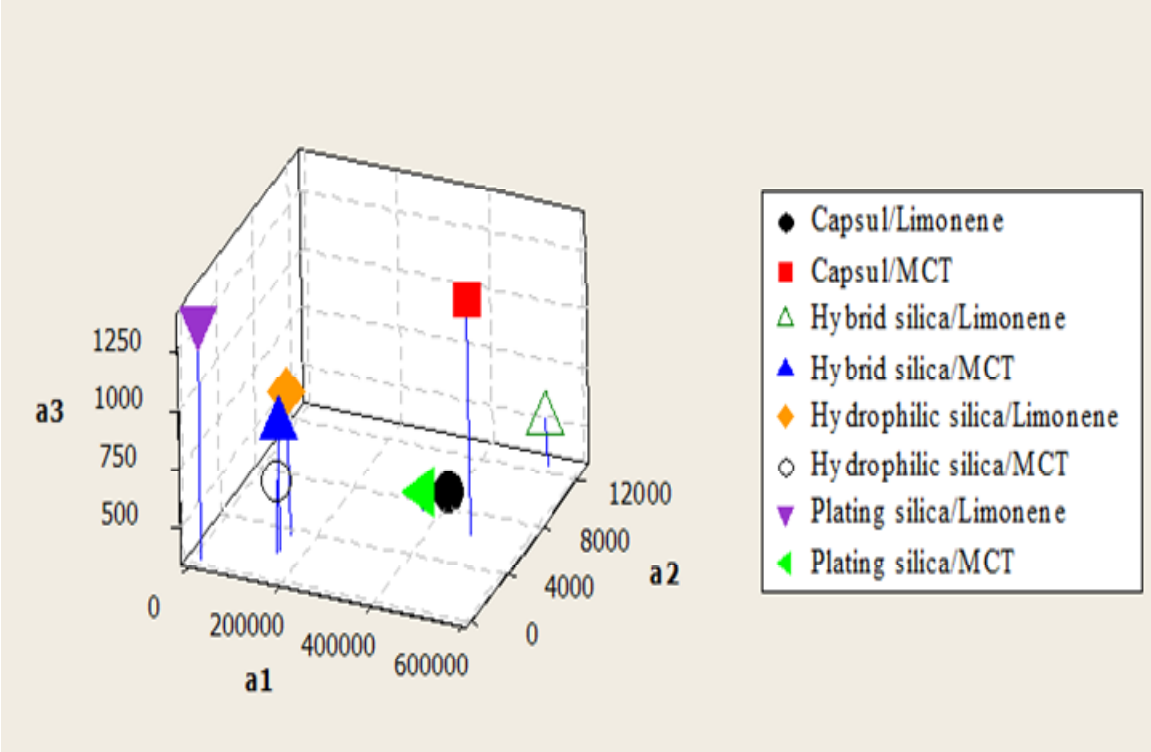

Figure 6-2: Three dimensional scatter plot for methyl propanal, a1- AUC (ppb); a2-I_{max} (ppb); a3 – surface release, (ppb)

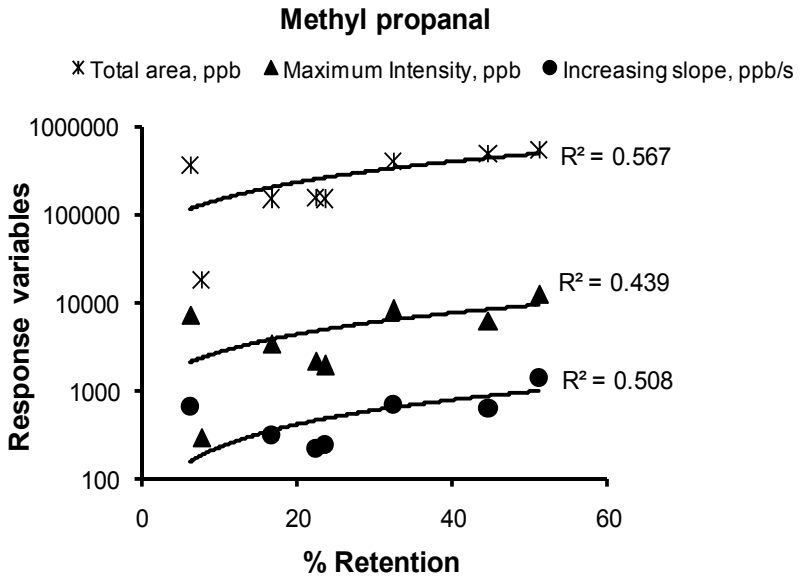

Figure 6-3: The influence of volatile retention during drying on volatile release

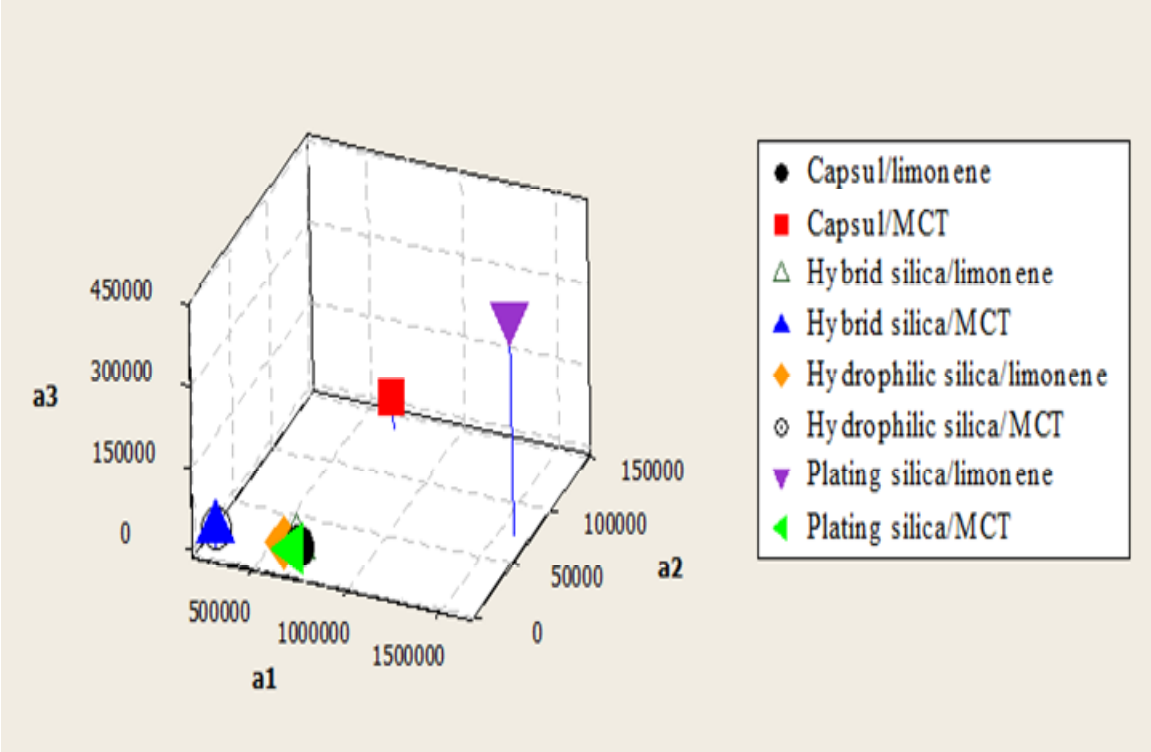

Figure 6-4: Three dimensional scatter plot for methyl pyrrole, a1- AUC (ppb); a2-I_{max} (ppb); a3 – surface release, (ppb)

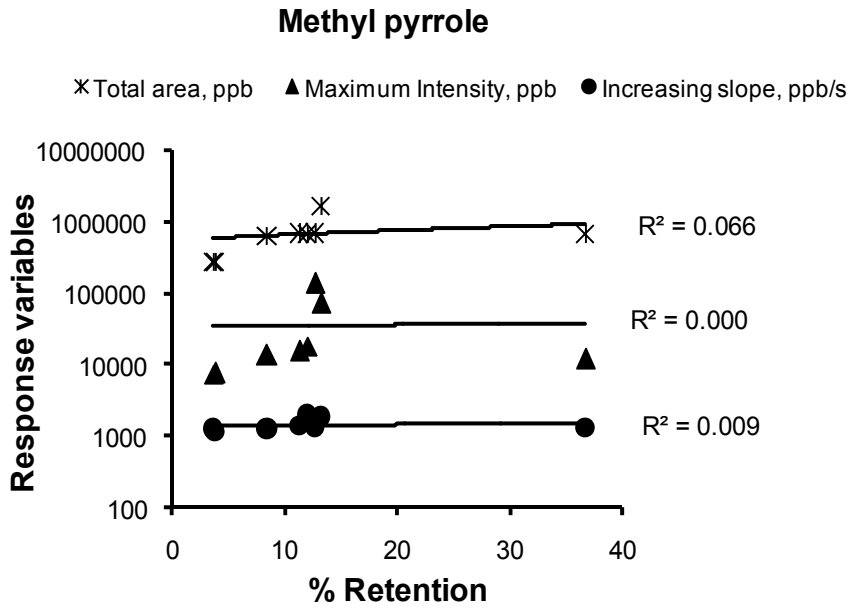

Figure 6-5: The influence of volatile retention during drying on volatile release

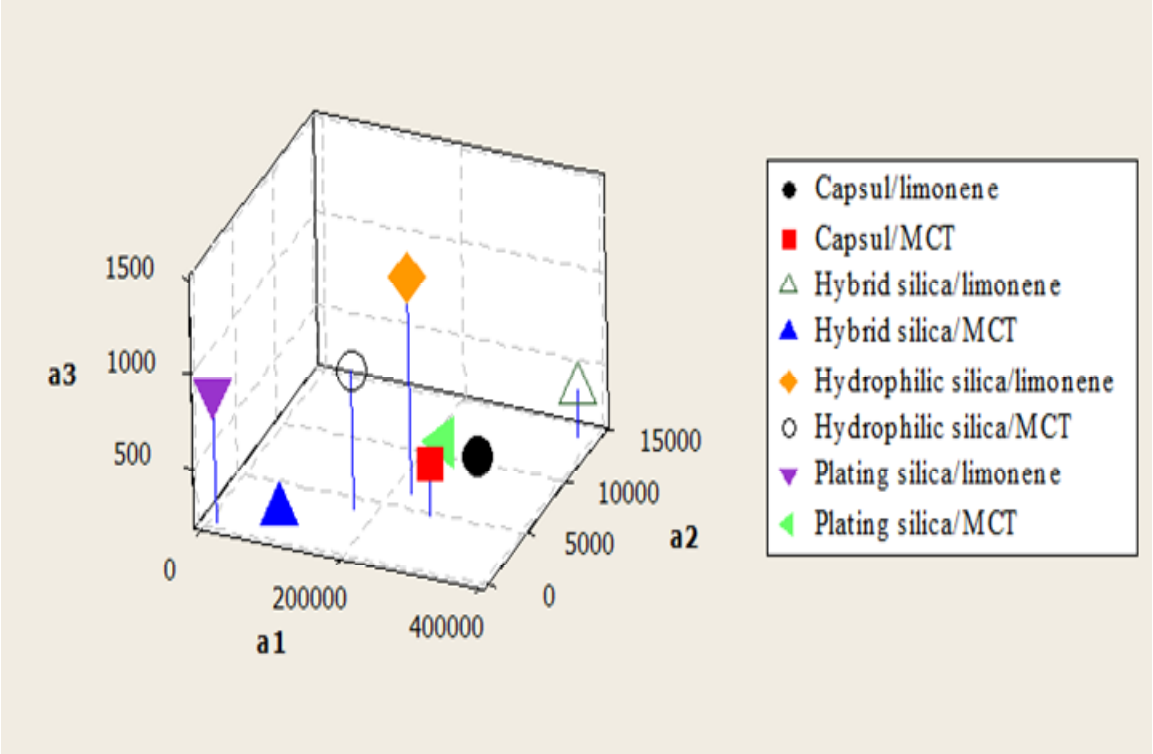

Figure 6-6: Three dimensional scatter plot diacetyl, a1- AUC (ppb); a2-I_{max} (ppb); a3 – surface release, (ppb)

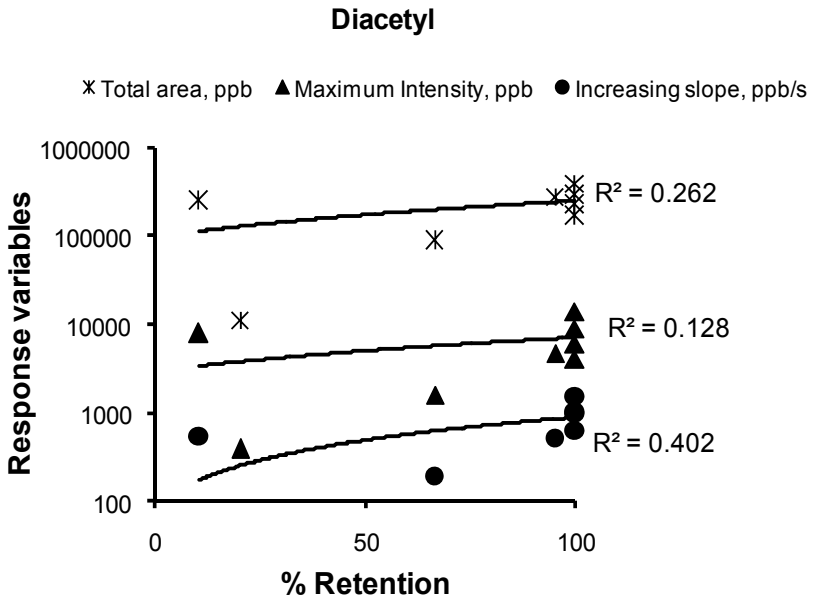

Figure 6-7: The influence of volatile retention during drying on volatile release

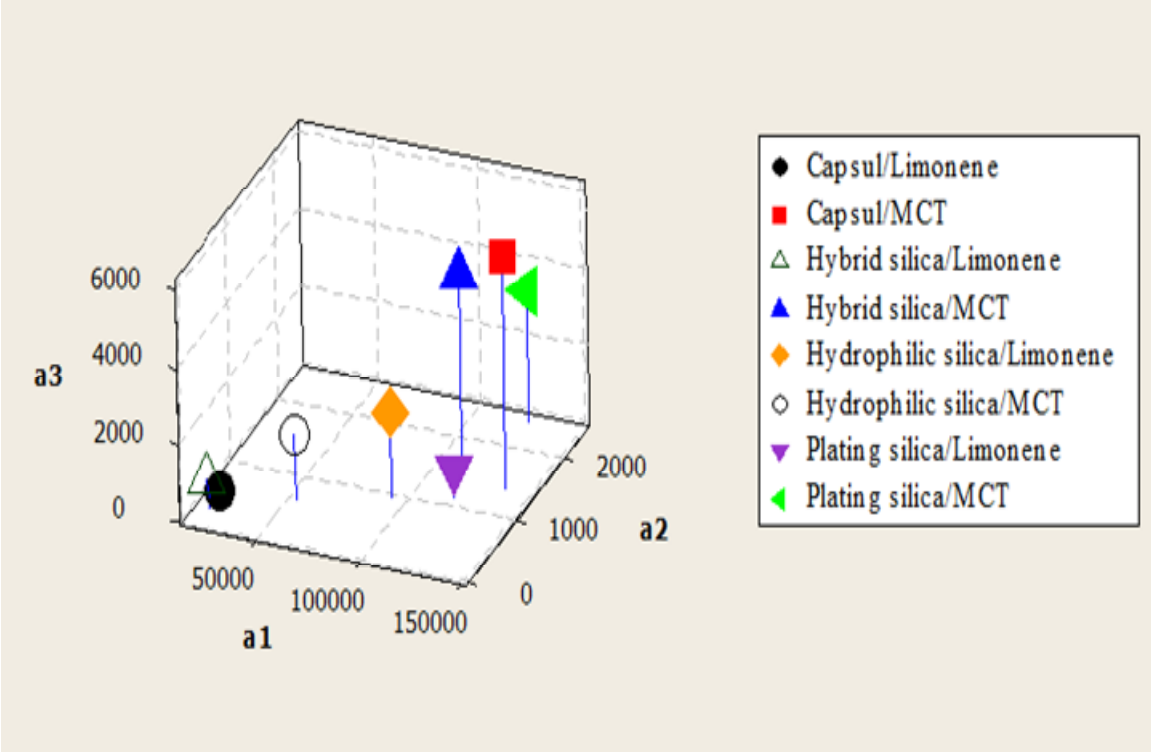

Figure 6-8: Three dimensional scatter plot for damascenone, a1- AUC (ppb); a2-I_{max} (ppb); a3 – surface release, (ppb)

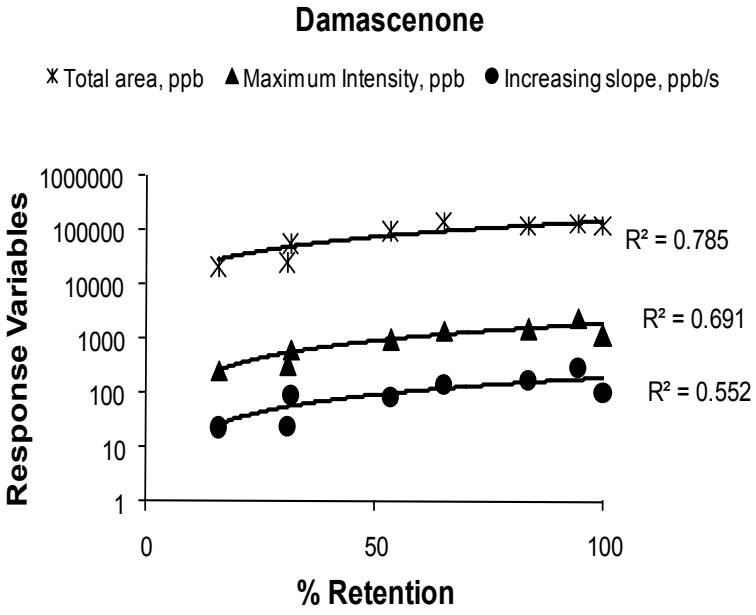

Figure 6-9: The influence of volatile retention during drying on volatile release

Table 6-1: Fischer LSD on the properties of the release curves for methyl propanal

Matrices	Cumulative area of the curve (ppb)	I_{max} (ppb)	Surface release (ppb)	Increasing slope of the curve (ppb/s)	T_{max} (s)	% Retention during drying
Capsul/MCT	489693.6 a	6219.7 c	1357.0 a	618.4 bc	73.3	44.7 b
Capsul/limonene	400569.8 b	8220.5 b	394.0 d	693.3 b	73.6	32.5 c
Hybrid silica/MCT	152738.3 c	2221.4 d	875.2 bc	220.6 d	72.3	22.4 d
Hybrid silica/limonene	531656.6 a	12550.0 a	530.3 cd	1417.7 a	69.8	51.2 a
Hydrophilic silica/MCT	150739.1 c	1921.3 d	656.2 bcd	238.6 d	70.3	23.6 d
Hydrophilic silica/limonene	149584.6 c	3480.7 d	960.3 b	309.0 cd	72.5	16.7 f
Plating silica/MCT	365406.5 b	7325.8 bc	426.1 d	669.1 bc	73.0	6.3 g
Plating silica/limonene	17915.1 d	299.8 e	1365.5 a	39.2 d	68.8	7.7 g

*Different letters note significant differences between matrices

Table 6-2: Fischer LSD on the properties of the release curves for methyl pyrrole

Matrices	Cumulative area of the curve (ppb)	I_{max} (ppb)	Surface release (ppb)	Increasing slope of the curve (ppb/s)	T_{max} (s)	% Retention during drying
Capsul/MCT	685556.1 b	135784.8 a	46635.3 b	1319.5 b	72.8	12.7 ef
Capsul/limonene	678316.9 b	15325.2 c	8169.4 b	1358.2 b	73.5	11.4 fg
Hybrid silica/MCT	269314.0 c	7331.5 c	27898.9 b	1230.0 b	70.4	3.7 h
Hybrid silica/limonene	654531.6 b	18242.1 c	8113.1 b	1951.1 a	69.3	12.1 ef
Hydrophilic silica/MCT	265877.5 c	7534.9 c	25897.1 b	1151.2 b	68.6	3.9 h
Hydrophilic silica/limonene	604910.6 b	13530.7 c	11512.7 b	1254.9 b	72.5	8.5 g
Plating silica/MCT	656538.0 b	11707.6 c	8150.9 b	1305.9 b	72.8	36.7 c
Plating silica/limonene	1587200.2 a	71085.5 b	394181.8 a	1822.5 a	69.6	13.3 ef

*Different letters note significant differences between matrices

Table 6-3: Fischer LSD on the properties of the release curves for diacetyl

Matrices	Cumulative area of the curve (ppb)	I_{max} (ppb)	Surface release (ppb)	Increasing slope of the curve (ppb/s)	T_{max} (s)	% Retention during drying
Capsul/MCT	272621.5 bc	4611.1 cde	464.0 c	501.5 bcd	73.3	95.2 b
Capsul/limonene	292687.8 b	8833.7 b	292.9 c	1020.2 ab	73.0	100.0 a
Hybrid silica/MCT	89721.52 e	1583.4 ef	241.8 c	186.7 cd	70.6	66.8 c
Hybrid silica/limonene	380681.3 a	13732.5 a	433.1 c	1482.1 a	69.3	100.0 a
Hydrophilic silica/MCT	168281.5 de	4004.5 def	920.4 b	622.1 bc	69.1	100.0 a
Hydrophilic silica/limonene	228681.4 c	5953.4 bcd	1340.6 a	974.7 ab	71.5	100.0 a
Plating silica/MCT	253443.2 bc	7852.7 bc	382.5 c	523.1 bcd	73.0	10.5 f
Plating silica/limonene	10720.5 f	384.0 f	878.8 b	53.7 d	70.1	20.3 d

*Different letters note significant differences between matrices

Table 6-4: Fischer LSD on the properties of release curve for damascenone

Matrices	Cumulative area of the curve (ppb)	I_{max} (ppb)	Surface release (ppb)	Increasing slope of the curve (ppb/s)	T_{max} (s)	% Retention during drying
Capsul/MCT	138098.2 a	1399.9 bc	5963.3 a	138.8 b	72.8	65.2 c
Capsul/limonene	24905.6 e	317.5 e	354.7 e	23.0 c	75.5	31.0 f
Hybrid silica/MCT	115273.6 b	1454.6 b	5111.4 a	161.7 b	72.3	83.7 b
Hybrid silica/limonene	20491.5 e	258.0 e	657.6 de	22.7 c	71.3	15.8 g
Hydrophilic silica/MCT	54204.6 d	625.1 de	2101.8 c	89.3 bcde	69.1	31.6 f
Hydrophilic silica/limonene	92759.2 c	941.5 cd	1687.8 cd	82.5 bc	74.9	53.4 d
Plating silica/MCT	126211.8 ab	2381.9 a	3297.0 b	278.4 a	74.2	94.5 a
Plating silica/limonene	119062.9 b	1110.4 bcd	647.7 de	94.3 bc	73.0	100.0 a

*Different letters note significant differences between matrices

Chapter 7 : Conclusions

The primary objective of this thesis was to develop an encapsulation technique that was economical and suitable for encapsulating complex flavor mixtures. For several years, silica matrices developed by the sol-gel process have been employed for the encapsulation of several molecules such as enzymes, proteins, nutraceuticals and fragrances. The sol-gel process is a chemical technique that involves a series of hydrolysis and polycondensation reactions of inorganic compounds resulting in the transformation of a colloidal suspension (sol) into a three dimensional network (gel or precipitate). Depending on the processing parameters (concentration of alkoxysilanes, time of hydrolysis and polymerization), the products generated can be a gel or precipitate. Several studies conducted with hydrophilic silicate matrices have illustrated the poor retention of hydrophobic molecules. The rationale explained for this drawback was two fold: 1) lack of interactions between the hydrophobic molecules and the hydrophilic matrices, and 2) diffusion losses occurring due to the porous nature of silica. In order to address these issues, we developed alkyl modified silicate (hybrid) matrices through the sol-gel for encapsulating flavor molecules. These matrices were generated by co-hydrolyzing and co-polymerizing a simple alkoxysilane and a long chain alkylalkoxysilane.

Preliminary experiments (part 1) for the synthesis of silicate matrices undergoing gelation were performed using a protocol established in the literature. The simple alkoxysilane in the formulation was substituted with alkylalkoxysilane at different levels and the influence of this substitution was studied by evaluating the retention of limonene after drying (a hydrophobic compound present in orange oil) and the release of limonene an acetone-water mixture system. The results from this study showed that the addition of alkylalkoxysilane into the system had a positive effect; increasing the retention as well as providing controlled release of limonene. However, the formation of gels involved a grinding process resulting in enormous losses of the flavor compound.

Therefore, in preliminary experiments (part 2); the processing parameters of the sol-gel process were modified to result in the formation of precipitates. The product generated from this modified process settled at the bottom entrapping the molecule to be encapsulated. These experiments involved the development of a protocol for the formation of precipitates and identification of reaction variables (concentration of simple alkoxysilane and alkylalkoxysilane, time of hydrolysis of alkoxysilanes and time of polymerization) for the process. The results showed that increasing the concentration of alkoxysilanes higher than 6 % of water resulted in gels; which was not desirable. A colorimetric technique available in the literature was successfully employed to monitor the qualitative progress of the reaction.

In study 1, a response surface model (central composite design) was used to systematically study the influence of the various processing parameters on the characteristics of the product obtained. The observables chosen for the study were: 1) particle size of the system, and 2) % extractable or unencapsulated limonene from the system. A second order model was fit and the main effects of the predictor variables were studied on the means of the observables. The results from the study (regression analysis) indicated that all the predictor variables identified showed a significant effect on either of the response variables. However, no association was observed between the particle size of the system and % extractable limonene indicated by the R^2 value = 0.033. Therefore, the conditions of the optimized formulation that had delivered the lowest % extractable limonene were employed for our subsequent experiments. Followed by these, additional experiments were conducted specifically to study the influence of hydrophobic and hydrophilic silicas employing the conditions from the response surface design. The results from these experiments showed that increasing the concentration of hydrophilic silica precursor (simple alkoxysilane) decreased the % extractable limonene. This implies that more compact structures were generated at higher concentrations of simple alkoxysilanes. On the other hand, increasing the concentration of hydrophobic silica precursor (alkylalkoxysilane) increased the % extractable limonene. This was supported by observations from literature stating that the introduction of long chain alkyl groups

into matrices can result in less compact structures (due to steric hindrance offered by the long chain alkyl groups) resulting in lower encapsulation efficiencies.

In study 2, two optimized formulations of the sol-gel process (1) 6 % total silica precursor with no alkylalkoxysilane addition; and 2) 4 % total silica precursor with 25 % addition of alkylalkoxysilane) that delivered the lowest % extractable limonene were used for the encapsulation of a complex flavor mixture consisting of compounds having a wide range of partition coefficients. In order to further overcome the diffusion losses due to the porosity of silica, silicate matrices were blended with a commercial emulsifying starch prior to the freeze drying process. A model flavor mixture consisting of diacetyl, methyl propanal, methyl pyrrole, and damascenone was incorporated into solvents (medium chain triglycerides (MCT's), limonene and neat) before being added into the carrier matrix. In this particular study, we examined the efficacy of these proposed matrices by conducting a comprehensive evaluation of the stability of encapsulated flavor compounds in silica: starch blends during drying and storage. Their performance was compared to conventional flavor carriers Capsul and plating commercial silica. Results showed that Capsul (neat) had the highest retention for most compounds (except methyl pyrrole) during drying. Alternatively, commercial plating silicas (neat) exhibited the lowest loss (plating) of methyl pyrrole of all delivery systems. Overall**,** results from retention during drying/storage showed that diacetyl was retained relatively better than the other compounds. While Capsul (limonene) retained volatiles the best during storage (except damascenone); commercial plating silicas performed poorly irrespective of the flavor solvents used (retaining negligible amounts at the end of nine weeks).

In study 3, the influence of different flavor carrier materials and solvents was studied by evaluating the release profiles of flavor compounds from different matrices in a food application using the PTR-MS. Analysis of variance (ANOVA) was conducted on the properties of the curve: cumulative area under the curve (AUC), maximum intensity reached (I_{max}), time required to reach maximum intensity (T_{max}), increasing slope in the linear portion of the curve, and surface release. ANOVA revealed

that the interaction between the carriers and solvents showed a significant effect on most release characteristics (AUC, I_{max}, surface release, increasing slope) for all the matrices. The release patterns for each volatile were similar between matrices exhibiting a strong burst of release instantly after the addition of water. The differences in release properties between matrices were primarily attributed to the differences in retention during drying; the effect of which may have surpassed the effect of flavor solvents or manufacturing formulation/process. However, there were some compound specific deviations to this hypothesis. Other factors that may explain exceptions to the hypothesis proposed were the location of the volatile substance in the particle and the affinity of solvents for the flavor compound.

References

Askvold, B. (1977). Product for flavouring concentrated alcoholic beverages, preferably brandy and method for manufacturing the same. Danish patent 136,321. FSTA 76-06-H0808.

Baker, R.W. In *Controlled release of biologically active agents*; Eds., John Wiley and Sons, New York, **1987**, pp. 18-72.

Balassa, L. L.; Fanger, G. O. Microencapsulation in the Food Industry. *Crit. Rev. Food Technol.* **1971**, *2*, 245-247.

Bangs, W. E.; Reineccius, G. A. Influence of Dryer Infeed Matrices on the Retention of Volatile Flavor Compounds During Spray Drying. *J. Food Sci.* **1981**, *47*, 254-259.

Barbe, C.; Bartlett, J.; Kong, L.; Finnie, K.; Lin, H.Q. Silica particles: A novel drug delivery system. *Adv. Mater.* **2004**, *16*, 1959-1965.

Bell, J.W. (1993) Chewing gum or confection containing flavorant adsorbed on silica. U.S Patent 5,338,809.

Bhandari, B. R.; D'Arcy, B. R. Microencapsulation of flavour compounds. *Food Aust.* **1996**, *48* (12), 547-551.

Bhatia, R. B.; Brinker, C.J.; Ashley, C.S.; Harris, T.M. Synthesis of sol-gel matrices for encapsulation of enzymes using an aqueous route. *Mater. Res. Soc. Symp. Proc*. **1998**, *519*, 183-188.

Bolton, T.A.; Reineccius, G.A. The oxidative stability and retention of limonene-based model flavor plated on amorphous silica and other selected carriers. *Perfum. Flavor.* **1992a**, *17*, 2.

Bolton, T.A.; Reineccius, G.A. The oxidative stability and retention of limonene-based model flavor plated on amorphous silica and other selected carriers. *Perfum. Flavor.* **1992b**, *17*, 2.

Bottcher, H.; Slowik, P. Sol-gel carrier systems for controlled drug delivery, *J. Sol-Gel Sci.Technol.* **1998**, *13*, 277.

Buffo, R.; Reineccius, GA. Optimization of gum acacia/modified starches/maltodextrin blends for the spray drying of flavours. *Perfum. Flavor*. **2000,** *25*, 37–49.

Carturan, G.; Pagani, E.; Campostrini, R.; Ceccato, R. Hybrid gels as host matrices of perfumed essences. *J. Sol-Gel Sci. Technol.* **1997,** *8,* 1115-1117.

Cellesi, F.; Tirelli, N. Sol-gel synthesis at neutral pH in W/O microemulsion: A method for enzyme nanoencapsulation in silica gel nanoparticles. *Colloids and Surfaces A.* **2006,** 52-61.

Chandrasekaran, S. K.; King, C. J. Retention of Volatile Flavor Components During Drying of Fruit Juices. *Chem. Eng. Prog. Symp. Ser.* **1971**, *67*, 108.

Chang, Y.I.; Scire, J.; Jacobs, B. Effect of particles size and microstructure properties on encapsulated orange oil. In *Flavor Encapsulation*; Risch, S. J., Reineccius, G. A., Eds.; American Chemical Society: Washington, DC, **1988**; pp 55-64.

Chavez, J.L.; Wong, J.L.; Jovanoic, A.V.; Sinner, E.K.; Duran., R.S. Encapsulation in sub-micron species - A short review and alternate strategy for dye encapsulation. *IEE Proc – Nanobiotechnol*, **2005**, *152*, 273 – 283.

Constantin, S.; Freitag, R. Preparation of stationary phases for open-tubular capillary electrochromatography using sol-gel method. *J. Chromatogr.* **2000,** *887,* 253-263.

Coradin, T.; Eglin, D.; Livage, J. The silicomolybdic acid spectrophotometric method and its application to silicate/biopolymer interaction studies. *Spectrosc.* **2004**, *18*, 567-576.

Cunningham, D.; Hans, R. (1968). Food release composition. U.S. Patent 3,397,065.

Dave, B.C.; Miller, J.M.; Dunn, B.; Valentine, J.S.; Zink, J.I. (1997). Encapsulation of proteins in bulk and thin film sol-gel matrices. *J. Sol-Gel Sci. Technol.* **1997**, *8*, 629-634.

De Roos, K.B. Physicochemical models of flavour release from foods. In*: Flavour Release*; Roberts, D.D.; Taylor, A.J.; Eds.; American Chemical Society: Washington, DC, **2000**, pp. 126–141.

De Witte, B.M.; Commers, D.; Uytterhoeven, J.B. Distribution of organic groups in silica gels prepared from organo-alkoxysilanes. *J. Non-Cryst. Solids* **1996,** *202,* 35-41.

Dezarn, T. J. Food Ingredient Encapsulation: An Overview. *Encapsulation and Controlled Release of Food Ingredients*; Risch, S. J., Reineccius, G. A., Eds.; American Chemical Society: Washington, DC, **1995**; pp 74-86.

Doom, L; Campanile, F. Encapsulation of food ingredients: Principles and applications for flavours. *Gums and stabilizers for the food industry*. **2006**, 268-274.

Dunn, B.; Miller, J.M. ; Dave, C. ; Valentine, J.S. ; Zink, J.I. Strategies for encapsulating biomolecules in sol-gel matrices. *Acta Mater*. **1998**, *46(3*), 737-741.

Dunphy, P. Real time volatile flavor release monitoring and its flavor/food application using proton transfer reaction mass spectrometry. *Perfum. Flavor.* **2006**, *31*, 44-51.

Dziezak, J.D. Microencapsulation and encapsulated food products. *Food Technol.* **1988**, *42*, 136-151.

Edlund, U.; Albertsson, A.C. Degradable polymer microspheres for controlled drug delivery. *Adv. Polym. Sci.* **2002**, *157*, 67-112.

Jillavenkatesa, A; Dapkunas, S.J.; Lum, L-S.H. Particle Size Characterization, Practical Guide. NIST Special Publication 960-1, U.S. Government Printing Office: Washington, D.C., **2001**.

Gill, I.; Ballesteros, A. Encapsualtion of biologicals within silicate, siloxane, and hybrid sol-gel polymers: An efficient and generic approach. *J. Am. Chem. Soc.* **1998,** *120,* 8587-8598.

Goubet, I.; Le Quere, J.L.; Voilley, A.J. Retention of Aroma Compounds by Carbohydrates: Influence of Their Physicochemical Characteristics and of Their Physical State. A Review. *J. Agric. Food Chem.* **1998,** *46,* 1981-1990.

Hansel, A.; Jordan, A.; Holzinger, R.; Prazeller, P.; Vogel, W.; Lindinger, W. Proton transfer reaction mass spectrometry: on-line trace gas analysis at the ppb level. *Int. J. Mass Spectrom. Ion Processes*, **1995**, *149*, 609-619.

Heller, J. Controlled release of biologically active compounds from bioerodible polymers. *Biomaterials*. **1980**, *1*, 51-57.

Hench, L.L; West, J.K The Sol-Gel Process. *Chem. Rev.* **1990,** *90,* 33-72.

Huang, X.; Brazel, C.S. On the importance and mechanisms of burst release in matrix-controlled drug delivery systems, *J. Controlled Release*. **2001**, *73*, 121-136.

Iler, R.K. (1955). "The Colloid Chemistry of Silica and Silicates". Cornell Univesrity Press, Ithaca, New York, NY.

Iler, R.K. 1979. "The Chemistry of Silica". Wiley, NY.

Jackson, L. S.; Lee, K. Microencapsulation and the food industry. *Lebensm.-Wiss., Technol.* **1991**, *24*, 289-297.

Jovanaic, A.V.; Underhill, R.S.; Bucholz, T.L; Duran, R.S. Oil core and silica shell nanocapsules: Toward controlling the size and ability to sequester hydrophobic compounds. *Chem. Mater.* **2005**, *17*, 3375-3383.

Jeon, B.J.; Hah, H.J.; Koo, S.M. Surface modification of silica particles with organoalkoxysilanes through a two-step (acid-base) process in aqueous solution. *J. Ceram.Process.Res*. **2002**, *3*, 216-221.

King, A. K. *Encapsulation of Food Ingredients: A Review of Available Technology, Focusing on Hydrocolloids*. In *Encapsulation and Controlled Release of Food Ingredients*; Risch, S. J., Reineccius, G. A., Eds.; American Chemical Society: Washington, DC, 1995; pp 26-41.

Kortesuo, P.; Ahola, M.; Kangas, M.; Jokinen, M.; Leino, T. Effect of synthesis parameters of the sol-gel processed spray-dried silica gel microparticles on the release rate of dexmedetomidine. *Biomaterials*. **2002**, *23*, 2795-2801.

Kortesuo, P.; Ahola, M.; Kangas, M.; Kangasniemi, I. In vitro evaluation of sol-gel processed spray dried silica gel microspheres as carrier in controlled drug delivery. *Int. J. Pharm.* **2000,** *200,* 223-229.

Kusakabe, K.; Sakamoto, S.; Saie, T.; Morooka, S., 1999. Pore structure of silica membranes formed by a sol-gel technique using tetraethoxysilane and alkyltriethoxysilanes. *Sep. Purif. Methods.* **1999**, 16, 139-146.

Langer, R. New methods in drug delivery. *Science*. **1990**, *249*, 1527-1533.

Leahy, M.; Anandaraman, M.; Bangs, W.E.; Reineccius, G.A. Spray-drying of food flavors of food flavors II. A comparison of encapsulating agents for the drying of artificial flavor. *Perf. Flav.* **1983**, *8*, 49–52, 55–56.

Lev, O.; Tsionsky, M.; Rabinovich, L.; Sampath, S.; Pankratov, I.; Gun, J. Organically modified sol-gel sensors. *Anal. Chem*.**1995**, 67, 22-30.

Lindinger, W.; Hansel, A.; Jordan A. On-line monitoring of volatile organic compounds at pptv levels by means of Proton-Transfer-Reaction Mass Spectrometry (PTR-MS) Medical applications, food control and environmental research. *Int. J. Mass Spectrom. Ion Processes* **1998**, *173,* 191-241.

Livage, J.; Coradin, T.; Roux, C. Encapsulation of biomolecules in silica gels. *J. Phys.: Condens. Matter*, **2001**, *13*, 673-691.

Loy, D.A.; Baugher, B.M.; Baugher, C.R.; Schneider, D.A.; Rahimian, K. Substituent effects on the sol-gel chemistry of organoalkoxysilanes. *Chem. Mater.* **2000,** *12,* 3624-3632.

Madene, A.; Jacquot, M.; Scher, J.; Desobry, S. Flavour encapsulation and controlled release - a review. *Int.J.Food Sci.Technol.* **2006,** *41,* 1-21.

Mah, S. K.; Chung, I. J. Effects of dimethyldiethoxysilane addition on tetraethylorthosilicate sol-gel process. *J. Non-Cryst. Solids.* **1995**, 183, 252-259.

Mateus, M.L., Lindinger, C., Gumy, J.C.; Liardon, R. Release Kinetics of Volatile Organic Compounds from Roasted and Ground Coffee: Online Measurements by PTR-MS and Mathematical Modeling *J. Agric. Food Chem.* **2007,** *55,* 10117–10128.

Marmo, D.; Rocco, F.L. (1975). Chewing gum. U.S. Patent 3,920,849.

Mei, J.B.; Reineccius, G.A.; Knighton, W.B.; Grimsrud, E.P. Influence of strawberry yogurt composition on aroma release. *J. Agric. Food Chem.* **2004**, *52(20)*, 6257-6270.

Menting, L.C.; Hoogstad, B.; Thijssen, H.A.C. Aroma retention during the drying of liquid foods. *J.Food.Tech*. **1970**, *5*, 127-139.

Meyer, M.; Fischer, A.; Hoffman, H. Novel ringing silica gels that do not shrink. *J. Phys. Chem. B*. **2002**, *106*, 1528-1533.

Narasimhan, B.; Langer, R. Zero-order release of micro- and macromolecules from polymeric devices: the role of the burst effect, *J. Controlled Release*. **1997**, *47*, 13-20.

Noureddini, H.; Gao, X. Characterization of sol-gel immobilized lipases. *J. Sol-Gel Sci.Technol.* **2007**, *41*, 31-41.

Oshima, S.; Suzuki, T.; Tsuboi, T.; Soma, T. (1992). Taste substances adsorbed on silicon dioxide for pet foods and manufacturing of pet foods containing them. Nihon Nosan Kogyo K.K., Nitchika Yakuhin Kogyo Co., Ltd. JP 03,206,852.

Panitz, J.C.; Geiger, F. Leaching of anthraquinone dye solvent blue 59 incorporated into organically modified silica xerogels. *J. Sol-Gel Sci.Technol.* **1998**, *13*, 473-477.

Park, M.; Komarneni, S. Effect of substituted alkyl groups on textural properties of ORMOSILS. *J. Mater. Sci.* **1998,** *33,* 3817-3821.

Pierre, A.C. The sol-gel encapsulation of enzymes. *Biocatal. Biotransform.* **2004**, *22*, 145-170.

Pothakamury, U.R.; Barbosa-Canovas, G.V. Fundamental aspects of controlled release in foods. *Trends Food Sci. Technol.* **1995**, *6*, 397–406.

Prokopowickz, M.; Lukasiak, J.; Przyjazny, A. Utilization of a sol-gel method for encapsulation of doxorubicin. *J. Biomater. Sci., Polym.Ed.* **2004**, *15(3)*, 342-356.

Reetz, M.T.; Zonta, A.; Simpelkamp, J. Efficient immobilization of lipases by entrapment in hydrophobic sol-gel materials. *Biotechnol. Bioeng.* **1996,** *49,* 527-534.

Reineccius, G. A. Carbohydrates for flavor encapsulation. *Food Technol.* **1991**, 144-146.

Reineccius, G. A. *Controlled Release Techniques in the Food Industry.* In *Encapsulation and Controlled Release of Food Ingredients*; Risch, S. J., Reineccius, G. A., Eds.; American Chemical Society: Washington, DC, **1995**; pp 8-25.

Reineccius, G. A. Spray-Drying of Food Flavors. In *Flavor Encapsulation*; Risch, S. J., Reineccius, G. A., Eds.; American Chemical Society: Washington, DC, **1988**; pp 55-64.

Risch, S. J. Encapsulation: Overview of Uses and Techniques. In *Encapsulation and Controlled Release of Food Ingredients*; Risch, S. J., Reineccius, G. A., Eds.; American Chemical Society: Washington, DC, **1995a**; pp 2-7.

Risch, S. J. Review of Patents for Encapsulation and Controlled Release of Food Ingredients. In *Encapsulation and Controlled Release of Food Ingredients*; Risch, S. J., Reineccius, G. A., Eds.; American Chemical Society: Washington, DC, **1995b**; pp 196-204.

Robinson, J.R.; Lee, V.H.L. In Robinson, J.R.; Lee, V.H.L. *Controlled drug delivery: fundamentals and applications*, Eds.; Marcel Dekker, New York, **1987**, pp 555-570.

Robinson, J.R.; Lee, V.H.L. In: *Controlled drug delivery: fundamentals and applications*; Robinson, J.R.; Lee, V.H.L.; Eds.; Marcel Dekker: New York, **1987**, pp 555-570.

Rodriguez, S.A. and Colon, L.A. Investigations of a sol-gel derived stationary phase for open tubular capillary electrochromatograpy. *Anal. Chim. Acta* **1999,** *397,* 207-215.

Rodriguez, S.A. and Colon, L.A. Si-NMr studies of the sol-gel hybrid solution containing octadecyltriethoxysilane and tetraethoxysilane used to fabricate a stationary phase for open tubular capillary electrochromatography. *Appl. Spectrosc.* **2001,** *55,* 472-480.

Rodriguez, S.A. and Colon, L.A. Study of the solution in the synthesis of a sol-gel composite used as a chromatographic phase. *Chem. Mater.* **1999,** *11,* 754-762.

Roos, K.B. Effect of texture and microstructure on flavour retention and release. *Int. Dairy J.* **2003**, *13*, 593–605.

Rosenberg, M.; Kopelman, I. J.; Talmon, Y. Factors Affecting Retention in Spray-Drying Microencapsulation of Volatiles Materials. *J. Agric. Food Chem.* **1990**, *38*, 1288-1294.

Schmidt, H. Organic modification of glass structure. New glasses or new polymers? J. Non-Cryst.Solids. **1989**, *112*, 419-423.

Shahidi, F.; Han, X. Q. Encapsulation of Food Ingredients. *Crit. Rev. Food Sci. Nutr.* **1993**, *33*, 501-547.

Shimizu, K.; Del Amo, Y.; Brzezinski, M.A.; Stucky, G.D.; Morse, D.E. A novel fluorescent silica tracer for biological silicification studies. *Chem. Biol*. **2001**, *8*, 1051-1060.

Shchipunov, Y.A. Sol–gel derived biomaterials of silica and carrageenan. *J. Colloid Interface Sci.* **2003**, 68 -76.

Shchipunova, Y.A.; Karpenkoa, T.Y.; Bakunina, I.Y.; Burtseva, Y.V.; Zvyagintsevab, T.N. A new precursor for the immobilization of enzymes inside sol–gel-derived hybrid silica nanocomposites containing polysaccharides. *J Biochem Biophys Methods*. **2004**, *58*, 25-38.

Shimojima, A.; Kuroda, K. Structural control of multilayered inorganic-organic hybrids derived from mixtures of alkyltriethoxysilane and tetraethoxysilane, *Langmuir*. **2002**, *18*, 1144-1149.

Shimojima, A.; Sugahara, Y.; Kuroda, K. Synthesis of oriented inorganic-organic nanocomposite films from alkyltrialkoxysilane-tetraalkoxysilane mixtures. *J. Am. Chem. Soc.* **1998**, *120*, 4528-4529.

Shimojima, A.; Umeda, N.; Kuroda, K. Synthesis of layered inorganic-organic nanocomposite films from mono-, di, and trimethoxy(alkyl) silane-tetramethoxysilane systems. *Chem. Mater.* **2001**, *13*, 3610-3616.

Singh, K. S. W.; Everett, D. H.; Haul, R. A. W.; Moscou, L.; Pierotti, R. A.; Rouquerol, J.; Siemieniewska, T. Reporting physisorption data for gas/solid systems with special reference to the determination of surface area and porosity. *Pure Appl. Chem.* **1985**, 57, 603-19.

Sirisuth, N.; Eddington, N.D. Influence of Stereoselective pharmacokinetics in the development and predictability of an IVIVC for the enantiomers of metaprolol tartrate. *Pharm. Res.* **2000**, *17(8)*, 1019-1025.

Tan, C-T. Beverage Emulsions. In : *Food Emulsions*, *3rd edition* Friberg, S.; Larsson, K; Eds.; Marcel Dekker Inc.: New York, **1997**.

Thevenet, F. Acacia gums: Stabilizers for flavor encapsulation. In: In *Flavor Encapsulation*; Risch, S. J., Reineccius, G. A., Eds.; American Chemical Society: Washington, DC, **1988**; pp 37-44.

Underhill, R.S.; Jovanoic, A.V.; Carino, S.R.; Varshney, M.; Shah, D.O.; Dennis, D.M.; Morey, T.M.; Duran, R.S. Oil-filled silica nanocapsules for lipophilic drug uptake: Implications for Drug Detoxification Therapy. *Chem. Mater.* **2002,** *14*, 4919 – 4925.

Underhill, R.S.; Jovanoic, A.V.; Carino, S.R.; Varshney, M.; Shah, D.O.; Dennis, D.M.; Morey, T.M.; Duran, R.S. Oil-filled silica nanocapsules for lipophilic drug uptake: Implications for Drug Detoxification Therapy. *Chem. Mater.* **2002,** *14*, 4919 – 4925.

Unger, B.; Jancke, H.; Hahnert, M. The early stages of the sol-gel processing of TEOS. *J. Sol-Gel Sci. Technol.* **1994,** *2,* 51-56.

Unger, K.; Rupprecht, H.; Valentin, B.; Kircher, W. The use of porous and surface modified silicas as drug delivery and stabilizing agents. *Drug Dev. Ind. Pharm.* **1993**, *9(162)*, 69-91.

van Ruth, S.M.; O'Connor; Delahunty, C.M. (2000). Relationships between temporal release of aroma compounds in a model mouth system and their physico-chemical characteristics. *Food Chem*. **2000,** *71*, 393-399.

Veith, S.R.; Hughes, E.; Pratisnis, S. Restricted diffusion and release of aroma molecules from sol-gel made porous silica particles. *J. Controlled Release*. **2005**, *99*, 315-327.

Veith, S.R. Retention, diffusion and release of flavor molecules from porous silica sol-gel made particles. PhD Thesis. Swiss Federal Institute of Technology, Zurich, 2004.

Versic, R. J. Flavor Encapsulation. In *Flavor Encapsulation*; Risch, S. J., Reineccius, G. A., Eds.; American Chemical Society: Washington, DC, **1988**; pp 1-6.

Voilley, A.; Simatos, D. Retention of aroma during freeze and air-drying. In *Food Process Engineering*; Linko, P., Ma lkki, Y., Olkku, J., Larinkari, J., Eds.; Applied Sciences: London, **1980**; pp 371-384.

Voilley, A. Flavor Encapsulation Influence of Encapsulation Media on Aroma Retention During Drying. In *Encapsulation and Controlled Release of Food Ingredients*; Risch, S. J., Reineccius, G. A., Eds.; American Chemical Society: Washington, DC, **1995**; pp 169-179.

Washington, C. In Benita, S. *Drug release from microparticulate systems. Microencapsulation: methods and industrial applications*, Eds.; Marcel Dekker, New York, **1996**, pp 155-181.

Whorton, B.C. Effect of polymeric phase transitions on the controlled release and oxidative stability of flavor model systems encapsulated in traditional carbohydrate carriers. Ph.D. Thesis, University of Minnesota, St.Paul, 2000.

Whorton, C. Factors Influencing Volatile Release from Encapsulation Matrices. In *Encapsulation and Controlled Release of Food Ingredients*; Risch, S. J., Reineccius, G. A., Eds.; American Chemical Society: Washington, DC, **1995**; pp 134-144.

Whorton, C.; Reineccius, G. A. Evaluation of the Mechanisms Associated with the Release of Encapsulated Flavor Materials from Maltodextrin Matrixes. In *Encapsulation and Controlled Release of Food Ingredients*; Risch, S. J., Reineccius, G. A., Eds.; American Chemical Society: Washington, DC, **1995**; pp 143-160.

Yi, Y.; Newufeld, R.; Kermasha, S. Optimization of tetramethoxysilane-derived sol gel entrapment protocol stabilizes highly active chlorophyllase. *J Sol-Gel Sci Technol.* **2006***, 38*, 251–259.

Yoldas, B.E. Hydrolytic polycondensation of Si(OC2H5)4 and effect of reaction parameters. *J. Non-Cryst. Solids.* **1996,** *83,* 375-390.

Yoldas, B.E. Hydrolytic polycondensation of Si(OC2H5)4 and effect of reaction parameters. *J. Non-Cryst. Solids* **1996,** *83,* 375-390.

Zeller, B.L.; Saleeb, F.Z.; Ludescher, R.D. Trends in development of porous carbohydrate food ingredients for use in flavor encapsulation. *Trends Food Sci. Technol.* **1999,** *9,* 389-394.

Chapter 8 : Appendices

Appendix 1 (Chapter 3)

Analysis of Variance Table: Particle size of the system

	Df	Sum Sq	Mean Sq	F value	Pr(>F)
conc	1	72.53	72.53	5.3281	0.02516 *
time	1	2328.36	2328.36	171.0342	< 2.2e-16 ***
conc:time	1	365.18	365.18	26.8248	3.991e-06 ***
Residuals	50	680.67	13.61		

Significant codes: 0 '***' 0.001 '**' 0.01 '*' 0.05 '.' 0.1 ' ' 1

Least Significant Difference 2.469974
Means with the same letter are not significantly different.

	trt	means	M	N	std.err
1	trt2	41.40556	a	18	1.7948268
2	trt3	37.87778	b	18	2.4300751
3	trt1	35.03889	c	18	0.9697092

Appendix 2 (Chapter 3)

Pearson's Square for the addition of BVO

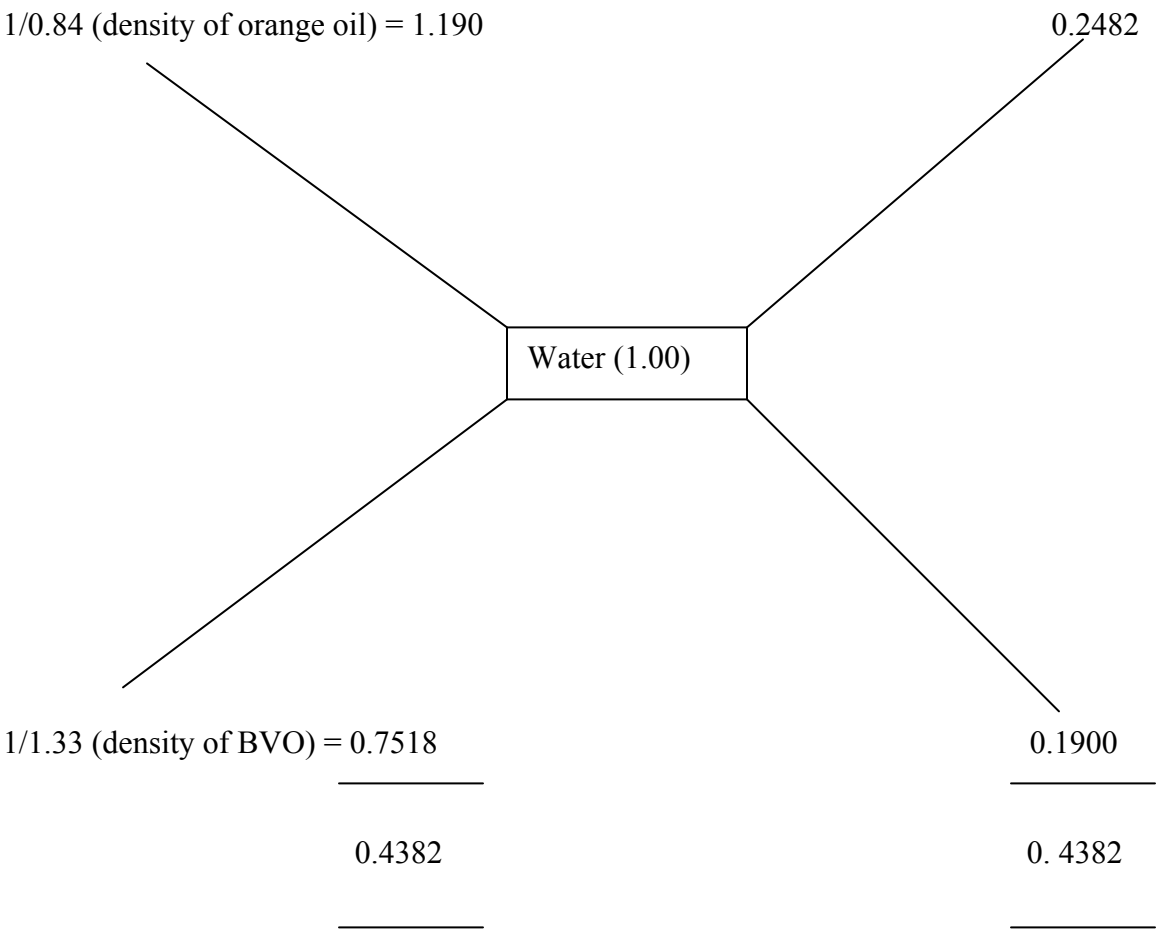

Amount of orange oil to be added = 0.2482/0.4382 * 100 = 56.6 %

Amount of BVO to be added = 0.1900/0.4382 * 100 = 43.3 %

Appendix 3 (Chapter 3)

Silicomolybdic acid spectrophotometric method

This method is commonly used to study the interactions between silica and living organisms. Literature cites the application of this method for sol-gel systems. However, there have not been any studies on the use of this method for sol-gel systems. Therefore, we tried to follow the protocol available in the literature to examine the compatibility of this method for our system. Briefly, silicic acid ($Si(OH)_4$) reacts with acidified ammonium heptamolybdate to form a yellow colored heteropolyacid (silico-12 molybdic acid). This resulting compound is titrated spectrometrically by monitoring the optical density at $\lambda = 400 \pm 10$ nm to determine the quantity of $Si(OH)_4$ formed (Coradin et al., 2004).

Application for our reaction system: Silicic acid formed during the hydrolysis of alkoxysilanes reacted with the acidified ammonium heptamolybdate and resulted in the formation of yellow compound providing us information that the reaction is occurring. As the hydrolysis progresses, the optical density should increase with the formation of silicic acid during hydrolysis (formation of silicic acid) and decrease as the polymerization starts (Si-O-Si bond formation and decrease in the amount of silicic acid).

Appendix 4 (Chapter 4)

Table 8-1: Experimental conditions of the sol-gel reaction (Central Composite Design)

Samples	Concentration alkyl-TEOS	Time of hydrolysis of alkyl-TEOS	Concentration of THEOS	Time of hydrolysis of THEOS	Time of polymerization	Particle size, micrometers
1	0.275	12.5	1	12.5	12.5	29.9
2	0.05	1	1	24	24	28.5
3	0.5	24	1	24	24	31.4
4	0.275	12.5	3.5	12.5	12.5	32.5
5	0.5	1	6	24	24	27.8
6	0.275	12.5	6	12.5	12.5	27.9
7	0.05	24	6	1	1	89.0
8	0.275	1	3.5	12.5	12.5	26.8
9	0.5	1	6	1	1	65.1
10	0.05	24	6	24	24	25.8
11	0.05	1	6	1	24	52.3
12	0.5	24	6	1	24	28.2
13	0.5	24	1	1	1	34.4
14	0.05	24	1	24	1	21.0
15	0.05	12.5	3.5	12.5	12.5	40.6
16	0.275	12.5	3.5	1	12.5	42.5
17	0.5	24	6	24	1	37.2
18	0.275	12.5	3.5	12.5	24	31.4
19	0.5	1	1	24	1	20.8
20	0.275	12.5	3.5	12.5	12.5	33.3
21	0.5	1	1	1	24	21.6
22	0.5	12.5	3.5	12.5	12.5	35.9
23	0.275	24	3.5	12.5	12.5	40.6
24	0.275	12.5	3.5	12.5	1	30.9
25	0.05	1	6	24	1	43.2
26	0.05	24	1	1	24	31.1
27	0.05	1	1	1	1	36.0
28	0.275	12.5	3.5	24	12.5	24.6
29	0.275	12.5	3.5	12.5	12.5	34.0
30	0.275	12.5	3.5	12.5	12.5	33.6
31	0.275	12.5	3.5	12.5	12.5	31.4
32	0.275	12.5	3.5	12.5	12.5	32.6
33	0.275	12.5	3.5	12.5	12.5	33.2
34	0.275	12.5	3.5	12.5	12.5	39.5

Appendix 5 (Chapter 4)

Regression Analysis for the central composite design

Table 8-2: Multiple regression on the particle size of system

	Estimate	**Std. Error**	**t value**	**Pr (>|t|)**
Intercept	27.217487	7.701091	3.534	0.003665 *
x1	-78.593952	40.971895	-1.918	0.077310
x2	0.291061	0.729168	0.399	0.696249
x3	**13.725281**	**4.135236**	**3.319**	**0.005540 ** **
x4	-1.103457	0.729168	-1.513	0.154128
x5	0.177726	0.729168	0.244	0.811238
x1^2	117.1621	69.024142	1.697	0.113414
x2^2	0.010445	0.026422	0.395	0.699028
x3^2	-0.546986	0.559096	-0.978	0.345762
x4^2	0.009311	0.026422	0.352	0.730201
x5^2	-0.008837	0.026422	-0.334	0.743379
x1:x2	-0.265700	0.529978	-0.501	0.624512
x1:x3	-4.844444	2.437899	-1.987	0.068396
x1:x4	**1.396135**	**0.529978**	**2.634**	**0.020617 ***
x1:x5	0.072464	0.529978	0.137	0.893339
x2:x3	0.041739	0.047698	-0.875	0.397415
x2:x4	-0.005955	0.010369	-0.574	0.575591
x2:x5	-0.014272	0.010369	-1.376	0.191940
x3:x4	**0.172174**	**0.047698**	**-3.610**	**0.003173****
x3:x5	**-0.219130**	**0.047698**	**-4.594**	**0.000503 *****
x4:x5	**0.039036**	**0.010369**	**3.765**	**0.002361 ** **

Significant codes: 0 '***' 0.001 '**' 0.01 '*' 0.05 '.' 0.1 ' ' 1
Residual standard error: 5.485 on 13 degrees of freedom; Multiple R-Squared: 0.9286; Adjusted R-squared: 0.8188; F-statistic: 8.457; on 20 and 13 DF, p-value: 0.0001524

model1 <- lm (particle size ~ x1 + x2 + x3 + x4 + x5 + (x1 ^2) + x1 * x2 + x1 * x3 + x1 * x4 + x1 * x5 + (x2 ^2) +x2 * x3 + x2 * x4 + x2 * x5 + (x3^2) + x3 * x4 + x3 * x5 + (x4^2) + x4 * x5 + (x5^2))

Table 8-3: Multiple regression on the % extractable release of limonene

	Estimate	**Standard Error**	**t value**	**Pr(>|t|)**
Intercept	2.699e-02	5.689e-02	0.474	0.64302
x1	-3.377e-01	3.027e-01	-1.116	0.28473
x2	-3.142e-03	5.387e-03	-0.583	0.56968
x3	1.286e-02	3.055e-02	0.421	0.68063
x4	2.995e-03	5.387e-03	0.556	0.58768
x5	-4.409e-03	5.387e-03	-0.818	0.42787
(x1^2)	1.591e-01	5.099e-01	0.312	0.76003
(x2^2)	1.289e-05	1.952e-04	0.066	0.94835
(x3^2)	1.437e-03	4.130e-03	0.348	0.73340
(x4^2)	7.353e-05	1.952e-04	0.377	0.71247
(x5^2)	1.442e-05	1.952e-04	0.074	0.94224
x1:x2	**1.406e-02**	**3.915e-03**	**3.592**	**0.00328 ****
x1:x3	-2.693e-03	1.801e-02	-0.150	0.88342
x1:x4	1.448e-03	3.915e-03	0.370	0.71738
x1:x5	**1.524e-02**	**3.915e-03**	**3.893**	**0.00185 ****
x2:x3	-4.815e-04	3.524e-04	-1.366	0.19498
x2:x4	6.974e-05	7.660e-05	0.910	0.37919
x2:x5	**2.440e-04**	**7.660e-05**	**3.185**	**0.00717 ****
x3:x4	**-1.429e-03**	**3.524e-04**	**-4.056**	**0.00136 ****
x3:x5	1.151e-04	3.524e-04	0.327	0.74909
x4:x5	-1.850e-05	7.660e-05	-0.242	0.81291

Significant codes: 0 '***' 0.001 '**' 0.01 '*' 0.05 '.' 0.1 ' ' 1
Residual standard error: 0.04052 on 13 degrees of freedom; Multiple R-Squared: 0.8883, Adjusted R-squared: 0.7165; F-statistic: 5.17 on 20 and 13 DF; p-value: 0.001999

model1 <- lm (release ^ (-1) ~ x1 + x2 + x3 + x4 + x5 + (x1 ^2) + (x2 ^2)+ (x3^2) (x4^2) + (x5^2)+ x1 * x2 + x1 * x3 + x1 * x4 + x1 * x5 + +x2 * x3 + x2 * x4 + x2 * x5 + + x3 * x4 + x3 * x5 + + x4 * x5)

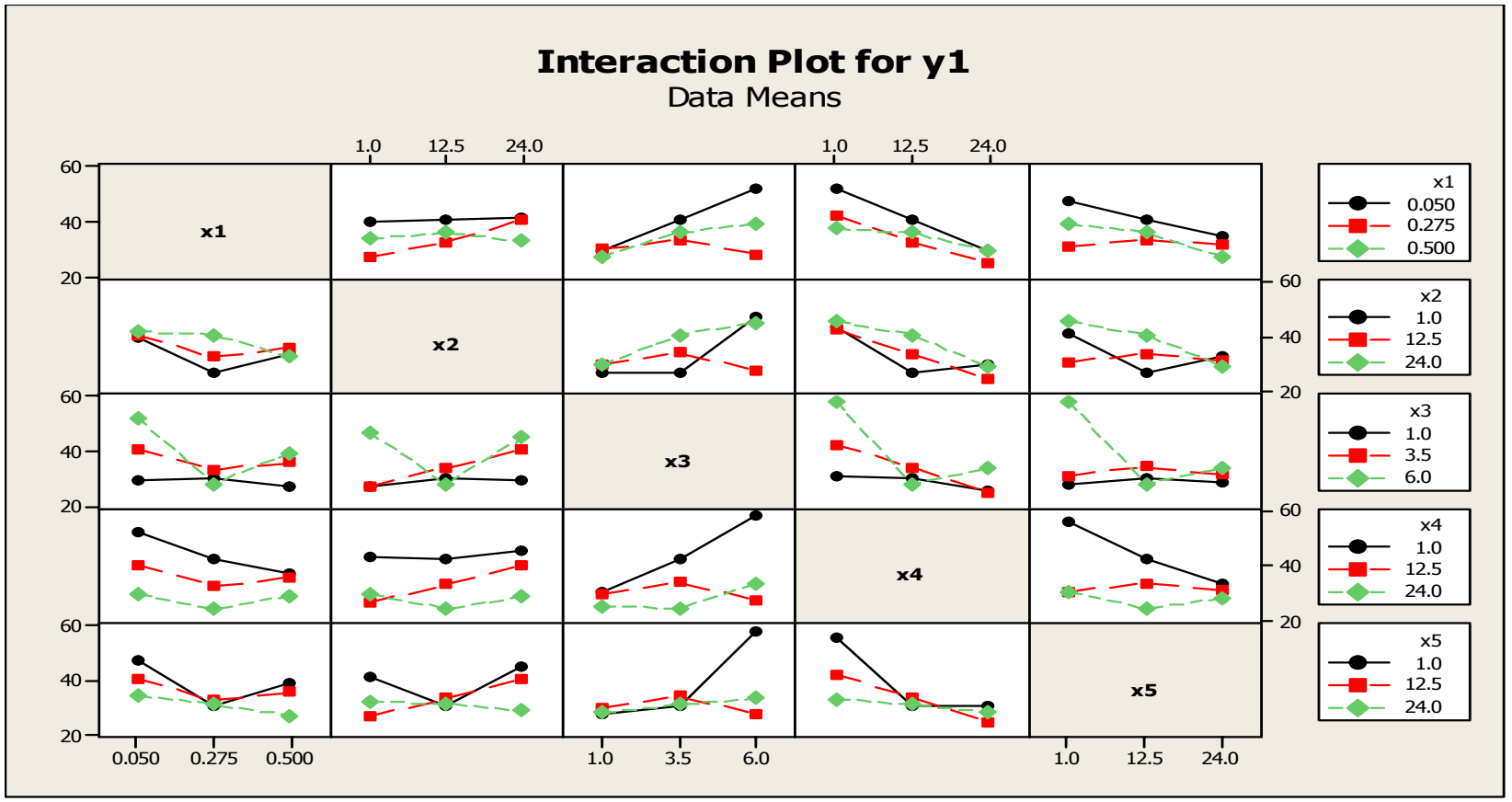

Figure 8-1: Interaction plot between predictor variables and response variable (particle size of the system)

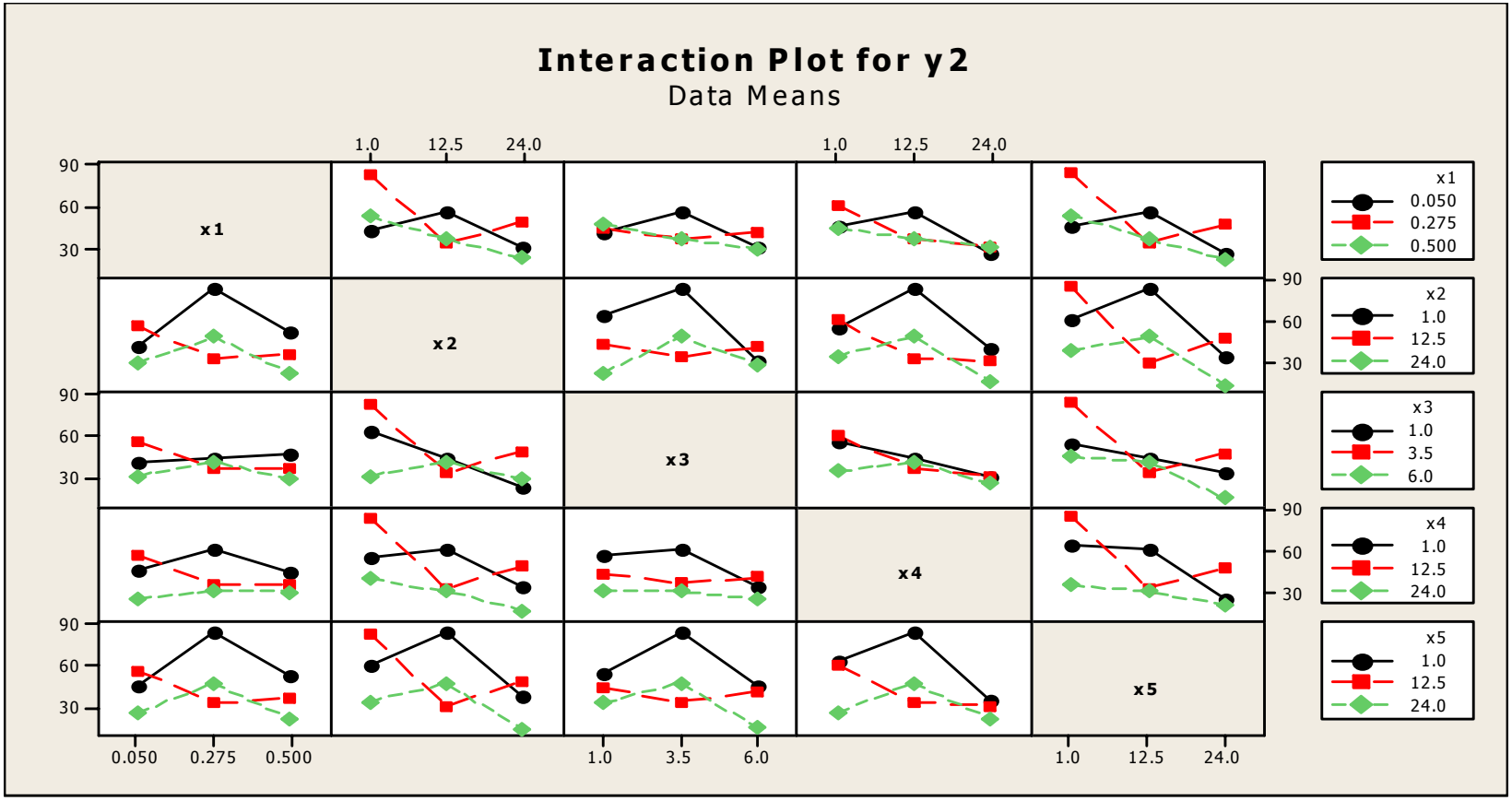

Figure 8-2: Interaction plot between predictor variables and response variable (% extractable limonene)

Release during polymerization of the sol-gel reaction

For sample 10 from Table 8-1, the % extractable limonene was measured at various intervals during the time of polymerization (1-24 h) of the reaction.

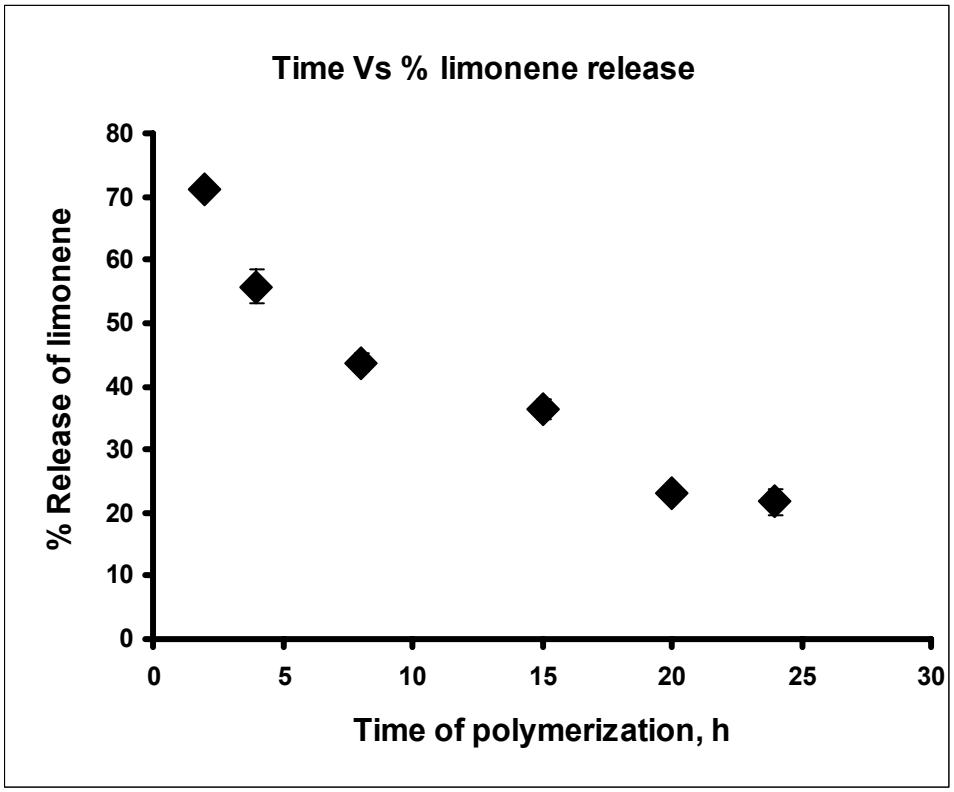

Figure 8-3: **%** Extractable limonene through the time of polymerization

It can be seen from the plot above, that the % extractable limonene release gradually decreased with the time of polymerization. As the polymerization leads to the formation of silicate shell (siloxane formation Si-O-Si), the shielding of orange oil in the silicate network likely resulted in the decreased release of limonene over time.

Appendix 6 (Chapter 4)

Controlled release of limonene from the synthesized precipitates

The controlled release of limonene was measured over a 24 h time interval for selected samples (samples 10 and 12 from Table 8-1). The rationale for doing this was to verify the protection offered by the silicate shell to the hydrophobic molecule. This can be well appreciated by looking at Figures 2 and 3.

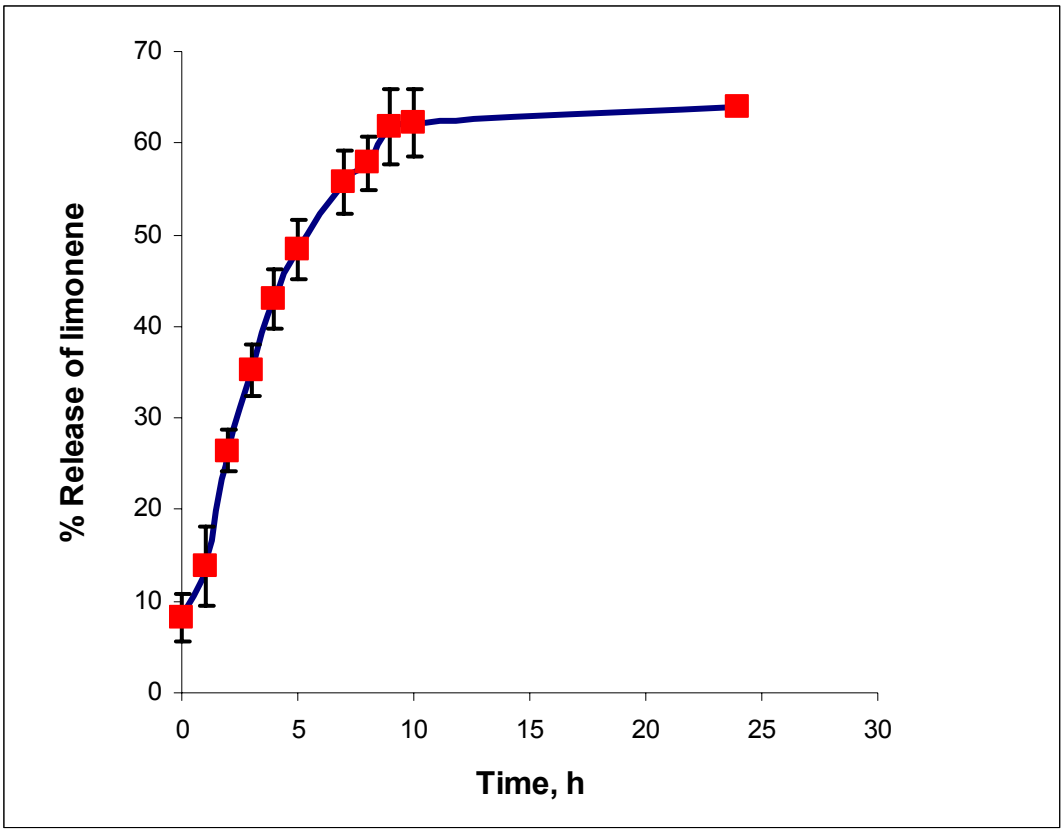

Figure 8-4: % Release of limonene from precipitates from in acetone-water mixture

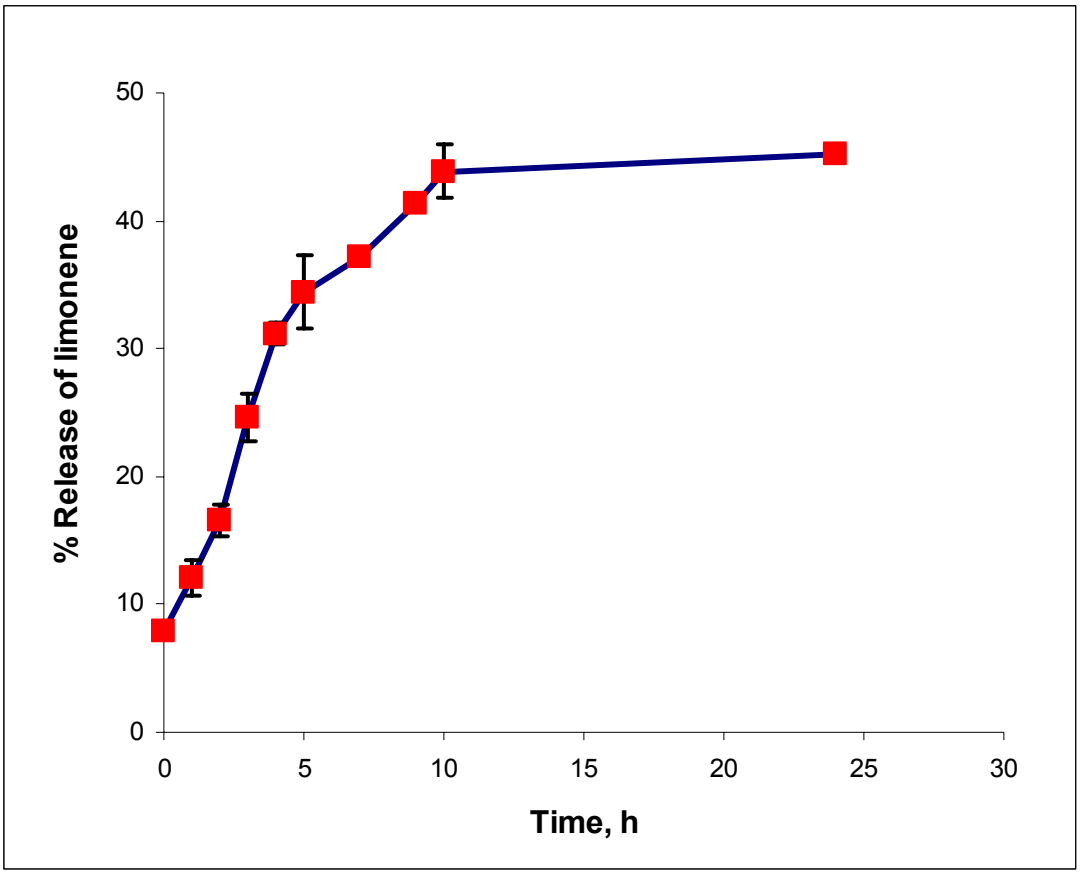

Figure 8-5: % Release of limonene from precipitates in acetone-water mixture

From the above Figures 8-2 and 8-3, it can be observed that the total release of limonene was only 65 % and 55 % of the theoretical (100 %) release for samples 10 and 12, respectively. For example, 1.4 g of orange oil is present in 50 ml of the solution; therefore 0.35 ml of the aliquot sample should contain 0.0098 g of orange oil (0.0093 g of limonene). However, the maximum release of limonene for samples 10 and 12 was around 0.006 g and 0.004 g, respectively. There can be three reasons for the decreased release of limonene 1) flavor loss during the process 2) strong flavor entrapment in the silicate network; or 3) solids generation during the reaction which has not been taken into account. In order to verify the reason for the decreased release, we ashed these samples. This would determine the actual amount of limonene in these samples.

Appendix 7 (Chapter 4)

Calculation of the amount of orange oil present in centrifuged silica precipitates by ash test and GC

For the ash test, blank samples containing no orange oil were prepared for sample formulations 10, 11 and 12 Table 8-1.

Centrifugation: The blank (contains silica and water) and the flavor loaded samples (orange oil, silica and water) were centrifuged for 30 min at 20,000 rpm. The centrifuged samples were studied for their flavor content by gas chromatography and ash content.

Ash Test: Two to three g of the centrifuged samples was weighed into a tared crucible and the crucibles were placed in a cool muffle furnace. The contents were ignited for about 12-18 h at about 550°C. The resulting samples were weighed and the amount of orange oil was calculated from the difference between the weight of the blank and the flavor loaded samples. Table 8-3 shows us the results of the ash test for the samples 10, 11 and 12. These tests were run in duplicate.

Table 8-4: Results for the ash test for the blank and flavor loaded samples

Samples	**W1(g)**	**W2 (g)**	**W2-W1 (g)**	**% Moisture**	**Orange Oil**	**% Orange Oil**
Blank sample 10	24.522 23.184	22.607 21.267	1.916 1.917	95.8 95.8		
Flavor sample 10	21.997 21.827	20.038 19.866	1.959 1.960	-	0.083 g 0.082 g	4.1 4.1
Blank sample 11	23.258 21.345	24.527 22.607	1.913 1.920	95.6 95.9		
Flavor sample 11	24.529 24.225	22.570 22.265	1.959 1.960	-	0.084 0.084	4.2 4.2
Blank sample 12	22.831 26.098	19.934 23.199	2.897 2.899	96.5 96.6		
Flavor sample 12	25.527 24.646	22.637 21.757	2.89 2.889	-	0.1011 g 0.1011 g	3.3 3.3

*Values are the average of at least three reproducible readings

The orange oil content of the flavor loaded samples from the ash test was calculated as follows,

Example: sample 10

From Table 8-4,

% moisture present in the blank sample = 95.8 %
Difference of weight in flavor loaded samples before and after ash test = 1.960 g
Weight loss due to moisture = 0.958 X 1.960 = 1.876 g
Weight loss due to orange oil = 1.960-1.876 = 0.083 g
% Orange oil = 0.083/2.00 = 4.1 %

Gas Chromatography

The orange oil content of the centrifuged samples (sample number 10 and 12) was calculated by measuring the amount of limonene present in the microcapsules using GC. This was done by sonicating 0.10 g of the sample in 10 ml of acetone containing 0.005 g/ml of 2-octanoane for 5 min. One μL of the resulting sample was injected into a GC.

Table 8-5: Percentage limonene present in the silica samples based on GC analysis

Samples	**Weight of sample (g)**	**Amount of limonene (g)**	**% limonene**	**% average limonene**
Sample 10	0.108 0.108	0.0043 0.0048	3.7 4.4	4.0 ± 0.49
Sample 11	0.113 0.113	0.0058 0.0053	5.1 4.6	4.8 ±0.35
Sample 12	0.104 0.100	0.0035 0.0042	3.3 4.2	3.8 ± 0.59

*Values are the average of at least three reproducible readings

Karl Fischer method for moisture determination

The moisture content of centrifuged flavor loaded samples (samples 10 and 12) were determined using the Karl Fischer method. Here 0.010 g of sample was equilibrated in 10 g of dry methanol for 12 h. One milliliter of the sample was injected into the Karl Fischer instrument to determine the moisture content. This was done in duplicate. The average moisture content in the samples 10 and 12 were 95.4 % (standard deviation= ± 0.28) and 95 % (standard deviation = ± 0.35), respectively. This was done to confirm the results obtained from ash test. From Tables 8-4, 8-5 and Karl Fischer method, it can be seen that the content of orange oil present in the silica precipitates determined from the ash test is comparable to the amount calculated from the GC. Therefore, we can conclude that the

entire amount of orange oil present in the silica precipitates is released during the determination of the controlled release of limonene.

Appendix 8 (Chapter 5)

Rate plots for encapsulated matrices

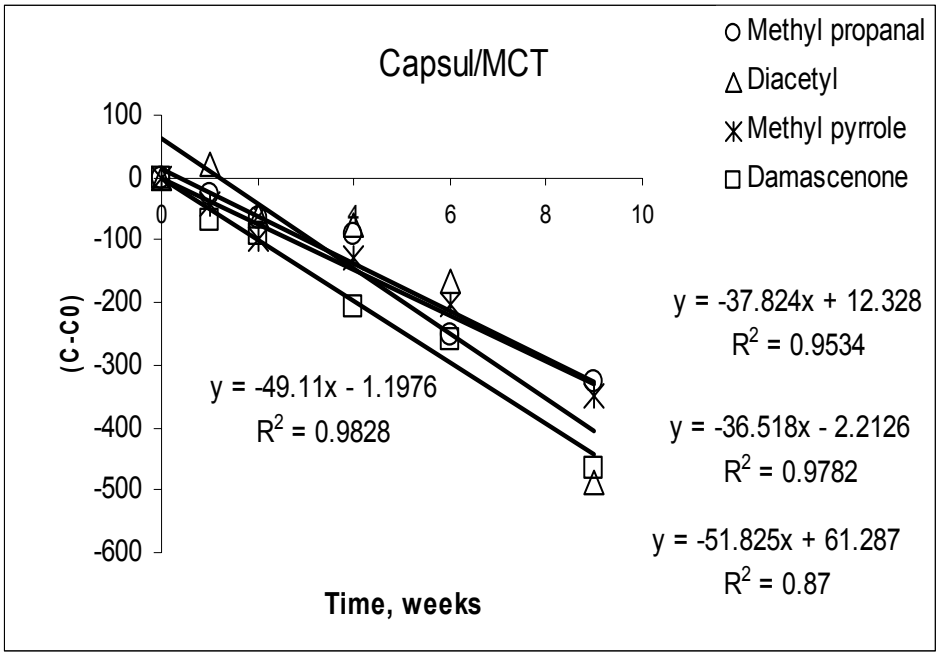

Figure 8-6: First-order rate plot for compounds encapsulated in Capsul/MCT matrix

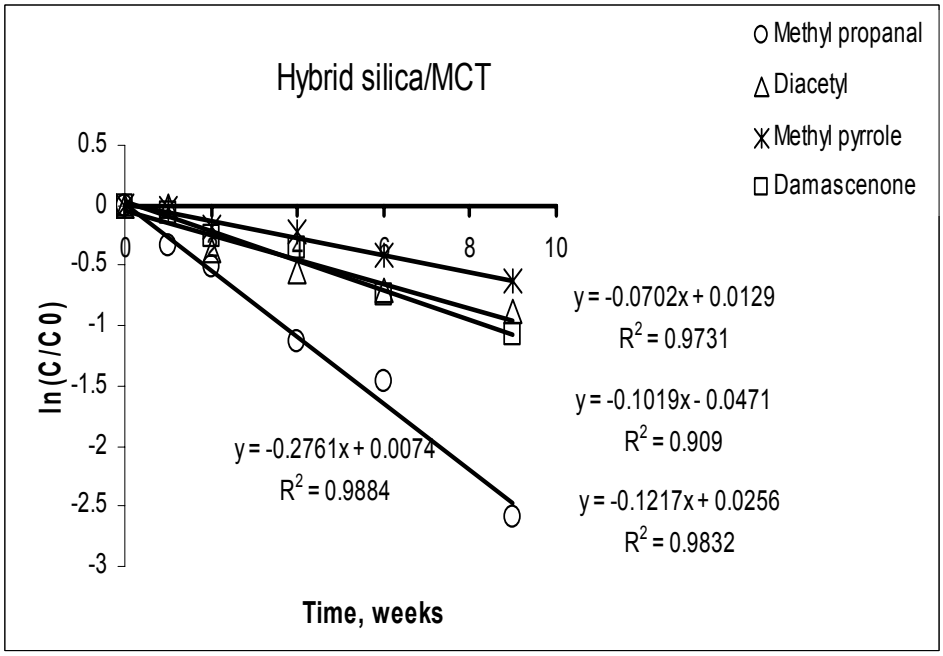

Figure 8-7: First-order rate plot for compounds encapsulated in hybrid silica sol-gel: starch blend/MCT matrix

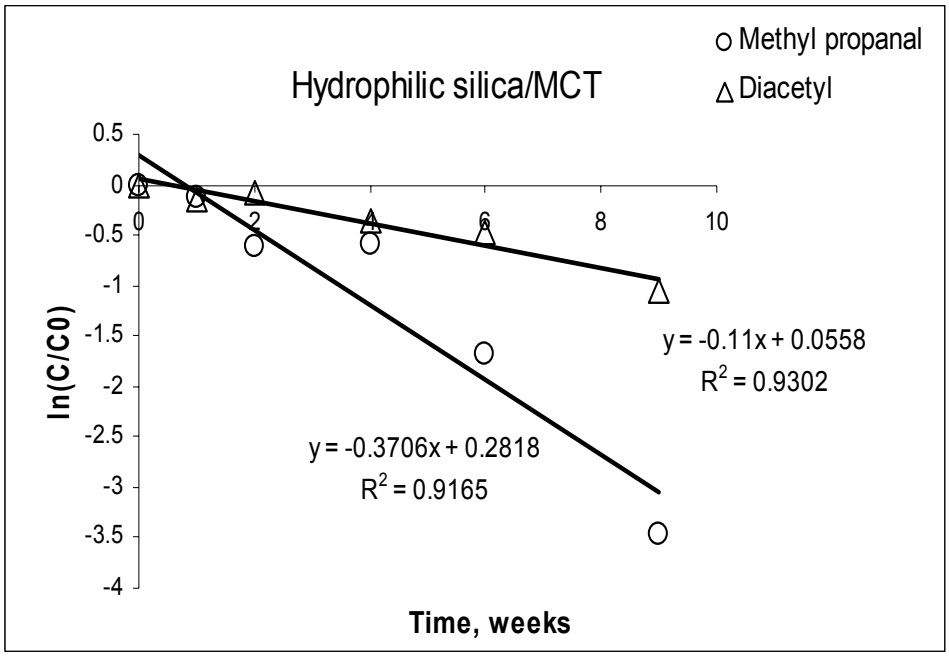

Figure 8-8: First-order rate plot for compounds encapsulated in hydrophilic silica sol-gel: starch blend/MCT matrix

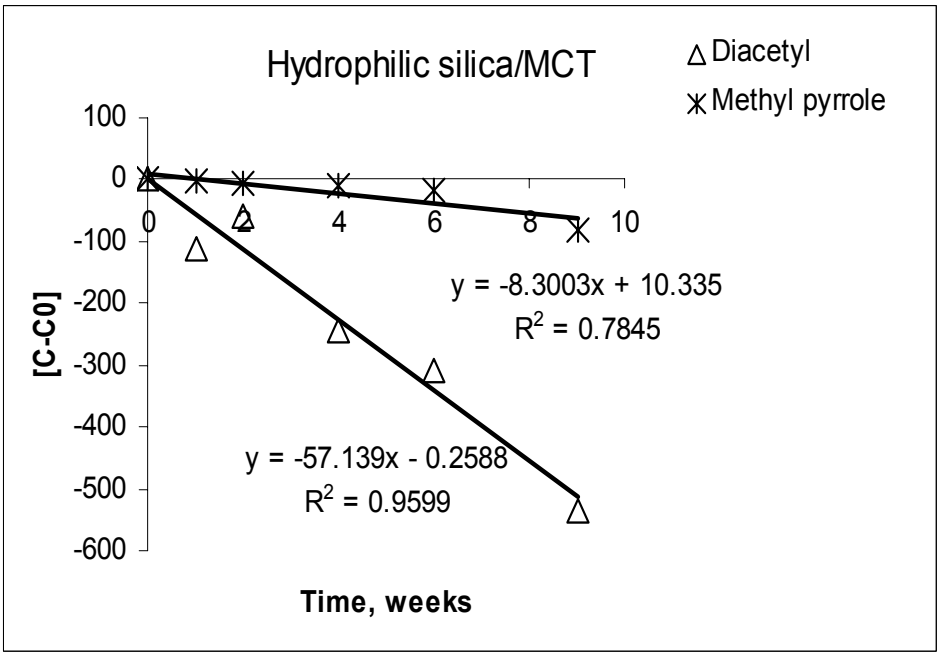

Figure 8-9: Zero-order rate plot for compounds encapsulated in hydrophilic silica sol-gel: starch blend/MCT matrix

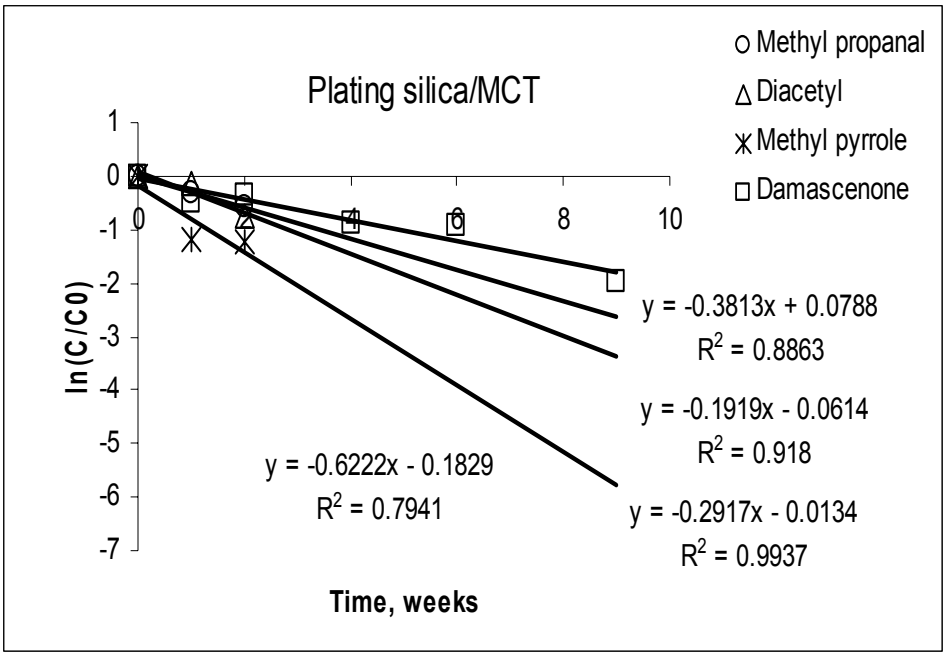

Figure 8-10: First-order rate plot for compounds encapsulated in plating silica/MCT matrix

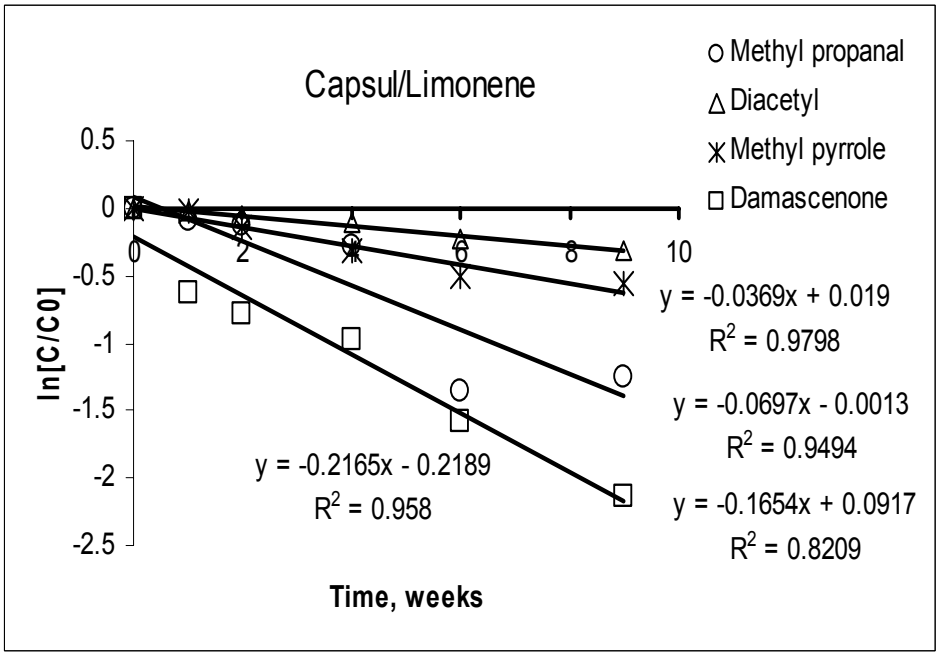

Figure 8-11: First-order rate plots for compounds encapsulated in Capsul/MCT matrix

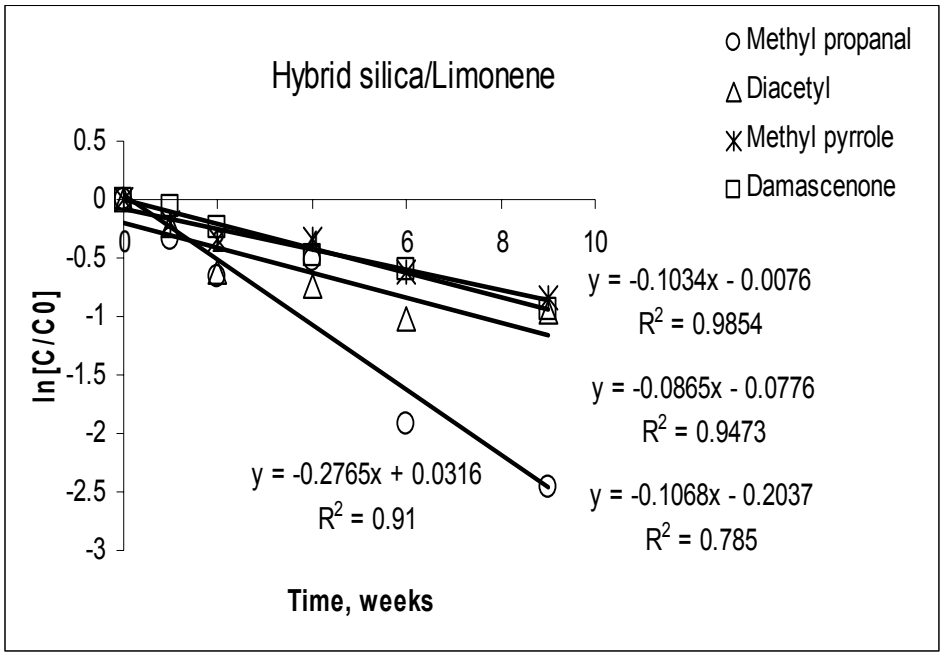

Figure 8-12: First-order rate plot for compounds encapsulated in hybrid silica sol-gel: starch blend/limonene matrix

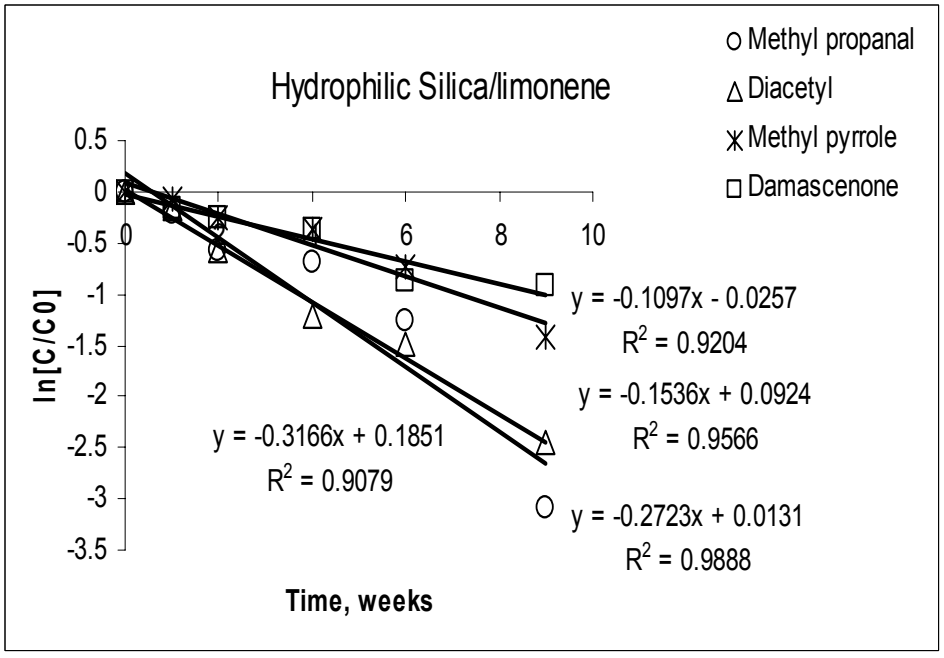

Figure 8-13: First-order rate plot for compounds encapsulated in hydrophilic silica sol-gel: starch blend/limonene matrix

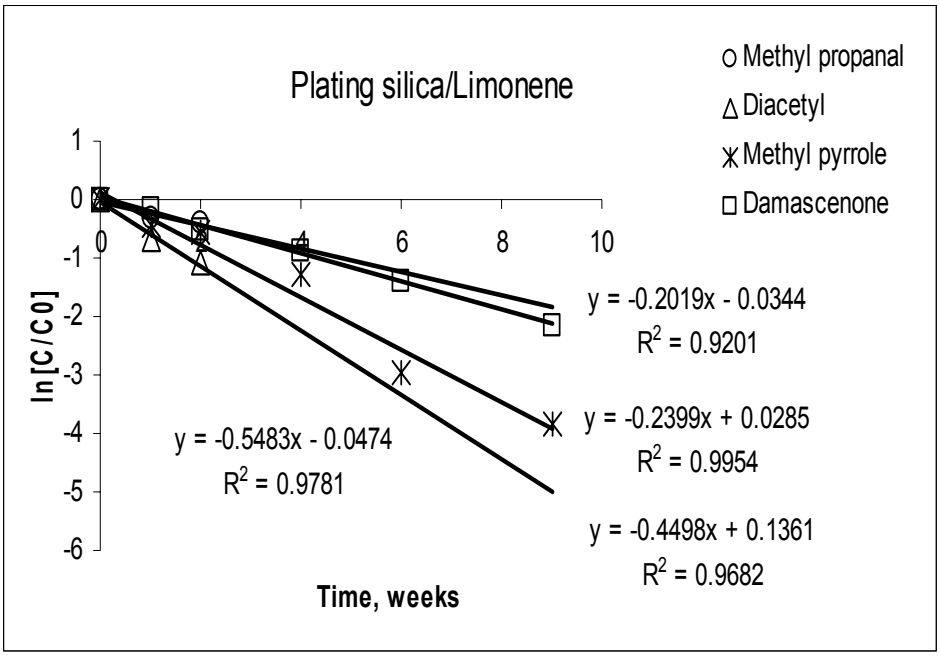

Figure 8-14: First-order rate plot for compounds encapsulated in hydrophilic silica sol-gel: starch blend/limonene matrix

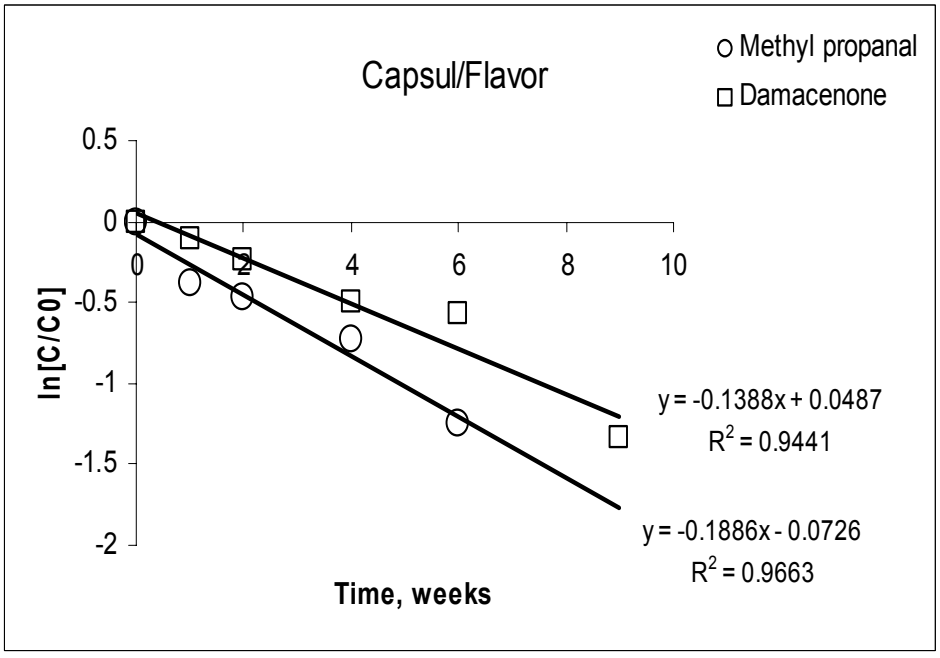

Figure 8-15: First-order rate plot for compounds encapsulated in Capsul/no solvent matrix

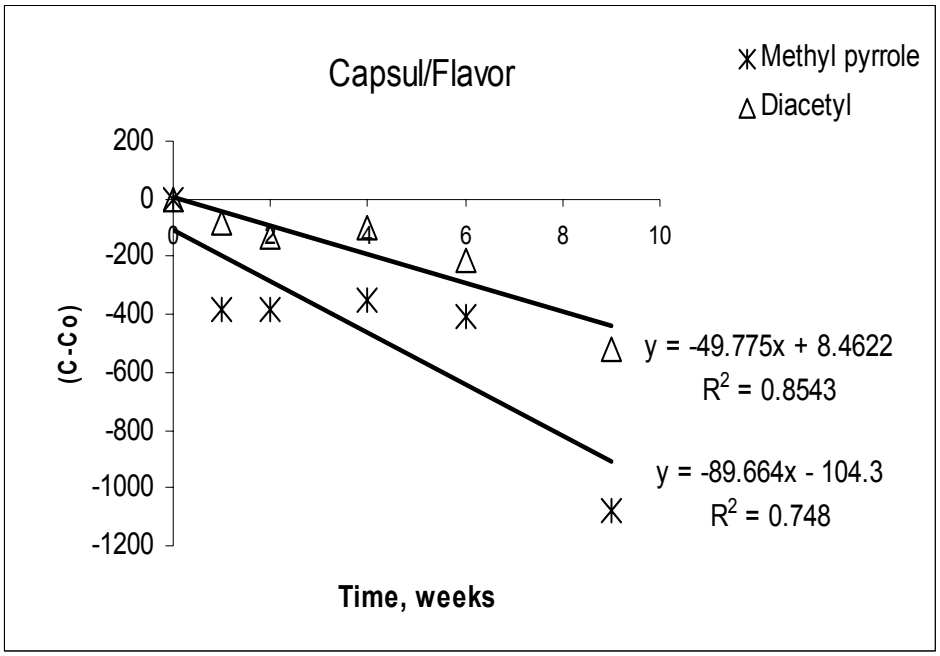

Figure 8-16: Zero-order rate plot for compounds encapsulated in Capsul/no solvent matrix

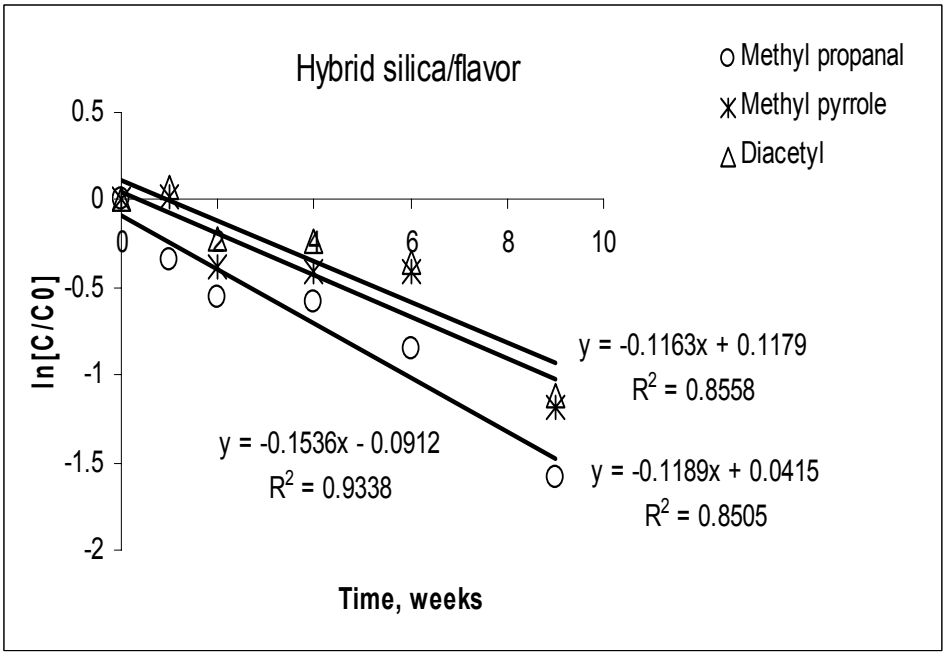

Figure 8-17: First-order rate plot for compounds encapsulated in hybrid silica sol-gel: starch blend /no solvent matrix

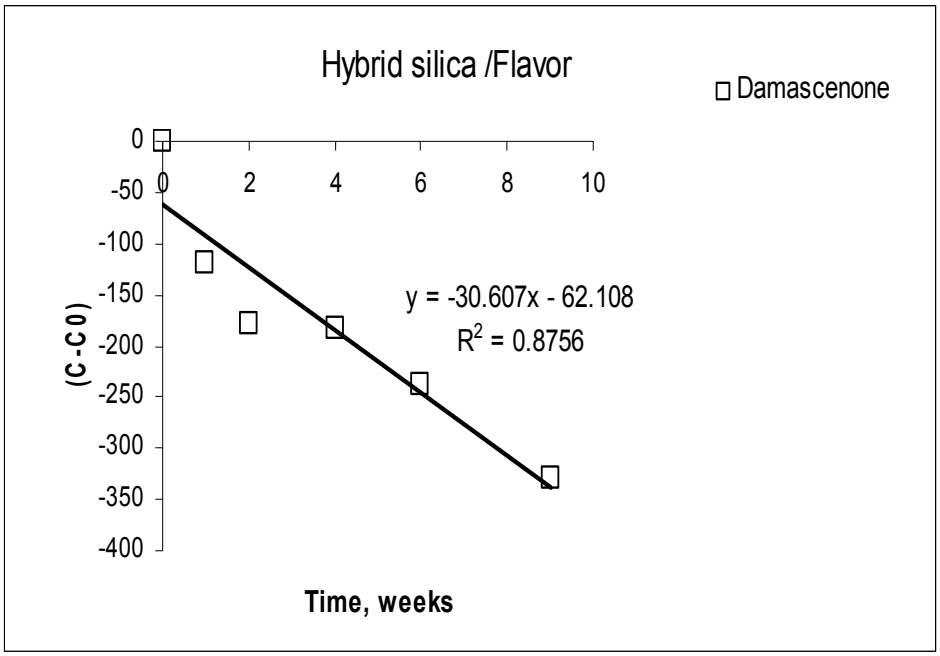

Figure 8-18: Zero-order rate plot for compounds encapsulated in hybrid silica sol-gel: starch blend/no solvent matrix

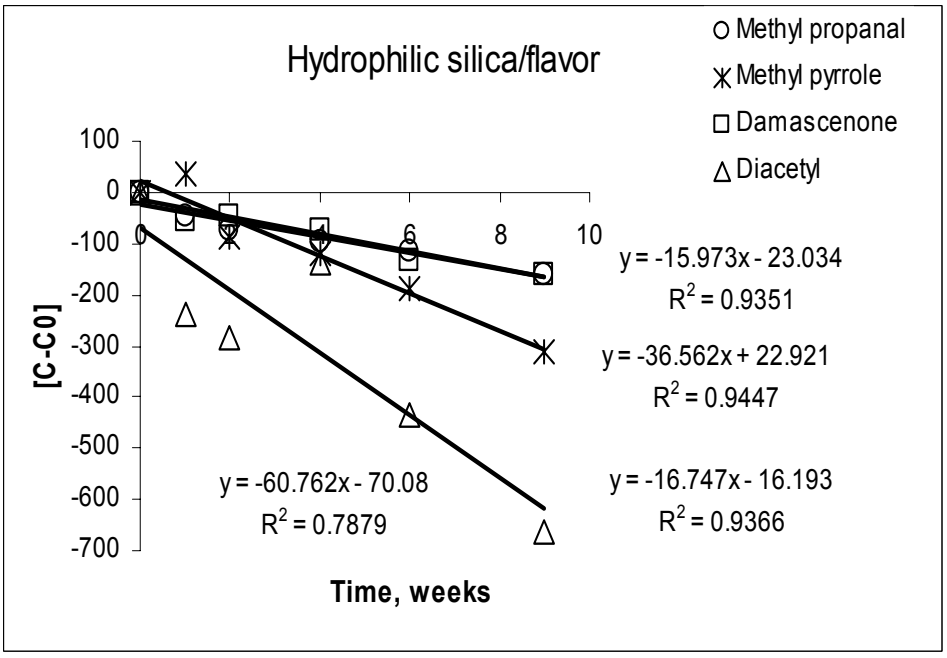

Figure 8-19: Zero-order rate plot for compounds encapsulated in hydrophilic silica sol-gel: starch blend/no solvent matrix

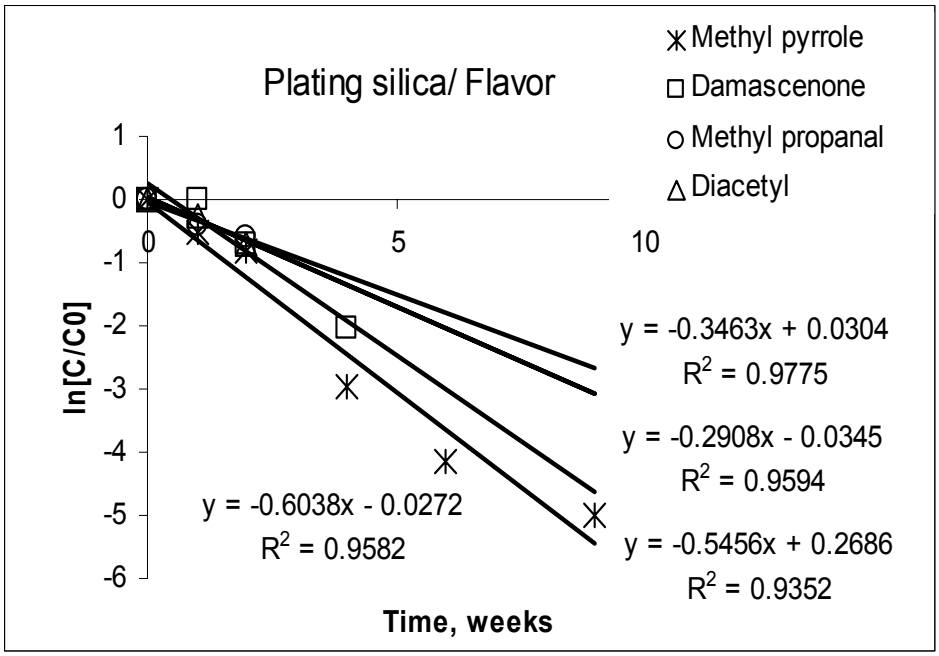

Figure 8-20: First-order rate plot for compounds plated on to commercial silica/no solvent matrix

Table 8-6 : Reaction kinetics of degradation of compounds encapsulated in different matrices

Carriers	Medium	Flavor compound	Order of Reaction	Equation	R^2
Capsul™	Limonene	Methyl Propanal	First	Y = -0.1654X +0.0917	0.8209
		Diacetyl	First	Y= -0.0369X + 0.19	0.9799
		Methyl Pyrrole	First	Y = -0.0697X -0.0013	0.9494
		Damascenone	First	Y= -0.2165X -0.2189	0.9580
Hybrid Silica	MCT	Methyl Propanal	First	Y= -0.2761X + 0.0074	0.9884
		Diacetyl	First	Y= -0.0702X+0.0129	0.9090
		Methyl Pyrrole	First	Y= -0.1019X-0.0471	0.9739
		Damascenone	First	Y= -0.1217X-0.0256	0.9832
Hybrid silica	Flavor	Methyl Propanal	First	Y= -0.1536X-0.0912	0.9338
		Diacetyl	First	Y= -0.1163X+0.1179	0.8558
		Methyl Pyrrole	First	Y= -0.1189X+0.0415	0.8505
		Damascenone	Zero	Y= -30.607X-62.108	0.8756
Hybrid silica	Limonene	Methyl Propanal	First	Y= -0.2765X+0.0316	0.9100
		Diacetyl	First	Y= -0.1085X-0.2037	0.785
		Methyl Pyrrole	First	Y= -0.0865X-0.0776	0.9473
		Damascenone	First	Y= -0.1034X -0.0076	0.9854
Hydrophilic silica	Limonene	Methyl Propanal	First	Y= -0.3166X+0.1851	0.9079
		Diacetyl	First	Y= -0.2723X+0.0131	0.9888
		Methyl Pyrrole	First	Y= -0.1536X+0.0924	0.9566
		Damascenone	First	Y= -0.1097X-0.0257	0.9204
Plating silica	Limonene	Methyl Propanal	First	Y= -0.2019X-0.0344	0.9201
		Diacetyl	First	Y= -0.5483X-0.0474	0.9781
		Methyl Pyrrole	First	Y= -0.4498X+0.1361	0.9682
		Damascenone	First	Y= -0.2399X+0.0285	0.9954
Hydrophilic silica	Flavor	Methyl Propanal	Zero	Y= -15.973X-23.034	0.9351
		Diacetyl	First	Y= -0.0929X+0.0778	0.9457
		Methyl Pyrrole	Zero	Y= -36.562X+22.921	0.9447
		Damascenone	Zero	Y= -16.747X-16.193	0.9366
Capsul™	MCT	Methyl Propanal	Zero	Y= -37.824X+12.328	0.9534

		Diacetyl	First	Y= -51.825 +61.287	0.8700
		Methyl Pyrrole	Zero	Y= -36.518X-2.2126	0.9782
		Damascenone	Zero	Y= -49.11X-1.1976	0.9828
Capsul™	Flavor	Methyl Propanal	First	Y= -0.1886X-0.0726	0.9663
		Diacetyl	Zero	Y= -89.664X-104.3	0.748
		Methyl Pyrrole	Zero	Y= -49.775X + 8.4622	0.8543
		Damascenone	First	Y= -0.1388X+0.0487	0.9441
Hydrophilic silica	MCT	Methyl Propanal	First	Y= -0.2908X-0.0345	0.9594
		Diacetyl	First	Y= -57.139X-0.2588	0.9599
		Methyl Pyrrole	First	Y= -0.6038X-0.0272	0.9582
		Damascenone	First	Y= -0.5456X+0.2686	0.9352
Plating silica	Flavor	Methyl Propanal	First	Y= -0.2917X-0.0134	0.9937
		Diacetyl	First	Y= -0.3813X+0.0788	0.8863
		Methyl Pyrrole	First	Y= -0.6038X-0.0272	0.9582
		Damascenone	First	Y= -0.5456X+0.2686	0.9352
Plating silica	MCT	Methyl Propanal	First	Y= -0.2917X-0.0314	0.9937
		Diacetyl	First	Y= -0.3813X+0.0788	0.8863
		Methyl Pyrrole	First	Y= -0.6222X-0.1829	0.7941
		Damascenone	First	Y= -0.1919X-0.0614	0.9180

Appendix 9 (Chapter 6)

Individual plots for release properties of the curve

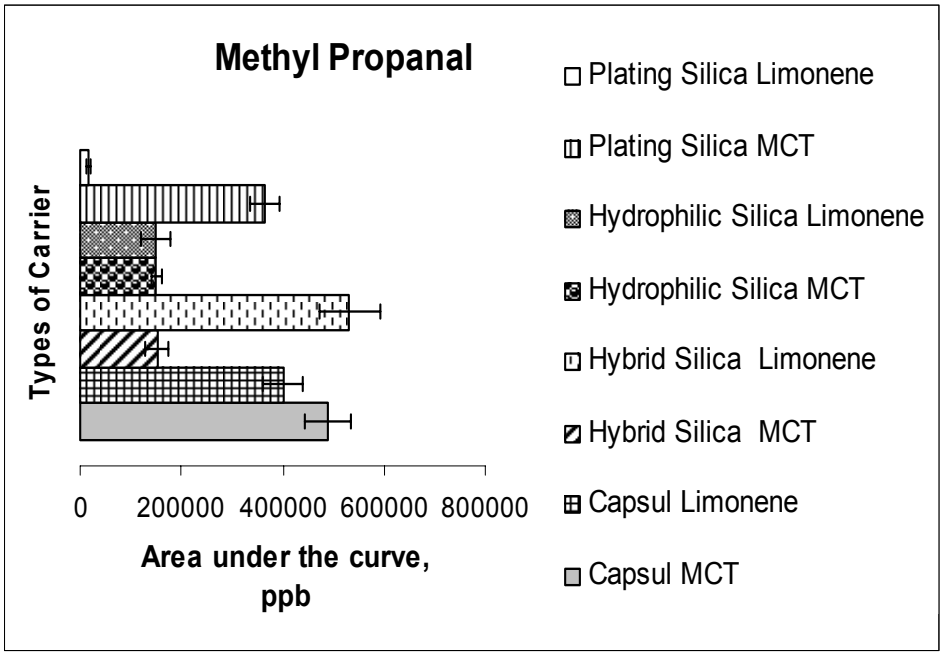

Figure 8-21: Cumulative area under the release curve for methyl propanal in different matrices

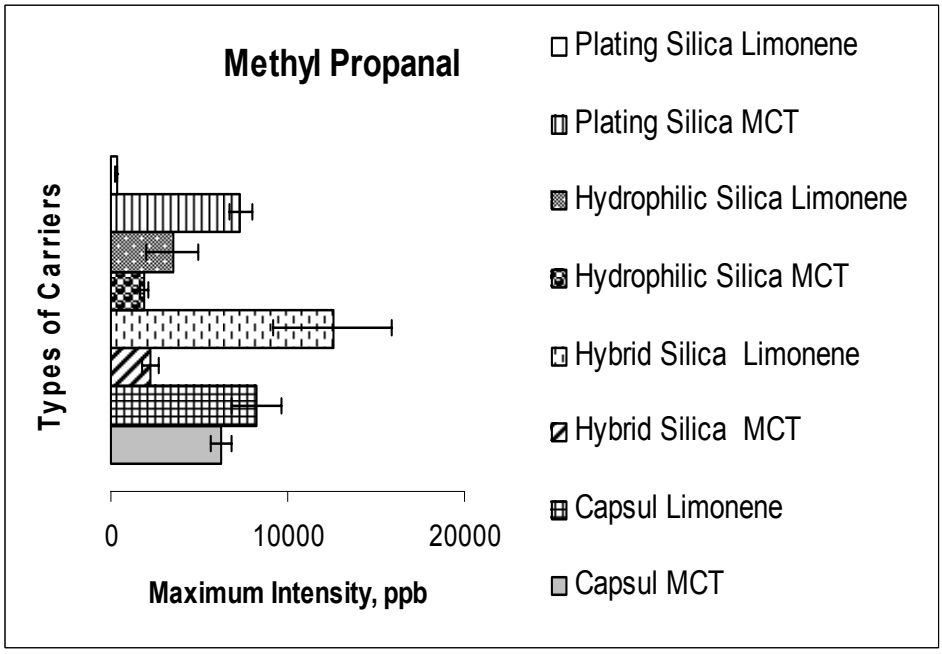

Figure 8-22: I_{max} of methyl propanal in different matrices

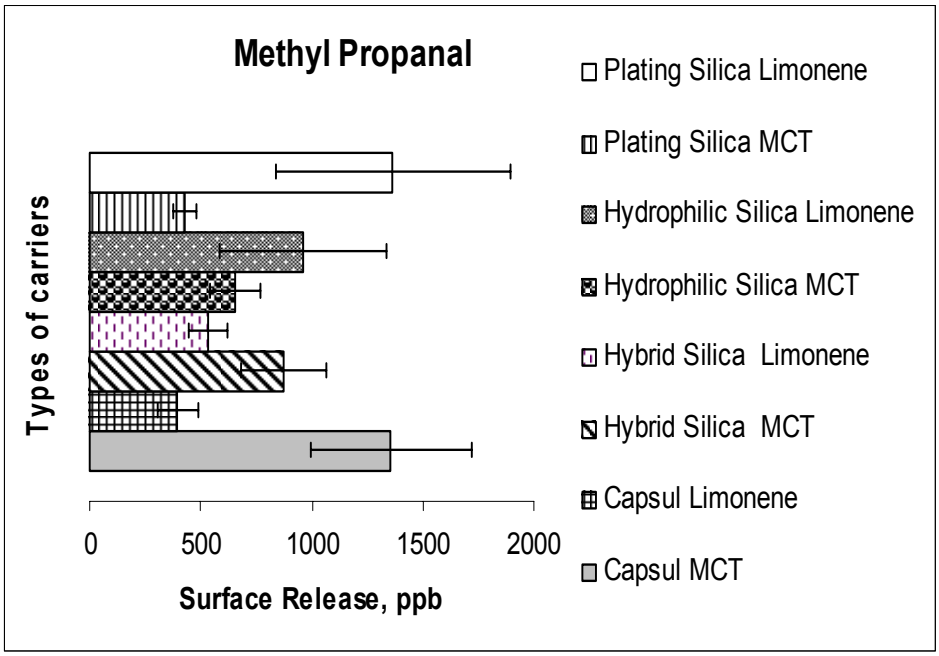

Figure 8-23: Area under the release curve for methyl propanal in different matrices before the addition of water (surface release)

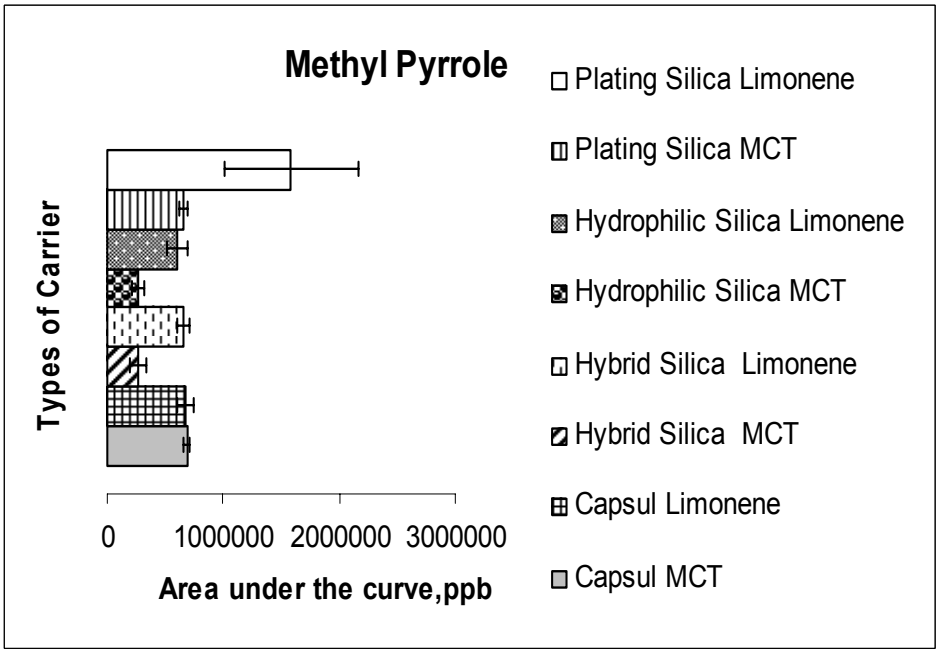

Figure 8-24: Cumulative area under the release curve for methyl pyrrole in different matrices

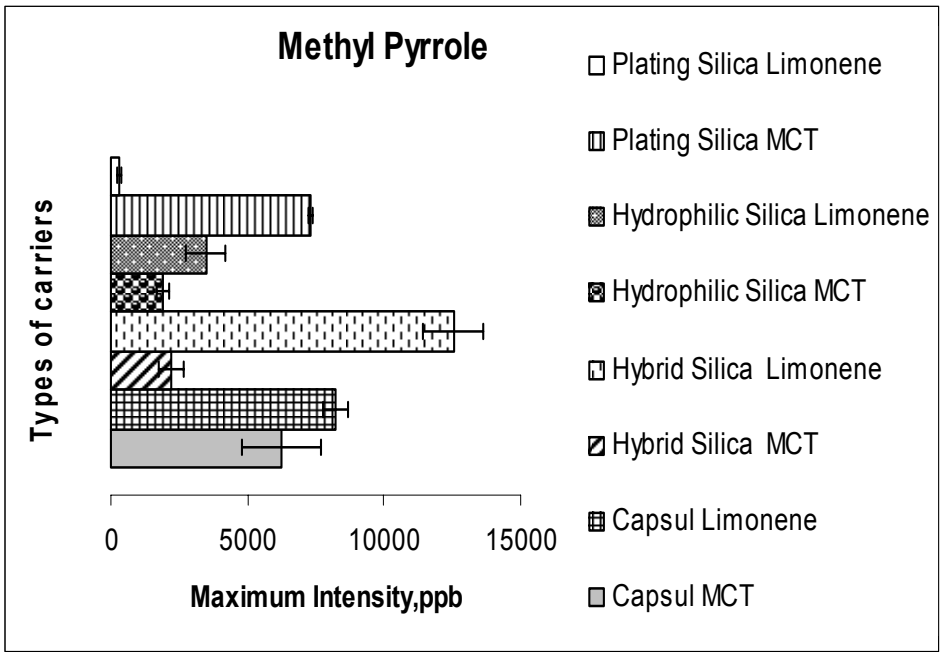

Figure 8-25: I_{max} of methyl pyrrole in different matrices

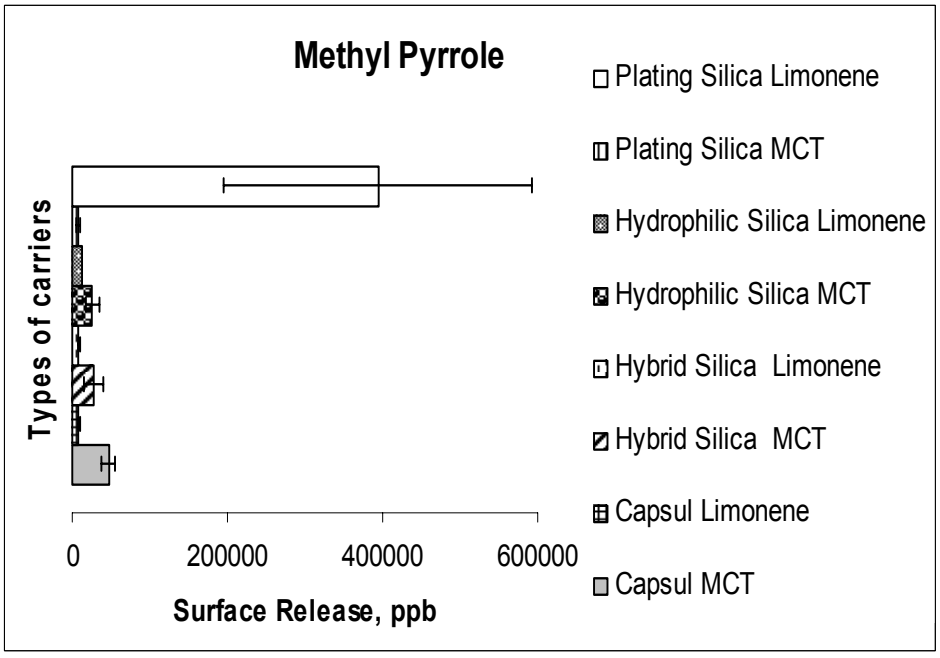

Figure 8-26: Area under the release curve for methyl pyrrole in different matrices before the addition of water (surface release)

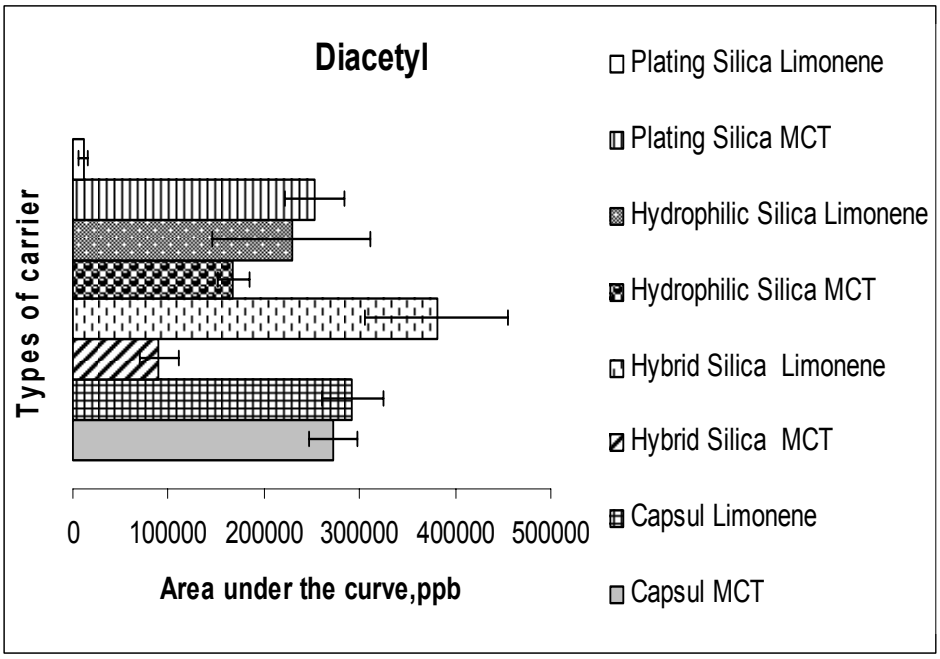

Figure 8-27: Cumulative area under the release curve for diacetyl in different matrices

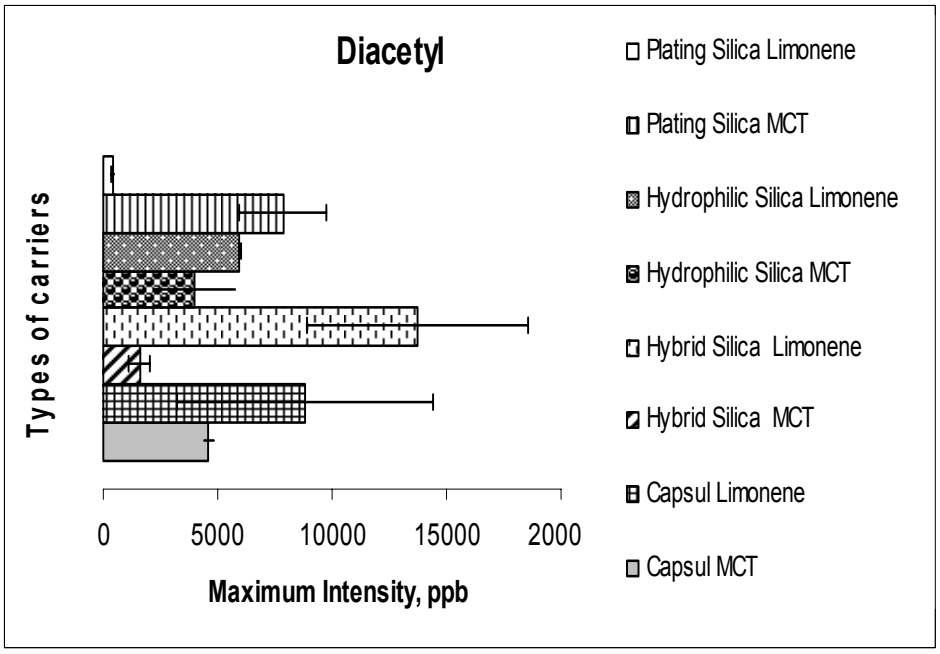

Figure 8-28: I_{max} of diacetyl in different matrices

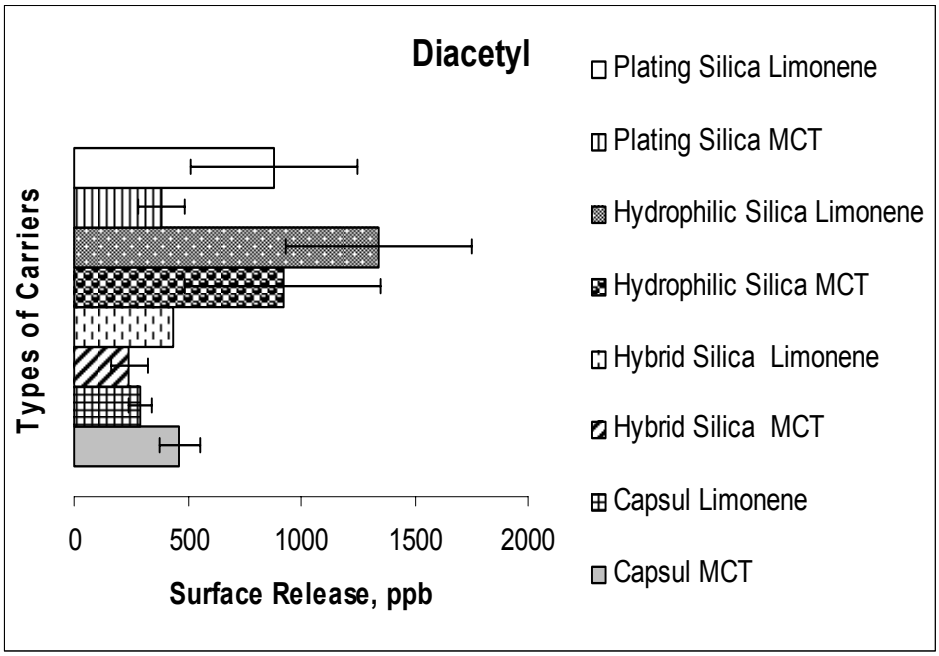

Figure 8-29: Area under the release curve for diacetyl in different matrices before the addition of water (surface release)

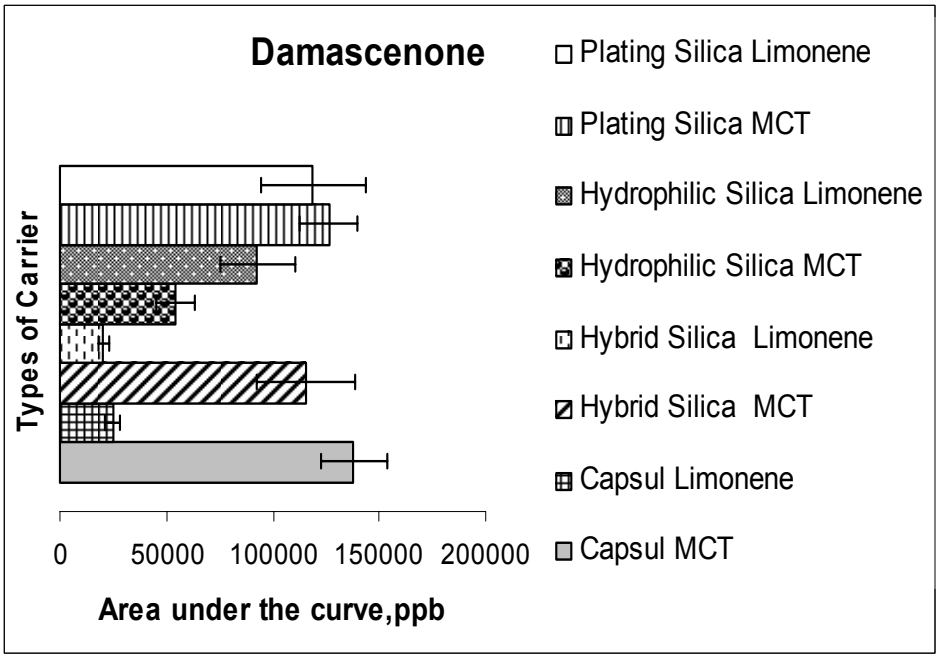

Figure 8-30: Cumulative **a**rea under the release curve for damascenone in different matrices

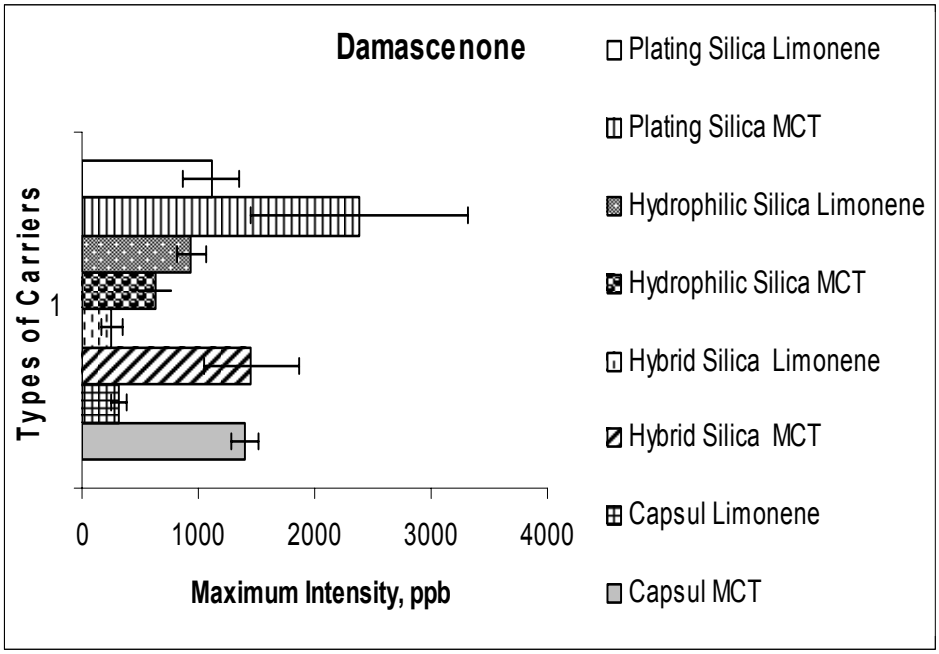

Figure 8-31: I_{max} of damascenone in different matrices

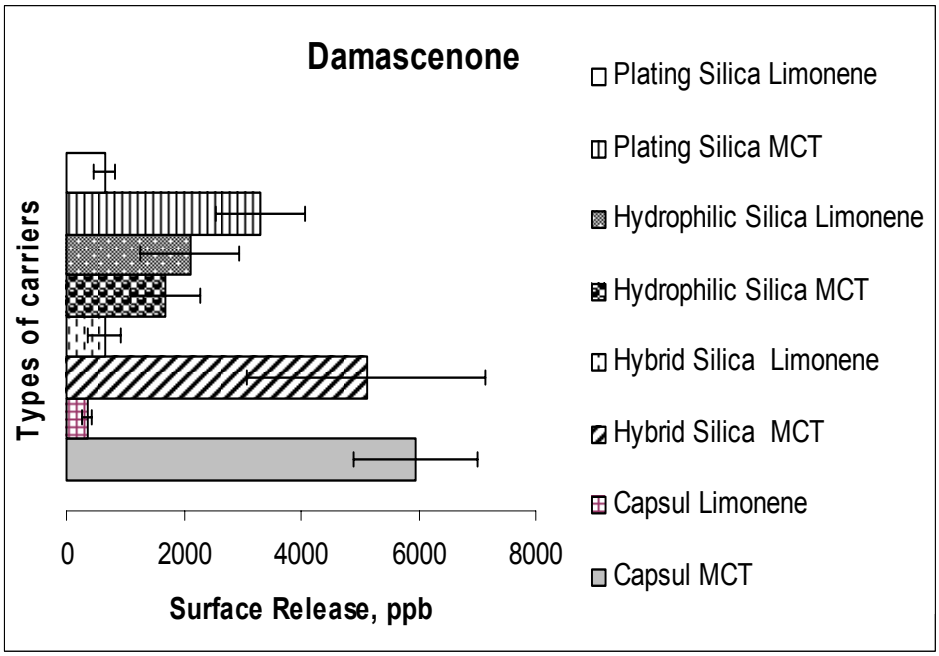

Figure 8-32: Area under the release curve for damascenone in different matrices before the addition of water (surface release)

Release patterns of encapsulated powders in water

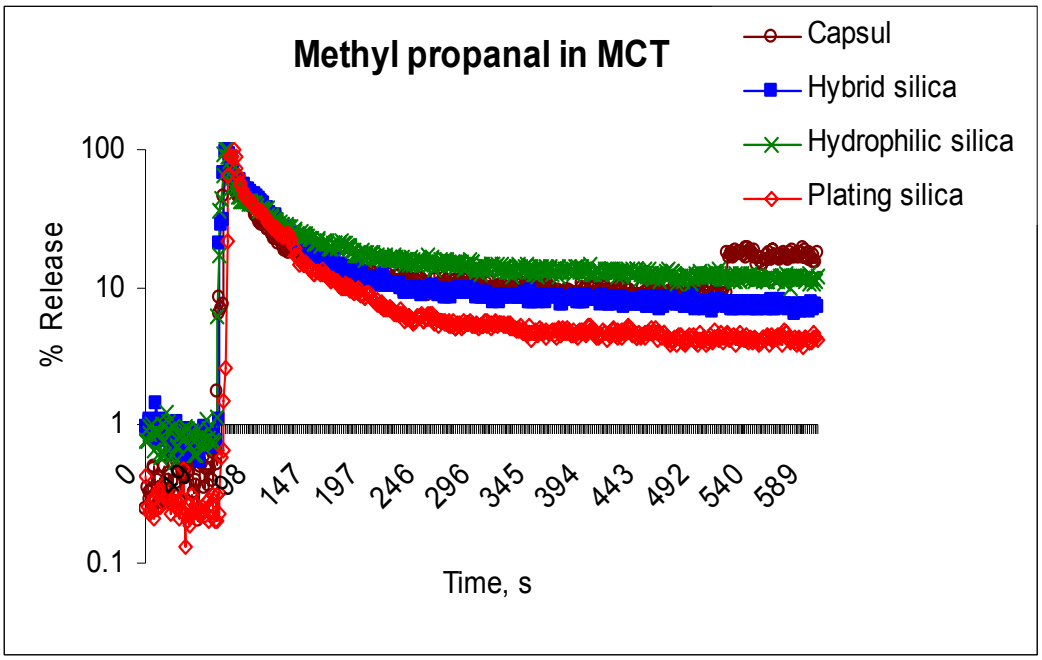

Figure 8-33: Release patterns of methyl propanal from encapsulated matrices using MCT as a solvent

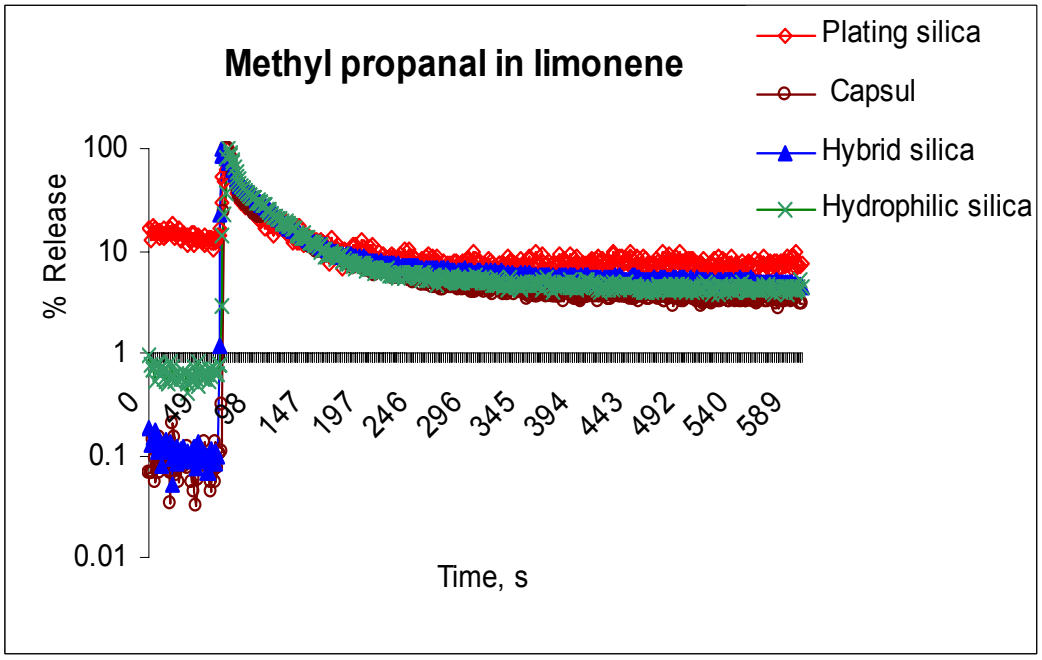

Figure 8-34: Release patterns of methyl propanal from encapsulated matrices using limonene as a solvent

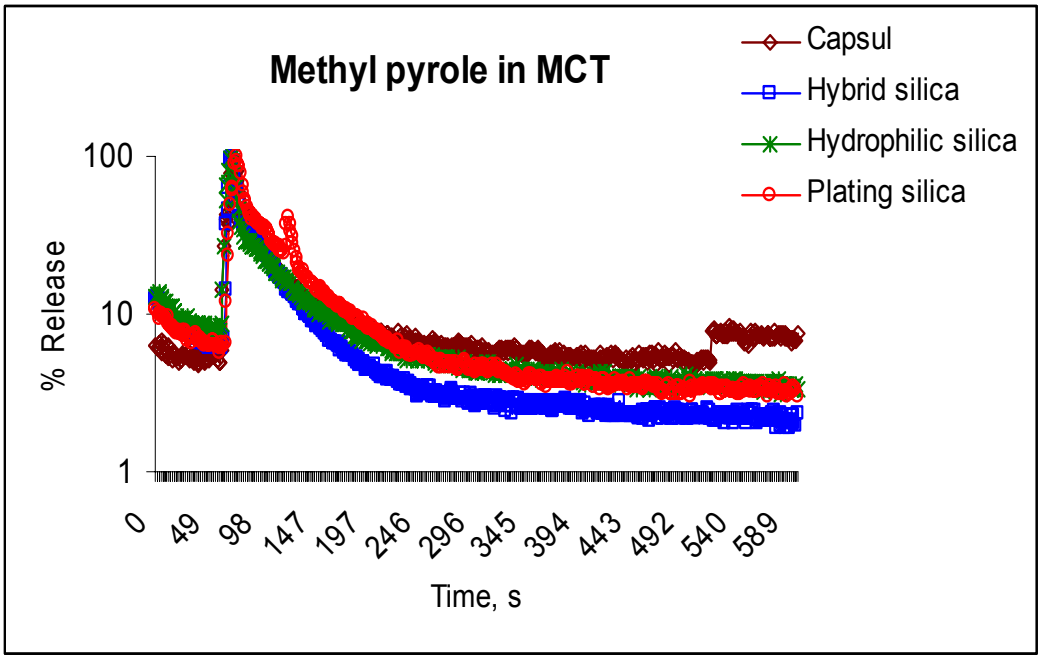

Figure 8-35: Release patterns of methyl pyrrole from encapsulated matrices using MCT as solvent

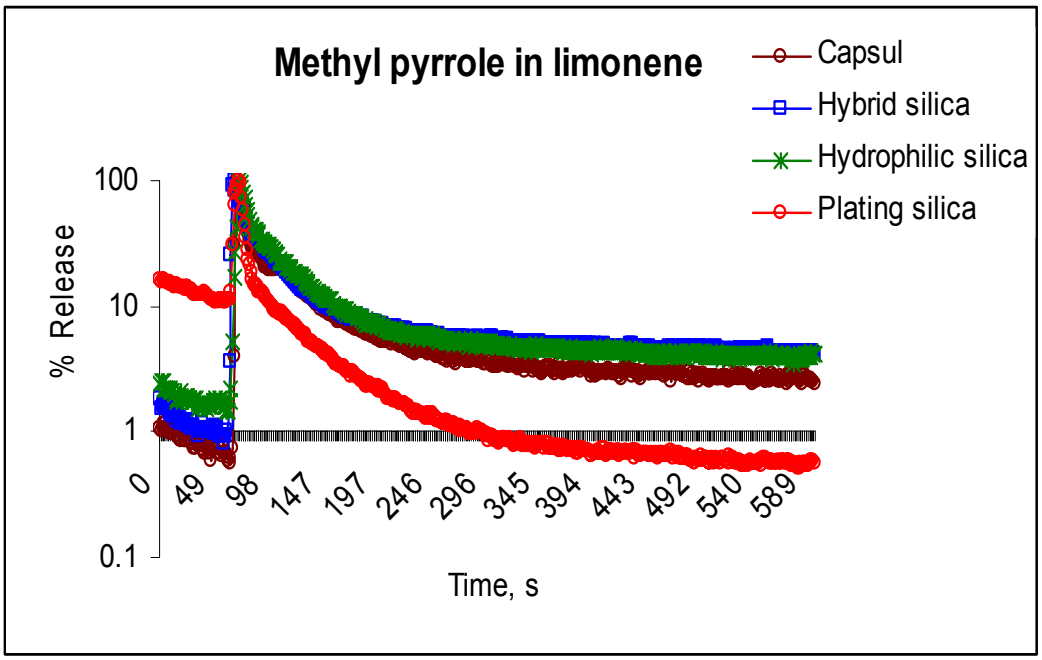

Figure 8-36: Release pattern of methyl pyrrole from encapsulated matrices using limonene as a solvent

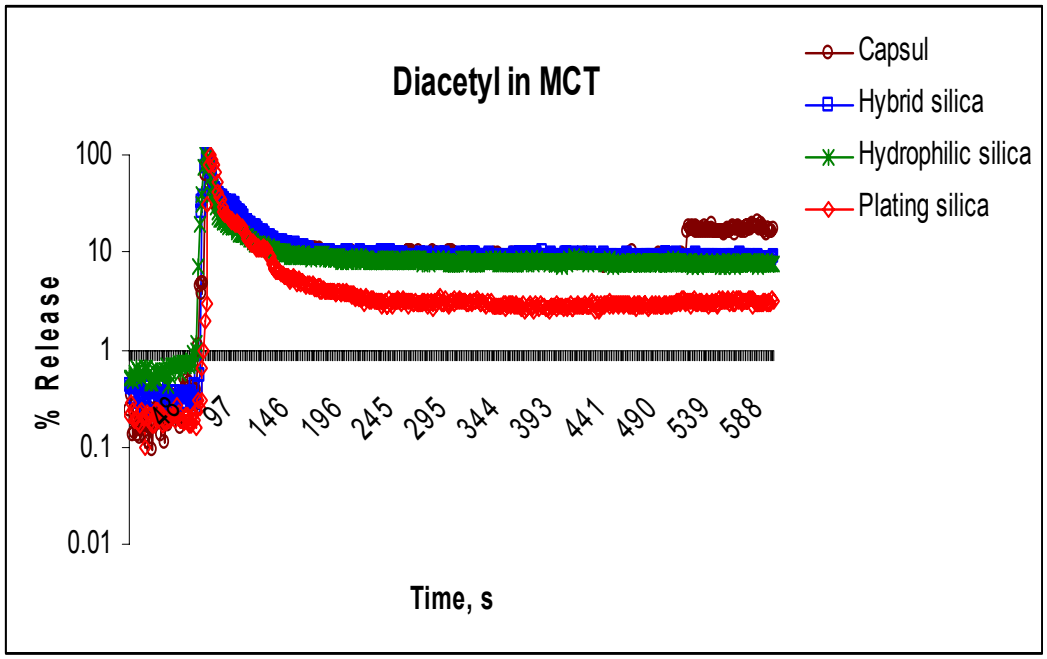

Figure 8-37: Release patterns of diacetyl from encapsulated matrices using MCT as a solvent

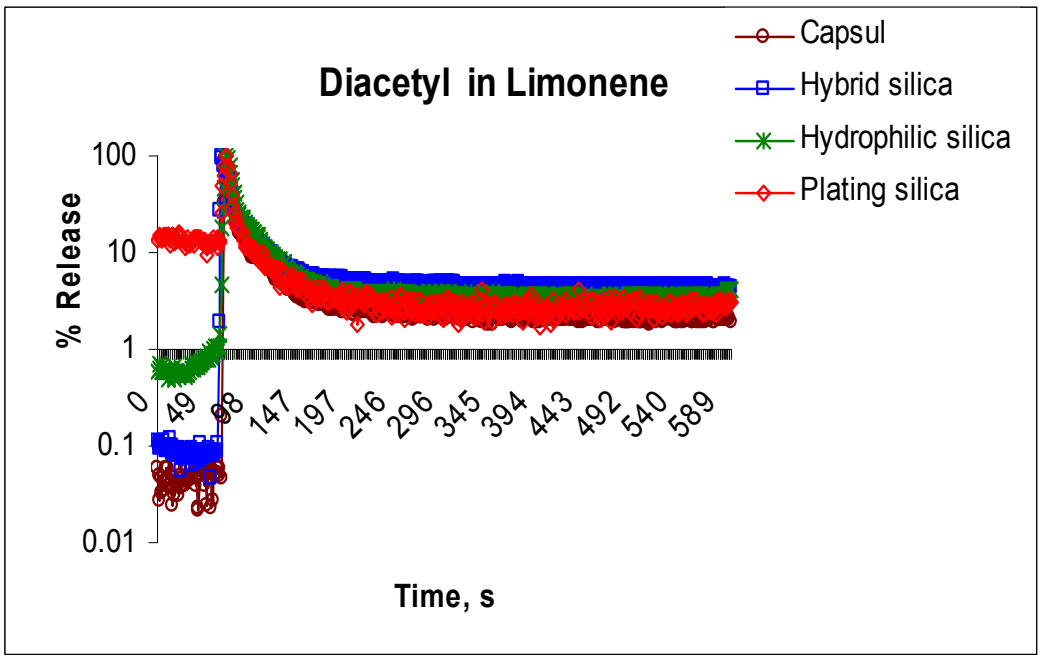

Figure 8-38: Release patterns of diacetyl from encapsulated matrices using limonene as a solvent

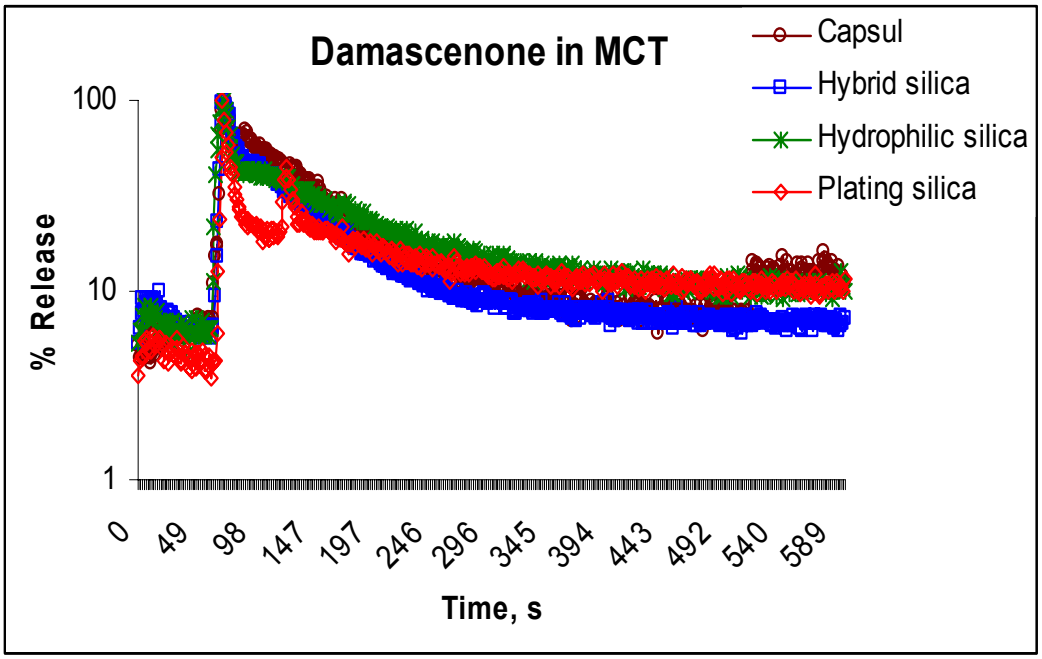

Figure 8-39: Release patterns of damascenone from encapsulated matrices using MCT as a solvent

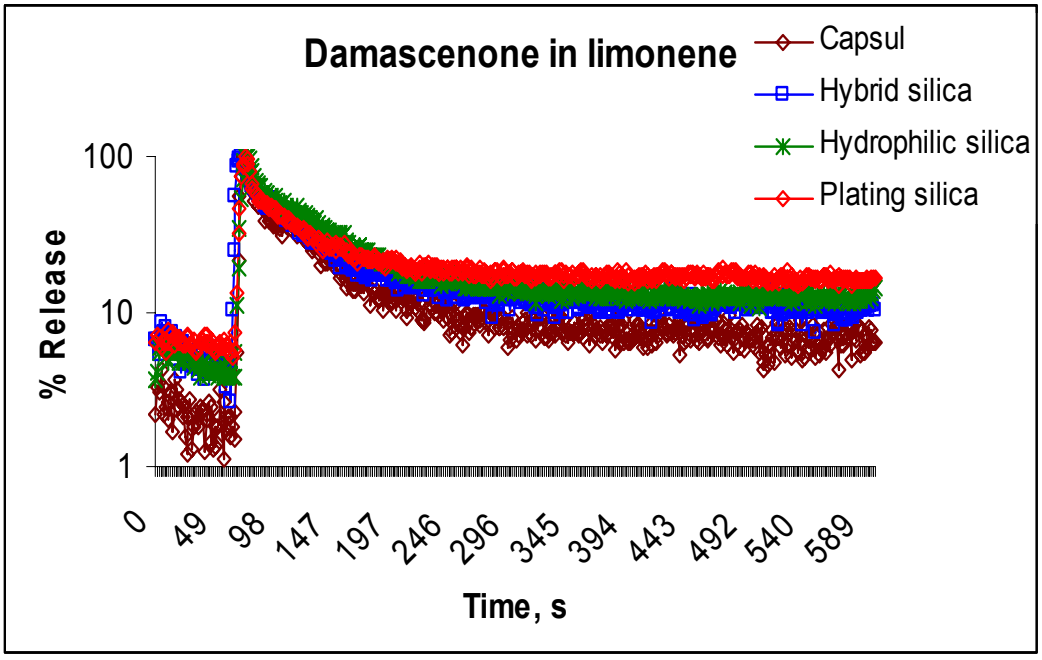

Figure 8-40: Release patterns of damascenone from encapsulated matrices using limonene as a solvent